Optimal Interconnections of PV Modules for Performance Enhancement of PV Array under Partial Shading Conditions

A thesis submitted to the
UPES

For the Award of
Doctor of Philosophy
In
Electronics Engineering

By
Isha Kansal

April 2023

Supervisor

Dr. Rupendra Kumar Pachauri

School of Engineering (SOE)
UPES
Dehradun – 248007, Uttarakhand

Optimal Interconnections of PV Modules for Performance Enhancement of PV Array under Partial Shading Conditions

A thesis submitted to the
UPES

For the Award of
Doctor of Philosophy
In
Electronics Engineering

By
Isha Kansal

(SAP ID-500057724)

April 2023

Supervisor

Dr. Rupendra Kumar Pachauri

Associate Professor,

Electrical Cluster,

UPES
UNIVERSITY OF TOMORROW

School of Engineering (SOE)
UPES
Dehradun- 248007: Uttarakhand

DECLARATION

I declare that the thesis entitled "**Optimal interconnections of PV modules for performance enhancement of PV array under partial shading conditions**" has been prepared by me under the guidance of **Dr. Rupendra Kumar Pachauri**, Associate Professor in Electrical Cluster, School of Engineering, University of Petroleum and Energy Studies, Dehradun. No part of this thesis has formed the basis for the award of any degree or fellowship previously.

Isha Kansal

School of Engineering [SOE]

University of Petroleum & Energy Studies

Dehradun-248007, Uttarakhand

UPES
UNIVERSITY OF TOMORROW

Great Place To Work. Certified MAR 2022 - MAR 2023 INDIA

CERTIFICATE

This is to certify that the thesis entitled "**Optimal Interconnections of PV Modules for Performance Enhancement of PV Array under Partial Shading Conditions**" is being submitted by **Isha Kansal** in fulfillment for the Award of DOCTOR OF PHILOSOPHY in **Renewable Energy** to the University of Petroleum and Energy Studies. Thesis has been corrected as per the evaluation reports dated **11/08/2023** and all the necessary changes / modifications have been inserted/incorporated in the thesis.

11.8.2023

Signature of Supervisor

Name of Supervisor: Dr. Rupendra Kumar Pachauri
Department: Electrical Cluster
Designation: Associate Professor
Contact address: UPES, Dehradun

Date: 11/08/2023

ABSTRACT

This thesis presents work that aims to optimize the connections between photovoltaic (PV) modules to improve performance metrics such as fill factor (FF), minimizing power loss (PL), global maximum power point (GMPP), accuracy and power enhancement (PE) of PV array in different partial shading scenarios (PSCs). Real-time data is collected via analogue sensors connected to a microcontroller system, allowing the electrical performance of a puzzle-based, optimized, interconnected PV array to be measured under varying shadowing conditions. The real-time data obtained in shading scenarios through data acquisition system on analysis is found to be reliable and cost-effective.

First, the advantages of total-cross-tied (TCT) electrical interconnections are weighed against those of symmetric-matrix-total-cross-tied (SM-TCT) for a variety of shadow test cases. Multiple power points (MPP) are mapped for the sake of local and global MPP to represent the non-linear conduct of PV systems in terms of power-voltage (P-V) and current-voltage (I-V) characteristics. Three types of shadow situations (lamp post, corner, and single vertex shadings) are used to assess and compare the efficacy of 8×8 size TCT and SM-TCT. The results of case-2 were found highly exceptional for the proposed SM-TCT based connection shows increase in power at GMPP from 7.382 to 8.769 kW, FF gets incremented to 0.634 from 0.538 % and PE is achieved as 15.81 %.

Secondly, experimental research on 4×4 size solar PV array installations with varying shading conditions will be verified through a MATLAB/Simulink study. Different hybrid Latin-square-Total-cross-tied (LS-TCT), series-parallel-Total- cross-tied (SP-TCT) and conventional PV arrangements have their

performance measured under shadowing conditions. The electrical performance (P-V and I-V curves) are demonstrated to have multiple MPP due to the partial shading. Each possible arrangement of PV panels is modelled. It has been found that when it comes to PSCs, the LS-TCT configuration is highly recommended with respect to the positioning of the GMPP, PL reduction, and improvisation of FF. To explore the efficacy of the Shape-Do-Ku (SPDK) topology is demonstrated and provided in-depth comparisons with existing TCT, Su-Do-Ku (SDK) and hybrid LS-TCT arrangements in the context of the novel shading pattern-4. SPDK puzzle-based PV array configurations are proposed, and their performance is best compared to GMPP, PL, and FF under shading cases-1 (63.89 W, 16.11 W, 0.727; MATLAB/Study; 62.25 W, 17.75 W, 0.807; experimental study) (pattern-4).

Thirdly, it introduces a 4×4 size new configuration known as the "SM-TCT", disperses shading with an idea of physically reallocating electrical connections that are fixed to PV modules. A comprehensive comparative analysis of traditional TCT and novel-TCT (NTCT) with the outcomes for the suggested SM-TCT arrangement prove its viability for maximizing performance can be demonstrated. The obtained results from Simulink and MATLAB are based on the non-linear I-V and P-V characteristics. Three realistic PSCs are used to assess the strengths and weaknesses of the SM-TCT, NTCT, TCT and Shape-do-Ku configurations with regards to voltage and power at GMPP, improved FF, decreased PL, power efficiency and performance ratio (PR).

Fourthly, it pinpoints DPVM-SEC methodology of 6×4 size validating as a trustworthy means of boosting PV system dependability, even in partially shaded environments. The power at GMPP was found to be greater in shadowing

conditions I-II, coming in at 79.81 W and 77.39 W, respectively. This is in contrast to more traditional configurations such as SP (65.1 W and 57.53 W) and TCT (68.79 W and 71.84 W), which both had a lower power output. PV accuracy can also be evaluated in the presence of such shading conditions using FF attributes. According to the evaluated shadowing scenario, the DPVM-SEC configuration's FF factors are 64.60 and 65.11 %. Reorganizing a PV module's structure with the DPVM-SEC method reduces power losses to 40.29 W and 42.71 W, respectively, in both shading cases. P-V and I-V characterization is utilized in testing the developed DAS to demonstrate its accuracy in comparison to conventional measurement techniques.

Fifthly, the primary objective is to advocate for a plan to reduce shadowing from PV systems so that significant GMPP can be attained. The magic square (MS) game puzzle of 4×4 size illustrates the PV system performance at higher side when exposed to irradiation that is not uniform and mimics real-world conditions. PSCs and their effects on PV system-based electricity production are disgraceful. TCT and SP, comparable to the MS puzzle approach, are the subjects of an extensive study and comparison. For parameters like minimal PL, PE, GMPP locations and FF, the MATLAB/Simulink analysis results matched the experimental validation very well. A pivotal statement motivates the duty to demonstrate the adequate results of the suggested PV system.

In this thesis, we present and evaluate the proposed shade dispersion approach, which has been shown to be effective at lowering PS losses on PV modules. Improvements in efficiency and MPP have been demonstrated through simulations and experimental validations of this approach in a variety of PS settings. Educators and researchers need access to a cost-effective, dependable, and low-priced sensor network for PV system monitoring and data acquisition.

ACKNOWLEDGEMENT

The trek to this paradise begins in the lush environment of UPES, Dehradun tucked in the valley at the Himalayan foothills in the eastern region of the Song River (which is a tributary of the Ganga) and western region of the Asan River (which is a tributary of the Yamuna). Its mesmerizing and divine flow in my soul stimulates me to be successful. My nurtures within Mother Nature have embarked on a dream to be of little value to human society. Following the pathways set out by my parents, being fostered by my mentors and blossoming under their blessings takes me to enroll myself, where I had worked under the guidance of Dr. Rupendra Kumar Pachauri to develop my vision and research abilities.

He has been most humane and persist a very supportive soul in the premises. His perspicacity knowledge in the world of research is remarkable to a young and crude mind like mine. I gained a broad understanding of modern solar PV engineering, since I believe that he has the finest interests in technologies and keen interest in serving humanity at heart. Dr. Pachauri's followers including me persists only two qualities that is dedication and determination as a wisdom seeker.

I'd like to thank everyone who helped me out in the Electrical Cluster, SOE, UPES, Dehradun for helping me overcome obstacles and solve puzzles while conducting research under their watchful eye. The members of the School Research Committee at the UPES, Dehradun, deserve a great deal of credit for helping me improve the quality of my research with their insightful comments and suggestions.

Any researcher who aspires to go beyond the scientific necessities of society finds knowledge to be a never-ending fog. It is our friends that strain their personal boundaries on our behalf in order to keep anchors at bay. I would like to express my requital to everybody mentioned even to all those being hidden cheer.

My father, Mr. Prabhat Kumar Kansal showed perseverance at every stage of my journey up to this point and my mother, Mrs. Sandhya Agarwal gave-off her dreams to spotlight my fortune and it is the result of their countless blessings. I am who I am today. To balance their blessings and struggle that makes this smile today, any word or action will always be insignificant. They made a tremendous choice by finding me a lifelong partner Mr. Adhish Agarwal, who does everything in his power to make any situation or whim of mine easier. He is the one who has consistently pleasantly surprised me or supported my dedicated service to science and mentors. His presence is exceptional and far surpasses any comfort that life can provide. Throughout this time, my brother Mr. Pranjal Kansal spoke to me in the most sincere and loving ways possible. He will always be a joyful and kind place for me to breathe. Finally, it is eternally heartwarming that the Almighty had the grace to bestow his blisses.

Isha Kansal

TABLE OF CONTENTS

	Page No.
TITLE PAGE	I
DECLARATION	III
CERTIFICATE	IV
ABSTRACT	V
ACKNOWLEDGEMENT	VIII
TABLE OF CONTENTS	X
LIST OF FIGURES	XVII
LIST OF TABLES	XXIV
NOTATIONS AND ABBREVIATIONS	XXV
CHAPTER- 1: Introduction	1-6
1.1 OBJECTIVES	6
CHAPTER-2: Literature Review	7-33
2.1 INTRODUCTION	7
2.2 IMPACT OF SHADING ON ARRAY CONFIGURATION	8
2.2.1 PV Array Conventional Configurations	20
(a) Series Configuration	20
(b) Parallel Configuration	22
(c) SP, TCT, BL And HC Configurations	23
2.2.2 Hybrid PV array Configurations	27
(a) SP-TCT, BL-TCT and BL-HC PV Array Configuration	27
2.2.2 Modified PV Array Configurations	28
(a) RTCT, RSP-TCT, RBL-TCT, RBL-HC and S-M-TCT	28
2.2.4 Puzzle Based Advanced PV Array Configuration	29

(a) Su-Do-Ku Configuration 29
(b) Physical Reallocation of Module-Fixed Electrical Connections Configuration (PRM-FEC) 30
(c) Optimal TCT and Novel TCT Configuration 30
(d) Magic Square Configuration 31
(e) Futoshiki Configuration 32
(f) Novel Configuration 32
(g) Latin Square Configuration 32
2.3 SUMMARY 33

CHAPTER- 3: PV system modelling and role of symmetric matrix-based PV array configuration for higher GMPP 34-46
3.1 INTRODUCTION 34
3.2 STRATEGIC CONFIGURATION AND PV SYSTEM 34
3.2.1 Solar PV system 34
3.2.2 The SM-TCT Size 8 Rules of Conduct 36
3.2.3 SM-TCT PV array configuration 36
3.3 CASE STUDIES AND PERFORMANCE EVALUATION OF SHADED TEXTURES 38
3.3.1 Shading scenarios 38
3.3.2 Partial shading losses 39
3.3.3 Fill Factor 40
3.4 RESULTS AND DISCUSSION 40
3.4.1 P-V and I-V curves for considered configurations 42
3.4.2 Power Loss 44
3.4.3 Performance Enhancement and Fill Factor 45
3.4.4 Performance Ratio 45
3.5 SUMMARY 46

Chapter- 4: Shape-Do-Ku Game Puzzle Based PV Array Reconfiguration for Higher GMPP 47-85

4.1 INTRODUCTION 47

4.2 PV SYSTEM TECHNOLOGY and ARRAY TOPOLOGIES 48

4.2.1 PV system modeling 48

4.2.2 PV array configurations 49

(a) Conventional Configurations 49

(b) Latin Square puzzle configuration 49

(c) Su-Do-Ku configuration 50

(d) Shape-Do-Ku configuration 50

4.3 ANALYSIS of PERFORMANCE PARAMETERS and SHADING PATTERNS 54

4.3.1 Performance Parameters 54

(a) Power Loss 54

(b) Fill Factor 55

(c) Performance Ratio 55

4.3.2 Analysis of Shading Scenarios 55

(a) Shading Pattern-1 55

(b) Shading Pattern-2 57

(c) Shading Pattern-3 58

4.4 RESULTS and DISCUSSION 59

4.4.1 P-V and I-V curves at STC 59

4.4.2 Effect of Shading Scheme-1 on PV Array 60

(a) P-V and I-V curves 60

(b) Power Loss 63

(c) Fill Factor 64

4.4.3 Effect of Shading Pattern-2 on PV Array 65

(a) P-V and I-V plots 65
(b) Power Loss 68
(c) Fill Factor 68
4.4.4 Effect of Shading Pattern-3 On PV Array 69
(a) P-V and I-V curves 69
(b) Power Loss 72
(c) Fill Factor 72
4.5 RESULTS AND ITS VALIDATION 73
4.5.1 Analysis of Shading Pattern-4 73
4.5.2 MATLAB/Simulink Analysis: P-V And I-V plots 73
4.5.3 Experimental Analysis: P-V And I-V Curves 77
(a) Power At GMPP 82
(b) PL 83
(c) FF 84
4.6 SUMMARY 85

CHAPTER-5: Comparative Study of Symmetric Matrix and Game Puzzle Based Configuration for Higher GMPP 86-109
5.1 INTRODUCTION 86
5.2 PV SYSTEM MODELLING AND GAME PUZZLE-BASED CONFIGURATIONS 87
5.2.1 PV System Modelling 87
5.2.2 Conventional TCT Configuration 88
5.2.3 Shape-Do-Ku Configuration 91
5.2.4 SM-TCT Configuration 91
5.3 PERFORMANCE PARAMETERS AND COMPARATIVE SHADE STUDY 94
5.3.1 FF 95

5.3.2 Analysis of Shading Patterns 95
5.4 RESULTS AND DISCUSSION 96
5.4.1 Analysis of P-V and I-V Characteristics using MATLAB/ Simulink 98
5.4.2 P-V And I-V Characteristics: Experimental Analysis 100
5.4.3 Power and Voltage at GMPP 105
5.4.4 PL 107
5.4.5 FF 107
5.4.6 PE 108
5.5 SUMMARY 109

Chapter 6: Experimental Validation of DPVM-SEC based methodology to reconfigure PV array 110-122
6.1 INTRODUCTION 110
6.2 PV SYSTEM TECHNOLOGY 110
6.2.1 Development of Photovoltaic System Layout 110
6.2.2 Development of DAS and Experimental Set-up 111
6.2.3 Conventional PV Array Configurations 113
6.2.4 DPVM-SEC Methodology for PV Array Re-Configuration 114
6.3 SHADING TRENDS ANALYSIS AND PERFORMANCE PARAMETERS 115
6.3.1 Power and Voltage at GMPP 117
6.3.2 PL and FF analysis 117
6.3.3 Execution Ratio 117
6.3.4 Power Gain 117
6.4 RESULTS AND DISCUSSION 118
6.4.1 I-V And P-V Curves during ideal conditions 118
6.4.2 I-V and P-V Plots Under Shading Conditions I-II 118

6.4.3 Power and Voltage at GMPP 120
6.4.4 FF and PL Analysis 120
6.4.5 ER and PG Analysis 121
6.5 SUMMARY 122

Chapter 7: Experimental Validation of Magic Square based PV array reconfiguration for higher GMPP under PSCs 123-140
7.1 INTRODUCTION 123
7.2 SOLAR PV TECHNOLOGY 124
7.2.1 PV Modelling 124
7.2.2 Conventional PV Array Configurations 124
7.2.3 Game Puzzle Based: Magic Square Configurations 125
7.2.4 Experimental Set-up 127
7.3 PERFORMANCE PARAMETERS AND SHADING SCENARIOS 129
7.3.1 Power and Voltage at GMPP 129
7.3.2 FF analysis 130
7.3.3 PL analysis 130
7.3.4 Execution Ratio 130
7.3.5 Power enhancement 130
7.3.6 Shading Scenarios I-II 130
7.4 RESULTS AND DISCUSSION 133
7.4.1 P-V and I-V curve at STCs, 133
7.4.2 I-V and P-V Curves for Shade Scenario I and II: A MATLAB/Simulink Analysis 133
7.4.3 Experimental Validation: I-V and P-V Plots under Shading Scenario-I 135
7.4.4 Power at GMPP 136
7.4.5 FF Analysis 137

7.4.6 PL Analysis 138
7.4.7 ER and PE Analysis 138
7.5 SUMMARY 140

Chapter 8: Conclusion 142
References 144
Publications 164

LIST OF FIGURES

Figure No.	Title	Page No.
1.1	Estimated Excess Primary Energy Use in Exajoules ($\times 10^{18}$ J)	1
1.2	Share of Primary Energy Consumption in 2021	2
1.3	Interconnections of solar cells to form modules turned into arrays	3
1.4(a)-(d)	I-V characteristics of identical solar cells	5
2.1	The effects of shade on a PV system's P-V characteristics and their causes	7
2.2	Total number of articles published on various configurations between 2008-22	9
2.3 (a)-(d)	Conventional array configuration	26
2.4(a)-(c)	Hybrid PV array configuration	28
2.5	SDK configuration	30
2.6	MS Configuration	31
2.7	LS-TCT configuration	33
3.1	PV cell equivalent electrical circuit	35
3.2(a)-(e)	Symmetric matrix: Properties	37
3.3(a)-(b)	Electrical connections of TCT and SM-TCT configuration	38

3.4(a)-(c)	Special shade cases for performance investigation on 8×8 size PV array	39
3.5(a)-(c)	P–V curves under shading test cases: I- III	42
3.6(a)-(c)	Obtained I–V curves under shading cases: I- III	43
3.7	PL analysis under regular shading cases: I-III	44
3.8	(a) % PE (b) FF of under shading cases: I-III	45
3.9	PR under regular shading cases: I-III	45
4.1	Various Shading Conditions affecting PV performance	48
4.2	Equivalent circuit of PV cell	48
4.3(a)-(m)	Conventional, hybrid, game puzzle-based configurations and their flow charts	53
4.4(a)-(b)	Shading impact on P-V and I-V characteristics	54
4.5(a)-(c)	Shading cases 1-3 for pattern-1	55
4.6(a)-(c)	Shading cases 1-3 for pattern-2	56
4.7(a)-(c)	Shading cases 1-3 for pattern-3	58
4.8(a)-(b)	P-V and I-V curves (STCs)	59
4.9(a)-(c)	I-V and P-V curves under shading scenerio-1	61
4.10	Power at GMPP for cases 1-3 under shading pattern-1	63

4.11	PL for cases 1-3 for shading pattern-1	64
4.12	FF for cases 1-3 for shading pattern-1	64
4.13(a)-(c)	I-V and P-V plots for shading pattern-2	66
4.14	Power at GMPP for cases 1-3 under shading pattern-2	68
4.15	PL for cases 1-3 under shading pattern-2	68
4.16	FF for cases 1-3 under shading pattern-2	69
4.17(a)-(c)	I-V and P-V curves under shading pattern-2	70
4.18	Power at GMPP for cases 1-3 under shading pattern-3	72
4.19	PL for cases 1-3 under shading pattern-3	72
4.20	FF for cases 1-3 under shading pattern-3	73
4.21(a)-(c)	Shading cases 1-2 for pattern-4	73
4.22 (a)-(b)	P-V characteristics of TCT, LS-TCT, SDK and SPDK systems	74
4.23 (a)-(b)	I-V characteristics of TCT, LS-TCT, SDK and SPDK configurations	75
4.24	Experimental setup of PV system	80
4.25 (a)-(b)	P-V characteristics of TCT, LS-TCT, SDK, and SPDK configurations	81
4.26 (a)-(b)	I-V characteristics of TCT, LS-TCT, SDK, and SPDK configurations	82

4.27	Power at GMPP for (a) Simulink (b) Experimental analysis	83
4.28	(a) MATLAB/Simulink Study (b) Experimental study	84
4.29	FF analysis for (a) Simulink (b) Experimental studies	84
5.1	Electrical circuit diagram of a PV cell	87
5.2	Zig-Zag arrangement for NTCT configuration	90
5.3	PV module arrangement of NTCT configuration	90
5.4(a)-(b)	Reconfiguration methodology of Shape-do-Ku array configuration	91
5.5(a)-(d)	SM properties	92
5.6(a)-(b)	Reconfiguration methodology of SM-TCT array configuration	93
5.7(a)-(b)	P-V and I-V characteristics	94
5.8(a)-(c)	Various types shading patterns for performance investigation of PV array	96
5.9(a)-(c)	P–V curves under PSCs	99
5.10(a)-(e)	I–V curves under PSCs	100
5.11	Hardware implementation of PV system	101
5.12(a)-(c)	P–V curves under PSCs	102
5.13(a)-(c)	I–V curves under PSCs	103

5.14	Power at GMPP (a) Simulation (b) Experimental study	104
5.15	Voltage at GMPP (a) Simulation (b) Experimental analysis	106
5.16 (a)-(b)	Power Loss	107
5.17	FF analysis under PSCs (a) Simulink study (b) experimental study	108
5.18	PE analysis under PSCs (a) Simulink study (b) experimental study	109
6.1	Arrangement in modules of PV array and equivalent circuit	111
6.2	Experimental setup	111
6.3	Wiring arrangement of DAS for real time electrical parameters	112
6.4	Flow chart to describe the operation of data logger system	113
6.5	(a) Nomenclature of PV system: 6×4 size (b) SP (c) TCT configurations	114
6.6	DPVM-SEC based PV array configurations	115
6.7	Shading scenarios I-II	116
6.8	(a) I-V (b) P-V curves during ideal conditions	118
6.9	(a) I-V (b) P-V characteristics during shading scenario- I	119
6.10	(a) I-V (b) P-V characteristics during shading scenario -II	119
6.11	(a) Power (b) voltage at GMPP	121

6.12	(a) FF (b) PL study	121
6.13	(a) ER (b) PG analysis	122
7.1	Development of PV array (4×4 size) and PV cell equivalent electrical circuit	124
7.2	(a) Nomenclature 4×4 size PV array (b) SP (c) TCT topologies	125
7.3	Methodology of attaining (4×4 Size) MS puzzle for PV array reconfiguration	127
7.4	Experimental setup	128
7.5	Wiring arrangement of DAS for real time measurement	128
7.6	Flow chart to describe the operation of data logger system	129
7.7	Shade profiles based on reconfigured PV array	131
7.8	Shade profiles based on redesign PV array	132
7.9	(a) I-V and (b) P-V curve at ideal conditions	133
7.10(a)-(b)	I-V and P-V curves under PSC-1	134
7.11(a)-(b)	I-V and P-V curves under PSC-I	134
7.12(a)-(b)	I-V and P-V plots under shading scenario-I	136
7.13	Power at GMPP for (a) Simulation (b) Experimental analysis	137
7.14	FF for (a) MATLAB/Simulink study (b) Experimental study	138

7.15	PL for (a) MATLAB/Simulink study (b) Experimenatl study	139
7.16	ER analysis for (a) MATLAB/Simulink study (b) Experimental study	139
7.17	PE analysis for (a) MATLAB/Simulink study (b) Experimental study	140

LIST OF TABLES

Table No.	Title	Page No.
2.1	Taxomony of available literature	10
3.1	Parameters of commercially available PV module	35
3.2	Performance parameters of proposed investigation	47
4.1	Parameters of commercially available PV module	49
4.2	Performance Matrices for each configuration under shading pattern-1	62
4.3	Performance matrices for each topology under shading pattern-2	67
4.4	Performance parameters for configuration experiencing shading pattern-3	71
4.5	Performance matrices for shading pattern-4	76
4.6	Specifications and role of components used in the developed experimental setup	78
5.1	PV module specifications at 1000W/m^2, 25^{o}C	88
5.2	MATLAB/Simulink based quantitative analysis of PV array configurations under three PSCs	104
5.3	Experimental study based quantitative analysis of PV array configurations under three PSCs	105
6.1	Placement of integer number to design puzzle for PV array reconfiguration	115
6.2	The quantitative outcomes of PV systems under PSCs	120
7.1	Quantitative performance indices during MATLAB/Simulink study	135
7.2	Quantitative performance indices during experimental study	136

NOMENCLATURE

RE	Renewable Energy
PV	Photovoltaic
PSCs	Partial Shading Conditions
P-V	Power-Voltage
I-V	Current-Voltage
MPP	Multiple Power Points
LMPP	Local Maximum Power Point
GMP	Global Maximum Point
GMPP	Global Maximum Power Point
PL	Power Loss
PE	Power Enhancement
FF	Fill Factor
PG	Power Gain
PR	Performance Ratio
ER	Execution Ratio
SP	Series-Parallel,
HC	Honey-Comb
BL	Bridge-Link
TCT	Total-Cross-Tied
SP-TCT	Series-Parallel-Total-Cross-Tied
LS-TCT	Latin Square- Total-Cross-Tied
SDK	Su-Do-Ku
SPDK	Shape-Do-Ku
MS	Magic Square
SM-TCT	Symmetric Matrix-Total-Cross-Tied
V_{oc}	Open circuit voltage

I_{sc}	Short circuit current
V_C	Cell Voltage
A	Ideality Factor
T_C	Cell Temperature
e	Electron Charge.
I_{ph}	Photo Current
I_o	Saturation Current
R_{series}	Series Resistance
I_C	PV cell Current.

CHAPTER- 1

INTRODUCTION

The demand for energy across the globe has skyrocketed in the last few centuries. The rise in energy demand is primarily caused by two factors: (i) world's population growth and (ii) countries mainly developing countries leading towards techno-economic growth [Woytea *et al.*, 2003; Ola *et al.*, 2020]. Primary energy refers to the total amount of energy used from all sources. This includes fossil fuels like coal, gas, nuclear, oil and hydro as well as renewable options like solar. In 2021, as shown in Fig. 1.1, the world used a total of 595.15 exa-joules (EJ), or 595.15 × 1018 joules, of primary energy. It had grown from 492.53 EJ since 2008 and its growth rate of energy demand is noticed as 5.8 % in 2021 [Energy Information Administration, IEA, 2021].

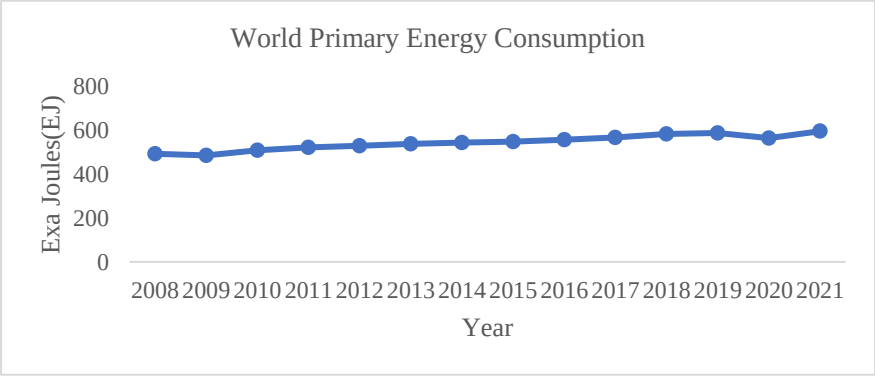

Fig. 1.1 Estimated Excess Primary Energy Use in Exajoules ($\times 10^{18}$ J)

The percentage of global energy demand met by primary sources is shown in Fig. 1.2. Primary energy requirement grew by 5.8 % in 2021, surpassing 2019 levels by 1.3 %. More than 8 EJ of RE was added to the grid between 2020 and 2021. As a whole, our use of fossil fuels hasn't changed. The percentage of primary

energy that came from fossil fuels was 82 % in 2018, down from 83 % in 2019 and 85 % in 2013 (when comparable data first became available). In 2021, the annual growth rate of renewable primary energy (including biofuels) was 15 %, stronger than the 9 % seen in the previous year and higher than that of any other fuel. This equates to an increase of about 5.1 EJ. Increases in solar and wind capacity of 226 GW in 2021 were nearly as high as the record 236 GW increase in 2020 [World Energy Outlook,2021].

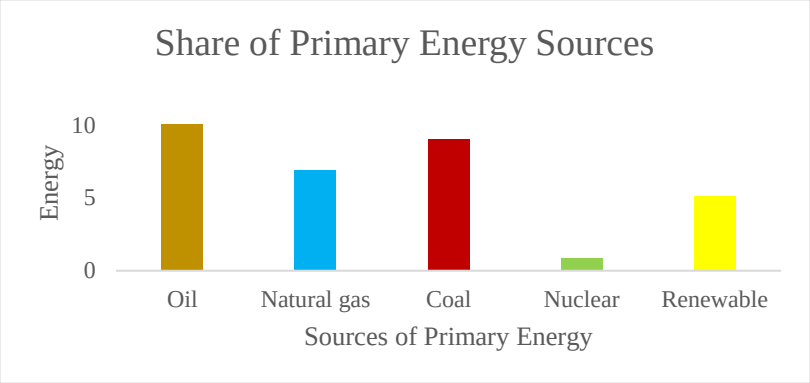

Fig. 1.2 Share of Primary Energy Consumption in 2021

Today, research into renewable energy (RE) based generation is expanding quickly due to concerns over environmental pollution and the depletion of fossil fuels [Manna *et al.*, 2014]. RE sources hold the key to solving the energy crisis. Solar radiation is the basis for solar collectors, PVs and thermal equipment. The technical and economic performance of these devices depends on how much sunlight is reaching at a particular location and time. At this point in time, the solar photovoltaic (PV) system is the authority with the greatest potential of renewable energy [Batzelis *et al*., 2015]. In order to provide power, solar modules, as opposed to individual solar cells, are established in situ. Several solar cells are needed to make up a PV module for solar power are combined with connections made in both series and parallel. The PV modules are suitably encapsulated so that they can

operate outdoors to a great extent and can be seen in Fig. 1.3, for quite some time.

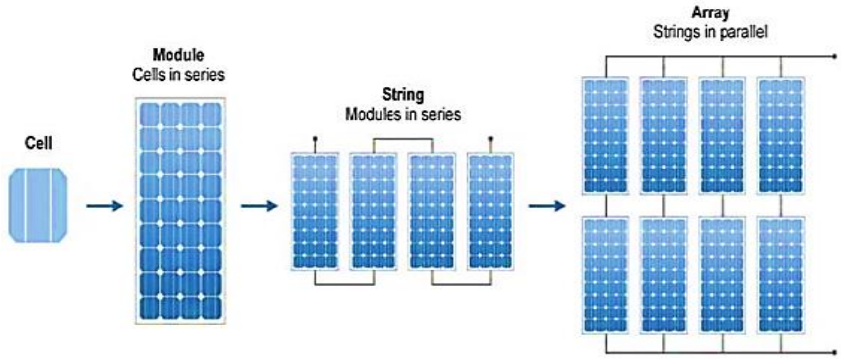

Fig. 1.3. Interconnections of solar cells to form modules turned into arrays [Manna *et al.*, 2014]

A greater amount of power can be generated by linking the cells in series and parallel using low power cells. Increasing the number of components in a series circuit increases both the output voltage and current when the components are connected in parallel. When cells are connected in series and parallel, it is generally presumed that all of the cells have the same characteristics, or that they are completely identical.

The following is generated voltage (0.6 V) and current (0.8 A) as observed through the I-V characteristics of these cells is presented in Fig. 1.4(a). The current through the series connection between two identical cells, is same as that through a single cell, and the V_{oc} of the two cells is added (see Fig. 1.4(b)). To create a serial connection between cells, the positive-negative terminal connected together. It's possible that two cells are linked in a parallel fashion when the I_{sc} from both of the cells is added together, but the combined cells have the same voltage as a single cell. Compared to a single cell, the current and voltage produced by a series (or parallel) connection of multiple cells is much higher. Fig.1.4(c) shows a parallel link between two series of cells in a schematic of a series connection. The

combination has a V_{oc} of 1.2 V and an I_{sc} of 1.6 A. In this manner, both voltage and current can be increased to the desired level.

The 36 cells in a module are connected in series, and their voltages are added to create the overall module output. Using the cells discussed in Fig. 1.4, a series combination of 36 cells will yield 21.6 V_{oc} and 0.8 I_{sc}. In solar PV array, where modules having identical electrical parameters linked in series and parallel, there is typically some variation, which can be significant or negligible.

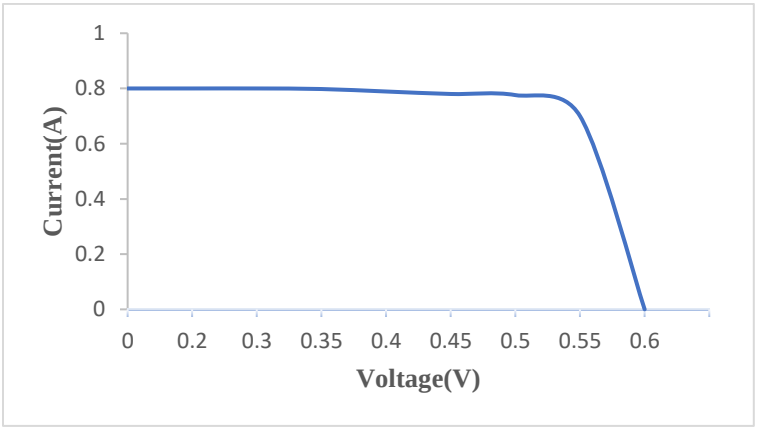

(a) An Individual Cell

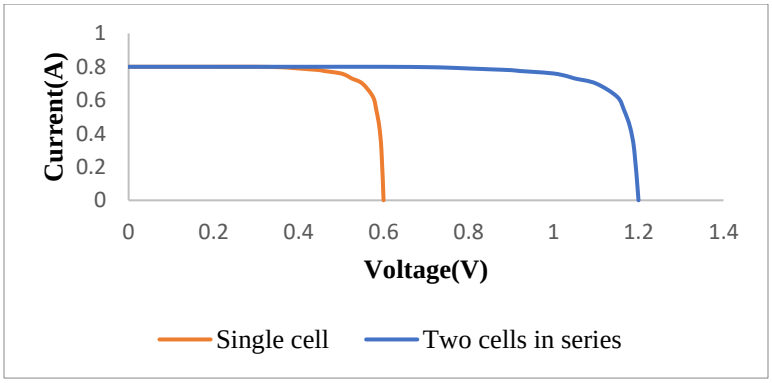

(b) Series connection between two cells

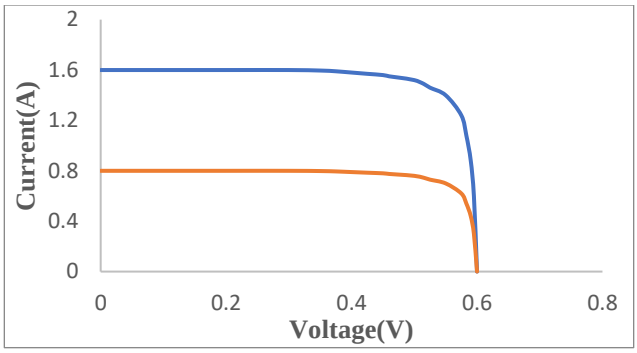

(c) Parallel connection between two cells

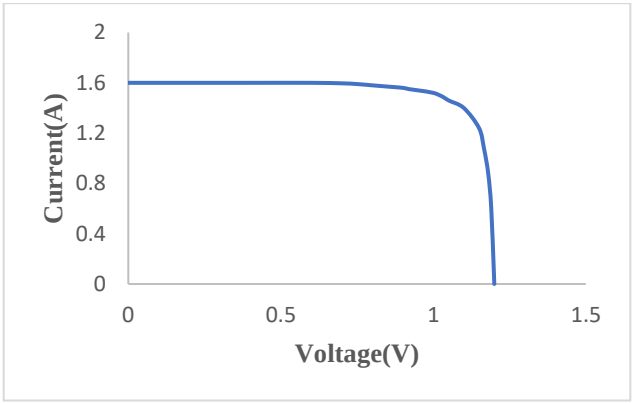

(d) Series and parallel combination of cells

Fig. 1.4 I-V characteristics of identical solar cells

Reasons for the discrepancies are:

- variations in processed cell
- modules or cells produced by different manufacturer with same rating
- harsh outside conditions i.e., partial shading
- Encapsulating material of cell is getting semi-transparent due to damage caused by UV light and
- Glass cover breaks etc.

These non-identical conditions give rise to loss of performance parameters

mainly output power.

1.1 OBJECTIVES

Our aim is to increase the PV array system's electrical power rating when it is shaded (Partially or fully). Shadowing has a major impact on the efficiency of the PV array. Additionally, PSCs are largely caused by architectural features, cloud cover, and tree cover. In this context, the existing literature reports numerous techniques for obtaining the maximum power.

Techniques introduced motivates us for obtaining optimized performance parameters includes: MPPT techniques, introducing by-pass diode in parallel to group of cells so that it is not affected by hotspots, methods for adaptive reconfiguration of PV arrays for power extraction, game puzzle based reconfigured array with fixed electrical connections etc. Here, we are using mathematical puzzle based reconfigured array for enhancing maximum output power and thus optimizing the performance parameters.

For analyzing the reconfigured array based on mathematical puzzle with conventional configurations firstly, we need to create a simulation model of the PV cell using the derived equations. Secondly, we need to simulate against different PS conditions in different module configurations, including the proposed rearrangement using their respective current-voltage (I-V) and power-voltage (P-V) characteristics curves. Thirdly, with the help of IoT-based data collection system (DAQ) we will collect the experimental data and compare it with simulated. Finally, realized that techniques responsible for shade dispersion and interconnections between PV modules, increase the performance of PV arrays in terms of accuracy, GMPP position, FF, minimum PL and PE in accordance with PSCs.

CHAPTER-2

LITERATURE REVIEW

2.1 INTRODUCTION

Renewably-sourced (RE) energy sources like solar, wind, tide, biofuel, and geothermal energy-based systems were developed in response to the world's energy crisis. Concerns over climate change and the finite supply of fossil fuels have boosted efforts to develop solar-assisted power plants. In recent years, solar photovoltaic (PV) technology has become widely adopted and is rapidly expanding around the world, from individual rooftops to massive multi-megawatt power plants. One enticing source of RE is solar energy [Woytea *et al.*, 2003; Ola *et al.*, 2020; Manna *et al.*, 2014; Batzelis *et al.*, 2015; Daliento *et al.*, 2016]. To be useful, a PV system must extract as much energy as possible given the lackluster PV cell efficiency [Ahmed and Salam, 2015; Jiang *et al.*, 2015; Tossa *et al.*, 2014]. Numerous PV array designs exist, each utilizing a unique combination of cells and modules wired in the more common series and parallel configurations to produce the required load power.

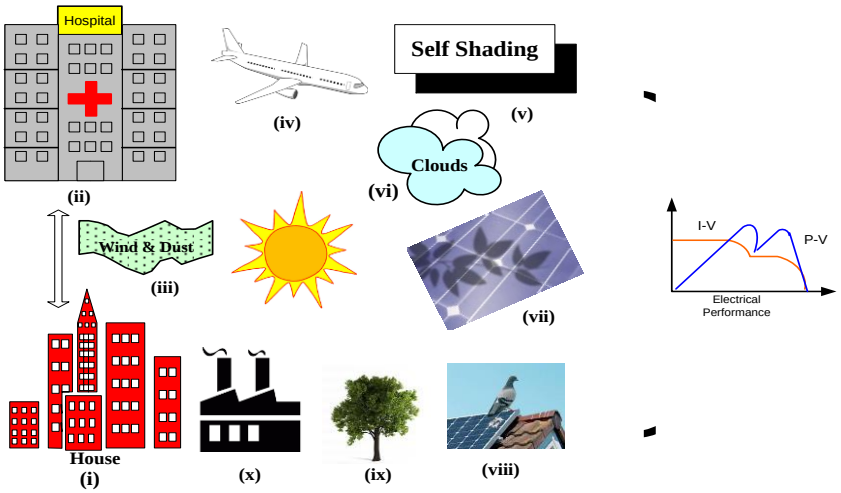

Fig. 2.1 The effects of shade on a PV system's P-V characteristics and their causes

Anywhere, from remote rural areas to urban neighborhoods, can benefit from having a PV system installed, frequently operate at non-uniform irradiation levels as a result of the characteristics of the surrounding barriers, necessitating the reduction of the installation land's size [Zheng *et al.*, 2014; Lorente *et al.*, 2014; Maki and Valkealahti *et al.*, 2014]. Due to the non-uniform solar irradiation levels, there exist multiple power maxima's i.e., GMPP and LMPP [Bishop *et al.*,1988; Blas *et al.*, 2002]. One of the most common causes of PSCs is the presence of static shading sources like trees, poles (especially telecom towers), tall buildings, bird poop, passing clouds (dynamic shade), etc. In order to investigate how PSCs influence PV array performance, the current research module closely follows the review analysis. Fig. 2.1 represents the causes of shading and its effects on the PV array with its P-V characteristics.

2.2 IMPACT OF SHADING ON ARRAY CONFIGURATION

In this study, several arrangements of PV array models performance in terms of accuracy, GMPP position, FF, minimum PL, PE, and the area of hardware implementation is evaluated and explored. The accuracy, robustness, execution ease, efficiency, simplicity, and applications are all examined in detail, highlighting both the advantages and disadvantages of each approach. The study subjects that pursue additional investigation are chosen and decided upon based on the body of literature that is currently available. A substantial number of research publications are taken into consideration for an exhaustive literature review. PV arrays can benefit from shade dispersion techniques and interconnections between PV modules, both of which are actively being studied in order to improve their performance under the PSCs. This is done in order to ensure that the review is as thorough as possible.

According to the author's best knowledge, Table 2.1 relevance of the categorize study is based on research articles that are currently available in literature. Fig. 2.2 shows the publication count on various arrangements as,

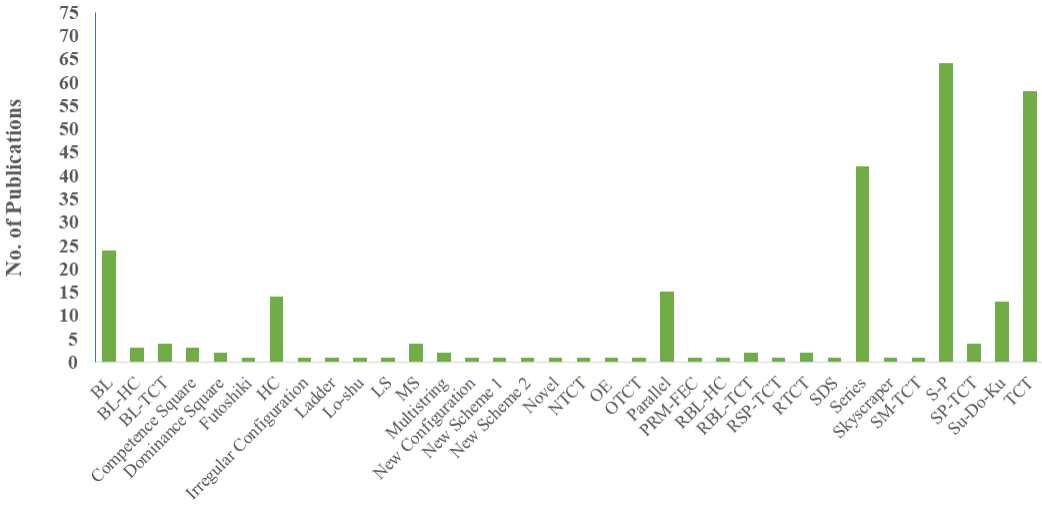

Fig. 2.2 Total number of articles published on various configurations between 2008-22

Performance factors considered in the present study include PV array design, partial shading, irradiance analysis, and power output.

Table 2.1-Taxomony of available literature

Authors, [Year]	Array Configurations	Best PV array	Array Size	Irradiation Level (W/m^2)	Shading Scenario	Output Power (W)
Patel and Agarwal, [2008]	SP	SP	30×10	500-1000	Passing clouds	1500
Patel and Agarwal, [2008]	SP	SP	10×90	500-1000	Passing clouds	230000
Silvestre and Chouder, [2008]	S	S	Small	300- 1000	Simulation	35.31
Dio *et al.*, [2009]	S, P, SP	SP	Small	500-800	Shaded Serially	28
Gao and Dougal, [2009]	S, P	P	20×4, 3×27	200-900	Shading due to tree	1.19
Quesada *et al.*, [2009]	S, SP	SP	72 series and 36 parallel cells	100-500	Simulation	230
Silvestre *et al.*, [2009]	S, SP	SP	36 PV cells	500-1000	Simulation	208.07
Bellini *et al.*, [2010]	S	S	4 PV modules	100-1000	Simulation	1760
Chowdhury and Saha, [2010]	S, P	P	Small	500-1000	Simulation	195
Piazza and Vitale, [2010]	Multistring, SP	Multistring, SP	Small	250- 750	Natural and artificial	205
Moreno *et al.*, [2010]	S, SP	SP	8 PV modules	100-1000	Simulation	125
Picault. *et al.*, [2010]	SP, T-C-T, BL	TCT	Medium	631-651	Simulation	1039
Tsai, [2010]	SP	SP	Mini	500-980	Simulation	60

Table 2.1 Continue……..

Authors, [Year]	Array Configurations	Best PV array	Array Size	Irradiation Level (W/m^2)	Shading Scenarios	Output Power (W)
Wang and Hsu, [2010]	S	S	Small	160-960	Simulation	80
El.-Dein *et al.*, [2011]	S-P, TCT	T-C-T	6x4	250-1000	Simulation	1528
Ishaque *et al.*, [2011]	SP	SP	20×3	200-1000	Simulation	1200
Maki *et al.*, [2012]	S	S	18×3	175-1000	Simulation	1350
Moballegh, and Jiang, [2011]	S	S	96 PV cells	130-992	Simulation	171.5
Patnaik *et al.*, [2011]	SP	SP	3×3, 4×4	250- 1000	Simulation	1.4 ,1.7 and 2.25
Renaudineau, *et al.*, [2011]	SP	SP	3×2	500-1000	Simulation	550
Santos *et al.*, [2011]	SP	SP	3×2	500-1000	Artificial	58
Li, *et al.*, [2011]	Multistring, SP, P	SP	4- 8 PV modules	NA	Artificial	10000
Wang, and Lin, [2012]	SP, TCT	TCT	36 PV modules	500-1000	Simulation	1256
Kadri, *et al.*, [2012]	S, P	NA	3 PV modules	400-1000	Artificial	180
Alahmad, *et al.*, [2012]	SP	SP	3×3	NA	Simulation and Artificial	3.7
Ding *et al.*, [2012]	S, P	P	3×2	220 -890	Simulation and Artificial	93.6

Table 2.1 Continue……..

Authors, [Year]	Array Configurations	Best PV array	Array Size	Irradiation Level (W/m^2)	Shading Scenarios	Output Power (W)
Dorado *et al.*, [2010]	S	S	36 PV cells	NA	Simulation	1164
Maki and Valkealahti, [2012]	S, P	P	18 PV modules	132- 729	Simulation	2350
Moschitta *et al.*, [2012]	S	S	20 PV modules	NA	Simulation	4900
Ramaprabha et al, [2012]	S, P, HC, TCT, BL, SP	TCT	2×6, 6×2, 3×4, 2×4, 4×2, 4×3, 3×3, 4×4,6×4, 4×6	325-1000	Simulation	676.8
Salam and Ramli, [2012]	SP	SP	4 PV modules	400-1000	Simulation	135.54
Villa, *et al.*, [2012]	SP, BL, HC, and TCT	TCT	3×3, 5×3	200-1000	Simulation	1000
Zhang *et al.*, [2012]	SP	SP	6×3	100-1000	Simulation	1000
Ziar *et al.*, [2012]	S	S	2 PV modules	150-300	NA	0.070
Alajmi *et al.*, [2013]	SP	SP	3×3	300-1000	Simulation	150
Bastidas *et al.*, [2013]	SP	SP	2×2	500-1000	Manually	689
Reinoso, *et al.*, [2013]	Conf 1-2 and 3	Conf. 1	9 PV module	75-525	Simulation	1100
El-Dein, *et al.*, [2013]	TCT, Half R-PVA, Full R-PVA	FRPVA	6×4	500-1000	Simulation	1834, 1630, 1786
Huynh *et al.*, [2013]	SP	SP	4×3	100-1000	Simulation	150
Jung, *et al.*, [2013]	SP	SP	6×5	500-1000	Simulation and artificial	144

Table 2.1 Continue……..

Authors, [Year]	Array Configurations	Best PV array	Array Size	Irradiation Level (W/m^2)	Shading Scenarios	Output Power (W)
Kouchaki *et al.*, [2013]	SP	SP	6×6	535-1000	Simulation and artificial	1355
Lu *et al.*, [2013]	S	S	72 PV modules	0-1000	Simulation	300
Nezhad *et al.*, [2013]	S	S	4 PV modules	250- 1000	Simulation	800
Ramos-Paza *et al.*, [2013]	SP, TCT	TCT	2×2 PV modules	322-560	Simulation and artificial	140
Pareek *et al.*, [2013]	S	S	2 PV modules	200-1000	Simulation	375
Rani, *et al.*, [2013]	TCT, SDK	SDK	9×9	200-900	Simulation	4532
Rodrigo, *et al.*, [2013]	S	S	24 PV modules	771-1000	Simulation	1100
Seyedmahmoudian *et al.*, [2013]	S	S	25 PV modules	400-1000	Simulation	350
Tian, *et al.*, [2013]	S, P, and SP	SP	4 modules	750-1160	Simulation	954.88
Batzelis *et al.*, [2014]	S	S	46 modules	200-1000	Simulation	1000
Bauwens *et al.*, [2014]	S	S	45 PV cells	NA	Simulation and artificial	43.16
Dorado *et al.*, [2014]	S, P	P	6×9	100-1000	Outdoor shading	2300
Fialho *et al.*, [2014]	S	S	2 PV module	700- 1000	Simulation	150
Parlak, [2014]	S	S	3 PV modules	300-1000	Simulation	165
Lun *et al.*, [2014]	SP, BL	BL	2×6	100- 1000	Artificial	173.9445
Ma *et al.*, [2014]	S	S	4 PV module	235-870	Natural shading	130.72
Moballegh and Jiang, [2014]	SP, TCT, and BL	TCT	2×4	279-992	Artificial shading	678.40

Table 2.1 Continue……..

Authors, [Year]	Array Configurations	Best PV array	Array Size	Irradiation Level (W/m^2)	Shading Scenarios	Output Power (W)
Pareek and Dahiya, [2014]	SP, TCT, and BL	TCT	4×4	200-1000	Simulation	2860
Qi *et al.*, [2014]	SP	SP	3×3	100-1000	Artificial	40
Ramaprabha, [2014]	SP, TCT, BL, and HC	TCT	2×6, 6×2, 2×4, 4×2, 3×4, 4×3, 3×3, 4×4,4×6, 6×4	200-1000	Simulation	234.57
Shirzadi *et al.*, [2014]	SP	SP	3×6, 4×10, 5×13,5×18	253-512	Simulation	3767
Storey, *et al.*, [2014]	SP, and TCT	TCT	2×6, 3×3	100-1100	Simulation	1340
Vijayalekshmy *et al.*, [2014]	S, P	P	10×3	0-1000	Simulation	290.5
Wang *et al.*, [2014]	S, P	P	4×4	500-1000	Simulation and Artificial	16.28
Bai *et al.*, [2015]	S	S	60 PV cells	733.1-751.1	Simulation	90
Belhachat, and Larbes [2015]	S, P, SP, TCT, BL, & HC	TCT	24 PV modules	300-1000	Simulation	1446
Celik, *et al.*, [2015]	SP, and TCT	TCT	2×2, 6×8, 8×3	100-1000	Simulation	2724

Table 2.1 Continue……..

Authors, [Year]	Array Configurations	Best PV array	Array Size	Irradiation Level (W/m^2)	Shading Scenarios	Output Power (W)
Deshkar, *et al.*,2015	TCT, SDK, and GA	GA	9×9	4802	Simulation	4802 W
Fathy, [2015]	S	S	3 PV module	200-1000	Simulation	480
Grisales, *et al.*, [2015]	SP, TCT, BL, & Irregular	Irregular	3×3	NA	Simulation	353
Malathy, and Ramaprabha, [2015]	TCT, Novel	Novel	3×3, 6×4	200-1000	Simulation	708. 57
Malathy, and Ramaprabha, [2015]	S, P, SP, TCT, BL, HC, novel	Novel	2×18, 3×12, 4×9, 12×3, 18×2, 6×6, 9×4	300-1000	Simulation	981.3
Potnuru, *et al.*, [2015]	TCT, SDK	Su-do-Ku	9×9	100-1000	Simulation	5554
Rao, *et al.*, [2015]	TCT, SDK, and I-SDK	I-SDK	9×9	200-900	Simulation	5168
Shankar, and Mukherjee, [2015]	SP	SP	10×100	500-1000	Simulation	40500
Sundareswaram *et al.*, [2015]	S, SP	SP	2×3	100-1000	Natural and Simulation	38.06
Vicente *et al.*, [2015]	SP	SP	2×2, 2×3	100-1000	Artificial	40
Vijayalekshmy, *et al.*, [2015].	SDK, HC, BL, TCT	SDK	6×6	200-1000	Artificial	1250

Table 2.1 Continue……..

Authors, [Year]	Array Configurations	Best PV array	Array Size	Irradiation Level (W/m^2)	Shading Scenarios	Output Power (W)
Vijayalekshmy. *et al.*, [2015]	TCT, RTCT	RTCT	6×6	200-1000	Simulation	1160
Xueye and Tianlong, [2015]	S, P, SP	SP	30 PV modules	400-1000	Simulation	5000
Yadav *et al.*, [2015]	SP-TCT, SDK, TCT	SDK	4×4	350-1000	Simulation	2278
Boukenoui, [2016]	S, SP	SP	2×4	100-980	Simulation	225
Braun, *et al.*, [2016]	SP, BL, TCT, BR	TCT	12×4	100-1000	Simulation	180
Forcan *et al.*, [2016]	S, SP	SP	3 PV modules	800- 1200	Simulation	375
Kumar *et al.*, [2016]	SP, TCT	TCT	4×4 PV cells	360- 500	Artificial	8
Mohammadnejad *et al.*, [2016]	SP, BL, TCT, & HC	TCT	4×4, 6×4	200-1000	Simulation	1123
Yadav *et al.*, [2016]	SP	SP	4×4 PV cells	360- 500	Artificial	8
Ram, and Rajasekar, [2016]	S, SP	SP	2×4	100-1000	Artificial	119.7
Rakesh, and Madhavaram, [2016]	TCT, MS	MS	4×4	200- 900	Artificial	960
Sahu, and Nayak, [2016]	TCT, PRMFEC	PRM-FEC	7×5	195-940	Natural	73.55
Sahu, *et al.*, [2016]	TCT, Futoshiki	Futoshiki	4×4, 5×5	220-950	Artificial	64.87

Table 2.1 Continue……

Authors, [Year]	Array Configurations	Best PV array	Array Size	Irradiation Level (W/m^2)	Shading Scenarios	Output Power (W)
Samikannu, *et al.*, [2016]	SP, TCT, BL, & MS	MS	3×3, 3×5, 4×8, 6×6	200-900	Artificial	2.8849
Pareek, and Dahiya, [2016]	TCT, Half-RPVA, Full-RPVA	FRPVA	6×4	500- 1000	Simulation	4354. 3
Vijaylekshmy, *et al.*, [2016]	TCT, OTCT, NTCT	NTCT	4×3	500-1000	Simulation	567
Yadav, *et al.*, [2016]	NS-1 &2, BL, HC, SP, TCT, BL-TCT, SP-TCT	NS-1, NS-2	5×4, 9×4	350 -1000	Simulation	2733
Ahmad, *et al.*, [2017]	SP	SP	4×4, 5×5	100-1000	Simulation	300
Yadav, *et al.*, [2017]	TCT, RTCT, RSP-TCT, BL-HC, MS, SP-TCT, RBL-TCT, RBL-HC	MS	4×4	350 -1000	Simulation	2733
Tabish and Asharaf, [2017]	S	S	Single PV module	500-950	Artificial	28
Bana. and Saini., [2017]	Novel, SP, TCT, BL, and HC	Novel	4×5	100-980	Experimental	1290
Belhaouas *et al.*, [2017]	SP, TCT, and S-M-TCT	S-M-TCT	3×3, 2×2	200-900	Artificial	540
Bosco and Mabel, [2017]	SP, SP-SDK, SP-CDV, TCT, TCT-SDK, and TCT-CDV	SPCDV, TCTCDV	9×9	200-1000	Artificial	7083

Table 2.1 Continue……..

Authors, [Year]	Array Configurations	Best PV array	Array Size	Irradiation Level (W/m^2)	Shading Scenarios	Output Power (W)
Pareek and Dahiya, [2017]	SP, TCT, Proposed	Proposed	2×2, 2×3	200-1000	Simulation	4419
Satpathy., *et al.*, [2017]	SDS, SP, BL, and TCT	SDS	3×3, 7×7	400-1000	Experimental	1746
Vengatesh and Rajan, [2017]	S, SP	SP	3 PV modules	800-1000	Simulation	581
Mishra *et al.*, [2017]	TCT, BL-TCT, BL-HC, SP-TCT, NS	NS	6×4	350-1000	Simulation	3419
Malathy and Ramaprabha, [2018]	TCT, MS	MS	5×5	500-1000	Experimental	300
Rodriguez., *et al.*, [2018].	HC, BL, SP, and TCT	TCT	3×3	70- 960	Experimental	400
Pachauri *et al.*, [2018]	TCT, and LS-TCT	LS-TCT	4×4	350, 1000	Simulation	2609
Pillai *et al.*, [2018]	TCT, DS	DS	9×9	200-900	Simulation	8000
Pachauri *et al.*, [2019]	SP, and TCT	TCT	3×3	380-710	Experimental	30
Krishna and Moger, [2019]	SDK and I-SDK, TCT, SP, BL, & HC	I-SDK	9×9	100-1000	Simulation	2280
Nasiruddin, *et al.*, [2019]	SP, TCT, BL, OE	OE	4×4	300, 600,1000	Simulation and Experimental	2512
Nihanth, *et al.*, [2019]	TCT, BS, Su-Do-Ku, Skyscraper	Skyscraper	9×9, 5×5	200-800	Simulation and Experimental	5658
Haq. *et al.*, [2020]	SP, BL, HC, TCT, RM	RM	6×6	400-1000	Simulation	9000

Table 2.1 Continue……..

Authors, [Year]	Array Configurations	Best PV array	Array Size	Irradiation Level (W/m^2)	Shading Scenarios	Output Power (W)
Fathy, [2020]	GWO, SP-TCT, NS, SP, TCT, & BOA	BOA	6×6	350-1000	Simulation	3766
Yousri. *et al.*, [2020]	MHHO, TCT, CS, PSO, & GA	MHHO	9×9	300-900	Simulation	3045
Premkumar. *et al.*, [2020]	SP, TCT, HC, BL, Ladder, BL-HC, BL-TCT, and SP-TCT	Ladder	4×4	300-1000	Simulation	3200
Sagar. *et al.*, [2020]	SRBL-TCT, SP, HC, BL, & BL-TCT,	SRBL-TCT	6×6	200-1000	Simulation and Experimental	8118
Srinivasan. *et al.*, [2020]	TCT, SDK	SDK	4×4	200-950	Experimental	140
Venkatiswari. and Rajasekar., [2020]	TCT, SDK, DS, CS, and Lo-Shu	Lo-Shu	9×9	300-900	Simulation	5601
Gul *et al.*, [2020]	SP, HC, and TCT	TCT	6×6	400, 500,1000	Simulation	5500
Chao. *et al.*, [2015]	SP, and TCT	TCT	4×3	700, 1000	Simulation	260
Penaranda. *et al.*, [2015]	SP, and GA	GA	3×3	400, 700, 1000	Simulation	230
Babu. *et al.*, [2020]	TCT, CS, FRA, GA, RAO, & SMO	FRA	9×9	200-900	Simulation	2731.10
Fathy., [2018]	GOA, TCT, SDK, & GA	GOA	9×9	200-900	Simulation	5042
Babu. *et al.*, [2018]	PSO, TCT, SDK, & GA	PSO	9×9	200-900	Simulation	5530

2.2.1 PV array: Conventional configurations

This is an especially difficult task for academic researchers to investigate ways that are both more efficient and more environmentally friendly in order to maximize the operation efficiency of PV devices. The best alternatives mean changing PV module placements to create a different PV array topology. Furthermore, a comprehensive review of current research is conducted for several PV array topologies currently in use, and the results are shown in Fig. 2.3(a)-(d).

(a) ***Series Configuration***

As the irradiation levels rise from 300 W/m^2 to 800 W/m^2, data shows that the PL has shot up from 8 % to 50 %, which is a substantial improvement. The shading effects on PV module outcomes was investigated [Gao and Dougal, 2009], and resulting from the tests, it was established that the output power of PV modules decreased. Two different layouts (S and P) were compared with see-through and opaque lighting. The use of parallel connection with translucent shading brought about an abrupt increase in GMPP, which went from 5 % to 50 % at irradiation levels of 97.8 % and 72.4 %, respectively. On the other hand, GMPP can be found at a rate of 5 % when exposed to 86.8 % irradiation and 50 % when exposed to 41.9 % irradiation when using the series connection. According to them [Bellini *et al.*,2010], the GMPP is 1760 W for optimal conditions and 1610 W for shaded conditions, respectively, with an increase in PL of 8.5 %. [Maki *et al.*,2012] provides a description of an examination of PV panel performance under various sorts of shadowing patterns. In a 50 % shaded and 70 % shaded environment, the GMPP value of 18 modules wired in series is calculated to be 1375 W. The authors have considered eight distinct shading scenarios, with radiation intensities ranging from 130 to 992 W/m^2 in [Moballegh and Jiang, 2011]. The calculated GMPP values are 171.5 W at 992 W/m^2 and 58 W at 279 W/m^2.

In [Ding *et al.*, 2012], two sets of three PV modules are connected in series for this experiment and simulation study, and irradiance values from 220 to 890 W/m^2 are tested. It has been shown that using a boost topology can reduce the GMPP error by as much as 0.56 %. Thirty PV modules in series were taken into account by the authors of [Dorado *et al.*,2010] for various shading scenarios. The efficiency of a PV array is measured in relation to its bypass diode's physical position. The experimental results demonstrate that the shadow losses are influenced by the PV module's bypass diode arrangement. According to the experimental data, the GMPP has the best deal of 70 mW. The study analyzes the SP configuration of 72 PV cells in [Lu *et al.*, 2013]. The simulation results show that under non-uniform irradiance, the SP configuration has the lowest PL and can generate up to 300 W of output power. The authors analyzed data from four solar panels wired in series and powered by PSCs in [Nezhad *et al.*, 2013]. The MPP is 800 W at 1000 W/m^2, and 230 W at 250 W/m^2.

In this experiment, by connecting two PV modules in series, we can analyze the impact of variables like series resistance, solar radiation, parallel resistance and temperature on the P-V and I-V curves in [Pareek *et al.*, 2013]. Moreover, a comparable investigation is also conducted in [Rodrigo *et al.*, 2013] made up of 24 individual PV modules, each producing 1.1 kW when connected in series and requiring a minimum of 771 W of solar radiation per square meter. It took 25 PV to power the experimentation necessary to assess performance of modules connected in series using PSCs in [Seyedmahmoudian *et al.*, 2013]. However, in a different study [Batzelis *et al.*, 2014], Hardware and software were evaluated for similarities and differences between systems that included and did not include bypass diodes in series with photovoltaic modules. While only the bypass diode was used by the authors of [Bauwens *et al.*, 2014] to lessen the impact of shade on PV panels. In a related experimental and modelling investigation, the authors [Bai

et al., 2015; Fathy, 2015] keep 60 photovoltaic cells at a minimum of three different densities of shading: 25 %, 50 %, and 75 %. Additionally, the practical outcomes used to verify the outcomes for each PSCs.

(b) ***Parallel Configuration***

The authors created a parallel PV system MATLAB/Simulink model in [Gao and Dougal, 2009; Chowdhury and Saha, 2010]. Under different PSCs and irradiance intensities of 200 W/m^2, 500 W/m^2 and 900 W/m^2, the maximum voltage, current, and GMPP of 3×27, 20×4 sizes of PV arrays are analyzed. The effects of shading are investigated in real-world settings to ensure accuracy of the findings. The authors of a study [Tsai, 2010] conducted an experiment in which they installed a real-time PV cell setup in a laboratory under controlled conditions, ranging from 31-34 °C with an irradiance of 500-980 W/m^2. We connected 60 W of PV modules in series and parallel to test how shade affects electrical performance. We look into how the shading design impacts the system's functionality in [Li *et al*., 2011] and [Kadri *et al*., 2012] using a developed Simulink model. The PV modules are typically set up in three, four, or eight-module groups to arrange conventional configurations (SP, parallel, and multi-string). The SP configuration yields the highest GMPP value.

There are four PV modules connected in series, parallel and SP configurations in [Tian *et al*., 2013] to test the system's performance under different shading conditions. Maximum GMPP was found to be 954.88 W at irradiation levels between 750 and 1160 W/m^2. In [Dorado *et al*., 2014], we use a real-world 69 PV array to evaluate the differences in shading between the series and parallel configurations for irradiance levels between 100 W/m^2 and 1000 W/m^2. As can be seen from the results of the experiments, the GMPP is highest when the PV modules

are set up in a parallel arrangement. Electrical performance of PV modules, as measured by GMPP and FF, is maximized when they are connected in parallel, according to the authors of [Vijayalekshmy *et al*., 2014]. There are three distinct shading styles under consideration: type A, B, and C. All three designs have different optimal GMPP values (290.5 W, 214.3 W, and 114.3 W).

(c) ***SP, TCT, BL and HC Configurations***

To evaluate PV modules of varying sizes efficiency, the author suggests running simulations in Simulink, including those with capacities of 158 W, 65 W and 28 W. These metrics are then compared to the maximum power that can be generated, not only the output voltage but also the output current. The simulation results demonstrate that a TCT arrangement with a 158 W GMPP performs well [Dio *et al.*, 2009]. In a study conducted [Quesada *et al.*, 2009], PV panel performance is analyzed in two different configurations, series and series-parallel, for a 9×9 array. At irradiance levels between 100 and 500 W/m^2, the SP configuration's 230 W GMPP value is found to be optimal. Scientists have analyzed the performance of 36 PV cells in both series and SP configurations when exposed to 500 W/m^2 and 1000 W/m^2 of light in [Silvestre *et al.*, 2009]. According to the results of the experiments, the SP configuration offers the highest maximum values of current (7.25 A) and voltage (28.7 V). Author developed a multi-string (SP) arrangement, and found that 205W is the optimal value of GMPP for irradiance levels between 250 and 750 W/m^2. Furthermore, hardware and simulation model-based experimental results are presented in [Moreno *et al.*, 2010; Patnaik *et al.*, 2011], and they illustrate that the finest value of GMPP for array sizes of 4×4 and 3×3 PV modules in SP configuration is 125 W. The authors in [Wang and Lin, 2012] designed a 9×4 PV array using SP and TCT topologies for 500 W/m^2 to 1000 W/m^2 of solar irradiance. At GMPP, the P-V characterization for a TCT

configuration is at its minimum PL and maximum voltage and power (1256 W).

In [Alajmi *et al.*, 2013], five different shading scenarios are considered, each utilizing an SP configuration for a 3×3 PV array, and the optimal values of GMPP are found to be 105 W and 65 W respectively, for cases 5 and 3. In [Bastidas *et al.*, 2013], an SP structure is used for a 2×2 PV array and under both irradiance levels (500 and 1000 W/m^2), the optimal GMPP value is found to be 689 W. Authors in [El-Dein *et al.*, 2013; Pareek and Dahiya, 2016] describes four different shading patterns, including oblique, quarter array, single row and double row shading modelled in MATLAB/Simulink for the total of three different configurations possible, including the TCT, full Reconfigured PVA, and half reconfigured PVA. Maximum GMPP is achieved under all four shading conditions with the FRPVA configuration at both the 500 W/m^2 and 1000 W/m^2 irradiation levels. In [Pachauri *et al.*, 2019], The efficiency of a 3×3 photovoltaic system was evaluated under occluded irradiance conditions, such as 380-710 W/m^2. The voltage and power at GMPP, FF and PL can be increased by making the change from SP to TCT configuration at these points with the help of a networked embedded system that regulates an electromechanical relay system from a remote location. Research was conducted on PV systems using SP, BL, HC and TCT configurations for flaws caused by 400-1000 W/m^2 of uneven irradiation (RM). Additionally, the effects of multiple PV array failures under consistent irradiance are examined and their cumulative impact on the various PV connections is analyzed in detail [Haq *et al.*, 2020; Gul *et al.*, 2020].

It is recommended that a PV module with shaded cells in SP arrangement be mathematically modelled for MPP tracking under circumstances of constant solar irradiance of 4×3, 6×5, and 6×6 sizes in [Huynh, *et al*, 2013; Jung *et al*, 2013; Kouchaki *et al*, 2013]. Furthermore, an experimental analysis has confirmed the

accuracy of the simulation results. The authors ran a simulation of a PV system (2×2) in both the SP and TCT configurations in [Ramoz-Paza *et al.*, 2013]. At an irradiation intensity of 332.63-560.60 W/m^2, the TCT arrangement is centered to have maximum voltage and power, 140 W GMPP; this is determined by analyzing the system's performance while shadowing is present. In [Qi *et al.*, 2014], at irradiance levels between 100 and 1000 W/m^2, the GMPP of a system of 3×3 PV modules interconnected in an SP configuration is 40 W. The authors examined the performance of PV array topologies with dimensions ranging from 4×2, 2×4, 6×2, 2×6, 4×3, 3×4, 3×3, 4×4, and 6×4 sizes under 100–1000 W/m^2 irradiances [Ramaprabha, 2014; Storey *et al.*, 2014]. Compared to other PV array arrangements, The TCT has the highest voltage and current in the vast majority of shadowing environments. In [Belhachat and Larbes, 2015], comprehensive investigation of 24 PV modules (6×4) with shaded S, P, SP, TCT, BL, and HC configurations is conducted in order to evaluate performance in terms of maximum power, voltage, and enhanced FF. At an irradiance level of 300-1000 W/m^2, the optimal GMPP value (1446 W) is found for TCT configuration. [Celik *et al.*, 2015] presents a Simulink modeling of different PV system topologies, including conventional 2×2, 6×8, and 8×3 sizes of S, P, SP, TCT, BL, and HC. The TCT configuration's highest power production (2724 W GMPP) under predefined shading circumstances is compared to other configurations at varying irradiance levels between 100 and 1000 W/m^2 is determined.

In [Shankar and Mukherjee, 2015], simulation study for SP configuration, the optimal GMPP value for a 10×100 PV array is determined to be 40.5 kW. Likewise, laboratory-based experimental and simulation work for S and SP configurations is reported in [Sundareswaram *et al.*, 2015]. Whereas, depending on the environment, SP arrangement outperforms with a GMPP of 38.06W at irradiance intensities between 100 and 1000 W/m^2. There are three configurations

S, P, and SP are used in [Xueye and Tianlong, 2015] with irradiation intensities ranging from 400–600–1000 W/m^2.There are thirty PV modules of various sizes and configurations. In an experimental and simulation study, the dimensions of a 2×4 PV array are considered for two configurations, S and SP, at irradiance levels ranging from 100 to 980 W/m^2. The SP configuration has the optimum performance when the GMPP is raised to 225 W [Boukenoui *et al.*, 2016]. These configurations are SP, BL, TCT, bypass and reconfiguration (BR) topology. [Forcan *et al.*, 2016] presents simulation work for S and P topologies, demonstrating that parallel systems with GMPPs of 375 W and irradiance levels between 800 and 1200 W/m^2 functioned well. The experimental work for a single PV module comprised of 16 cells as discussed in [Kumar *et al.*,2016; Yadav *et al.*, 2016] for configurations namely S, P, and TCT. The TCT configuration with a 3×3 PV array size and 400 W GMPP has proven to be the most efficient. TCT provides superior performance to other configurations under all shading conditions.

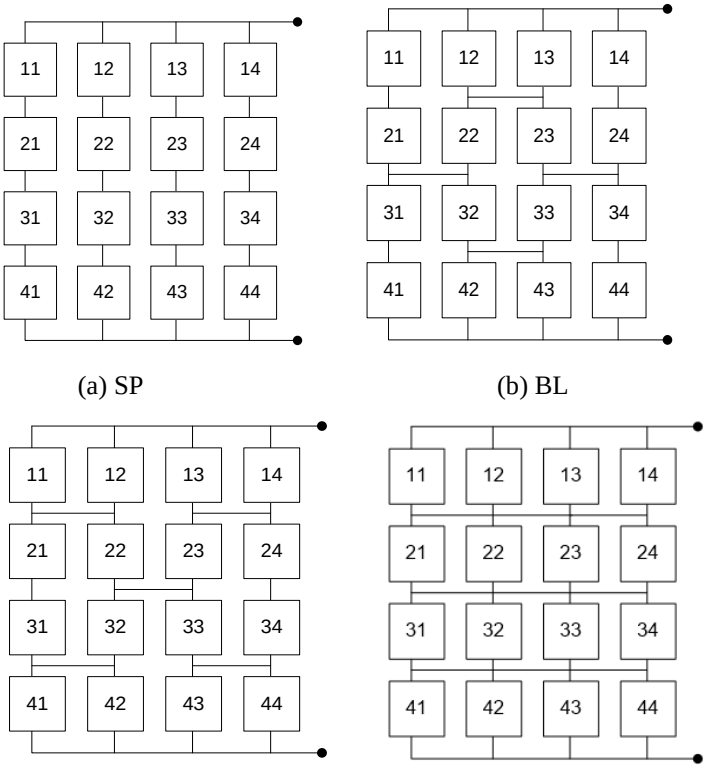

(a) SP (b) BL

(c) HC (d) TCT

Fig.2.3(a)-(d) Conventional array configuration

For SP, TCT, HC, and BL as shown in Fig. 2.3, simulation and experimental studies are provided in [Rodriguez *et al.*, 2018].

2.2.2 Hybrid PV Array Configurations

(a) ***SP-TCT, BL-TCT AND BL-HC PV Array Configuration***

Various studies have developed hybrid setups with the sizes of 4×4, 5×4, and 6×4 to evaluate and performance improvisation. Hybrid configurations are developed through the conventional configurations such as SP, BL, HC, and TCT. The authors perform a simulation study for three configuration types, comprising hybrid topologies (SP, SP-TCT, and SDK), for 4×4 PV array sizes with irradiance conditions between 350 and 1000 W/m^2, and find that the SDK arrangement is the most efficient, with a GMPP value of 2278 W [Yadav *et al.*, 2015]. Additionally, a MATLAB-based Simulink model is created in a later research investigation [Yadav *et al.*, 2016] Simulation of the SP, TCT, BL, HC, BL-TCT, SP-TCT, and noble structure (NS-1, NS-2) configurations. The optimal performance for PV module array sizes 5×4 and 9×4 with GMPP is 2733 W at 350–1000 W/m^2 irradiation is shown by the results for the NS-1 configuration. [Yadav *et al.*, 2017] Using TCT, RTCT, RSP-TCT, S-P, T-C-T, RBL-TCT, BL-HC, and MS are all developed in Simulink tool. The MS configuration with a GMPP of 2733 W was found to be the most efficient. Simulink model is proposed for a 6×4 size PV system in a later study [Mishra *et al.*, 2017] under 350 W/m^2, 500 W/m^2, 800 W/m^2, and 1000 W/m^2 of radiation to investigate the TCT and hybrid (SP-TCT, BL-TCT, and BL-HC), and NS puzzle layouts. While modelling a PV array configuration of the same size, it is determined through experimental analysis that there are less ties than in the TCT setup as shown in Fig.2.4(a)-(c).

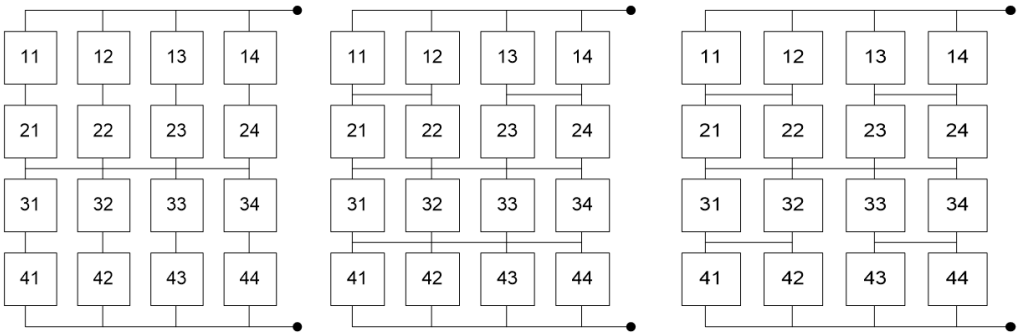

(a) SP-TCT (b) BL-HC (c) BL-TCT

Fig. 2.4(a)-(c) Hybrid PV array configuration

2.2.3 Modified PV Array Configurations

(a) ***RTCT, RSP-TCT, RBL-TCT, RBL-HC and S-M-TCT***

A hardware-based, PV arrays (6×6 size) are assessed to measure the power generated and the amount of current flowing through the system configurations for TCT and RTCT (TCT rearranged using the Su-Do-Ku puzzle) [Vijaylekshmy *et al.*, 2016]. At an irradiance of 200-1000 W/m^2, it is shown that the RTCT arrangement with a GMPP of 1160 W yields the best performance metrics. The authors of [Yadav *et al.*, 2017] reconfigured a standard 4×4 PV array into four distinct configurations—SDK based Reconfigured TCT, and hybrid (SP-TCT, and BL-TCT, and BL-HC) to assess the effect on electrical output. Then, the SDK puzzle is applied to reorganize these unique hybrid forms. The RSP-TCT configuration outperformed alternate configurations with regard to shading. A hardware-based model was developed for 3×3 and 2×2 PV array module sizes, the authors of [Belhaouas *et al.*, 2017] compared and contrasted conventional TCT and hybrid TCT (S-M-TCT arrangement: shifting the physical placement of PV modules while keeping their electrical connections the same). In terms of FF and PL, S-M-TCT has been shown to outperform traditional TCT configurations in experiments, with GMPP reaching an exquisite 540 W across a wide range of irradiances (200-900 W/m^2).

2.2.4 Puzzle-based PV Array

(a) *Su-Do-Ku Configuration*

The SDK and TCT topologies are modeled using simulations that include modules with a 9×9 array size, as shown in Fig. 2.5, with irradiation levels ranging from 200 W/m^2 to 900 W/m^2 in [Rani *et al.*, 2013]. For the performance analysis, when calculating the PE, maximum power, and voltage, it is necessary to take into account four distinct shading conditions (SW, LW, SN, and LN). The SDK configuration, which has the highest possible GMPP of 4532 W, exhibits the best performance, according to experimental results. In order to evaluate SDK and TCT topologies for highest power extraction, authors in [Deshkar *et al.*, 2015; Rao *et al.*, 2015] have utilized hardware-based experimental analysis to compare and minimization ML under varying PSCs, with results showing that the former yields better performance in most cases. The maximum GMPP (4802 W), and the electrical performance of both configurations is evaluated under LN to SW shading instances from 200- 900 W/m^2.

At non-uniform irradiation levels, including (200-900 W/m^2) the GMPP location was discovered as 5168 W for SDK configuration. This value was found to be optimal. The PL investigated during the experimentation study under a variety of PSCs on 6×6 PV array size in [Vijaylekshmy *et al.*, 2015]. The best GMPP value (1250 W) is observed in the SDK arrangement under effective shading impacts.

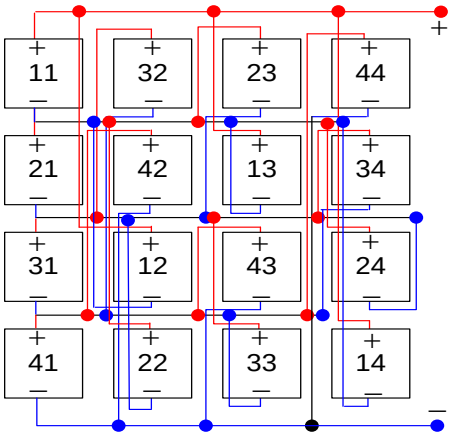

Fig. 2.5 SDK configuration

(b) ***Physical Reallocation of Module-Fixed Electrical Connections Configuration (PRM-FEC)***

The authors rearranged PV array (7×5 size) with modified electrical interconnection in the case of TCT arrangement based on the PRM-FEC approach in [Sahu and Nayak, 2016]. The best GMPP value as 73.55 W at considered irradiation level of 195-940 W/m^2 and observed simulation results are validated through experimentation.

(c) ***Optimal TCT And Novel TCT Configuration***

Mathematical modeling and comparative research for TCT and optimum total-cross-tied (OTCT) architecture determine PV module placement [Vijayalekshmy *et al.*, 2016]. A novel configuration known as the NTCT configuration is created where the TCT connections are reconfigured using the Zig-Zag pattern. In this study, we evaluate the relative merits of the TCT, OTCT, and NTCT configurations for 4×3 PV module arrays. At irradiance levels between 500 and 1000 W/m^2, it is found that a GMPP of 567 W is optimal for the NTCT configuration. Additionally, when subjected to the determined shading cases, the NTCT design outperforms compared to conventional schemes in aspect of GMPP, improved FF, % PE, and % PR.

(d) ***Magic Square Configuration***

The researchers in [Rakesh and Madhavaram, 2016] done in-depth research into TCT and MS topologies using 4×4 array size modules. In Fig. 2.6 explored four distinguished short and long shading scenarios are considered during the study. By analyzing the data obtained for both the TCT, and MS configurations, it is observed that the MS configuration has significantly higher FF, GMPP with lower PL. For the conventional (SP, BL, TCT), and MS configurations, the authors of [Samikannu et al, 2016] constructed a 3×3 and 6×6 PV array system for testing purposes, positioned in partial shade according to standard protocols. Here, the best results can be found with the MS puzzle configuration, which generates 2.88 W of maximum voltage under a widely irradiation intensities (200-900 W/m^2). In comparison to TCT and hybrid (SP-TCT, BL-TCT, and BL-HC) configurations, the authors found that a MS arrangement (4×4) deliberated the best performance GMPP, and enhanced FF). In a later study [Yadav *et al.*, 2017]. The authors of [Malathy and Ramaprabha, 2018] analyzed the PV array (6×6) and compared using hardware analysis to validate simulation study, with the most impressive GMPP of 300 W being achieved at irradiance levels of 500-1000 W/m^2.

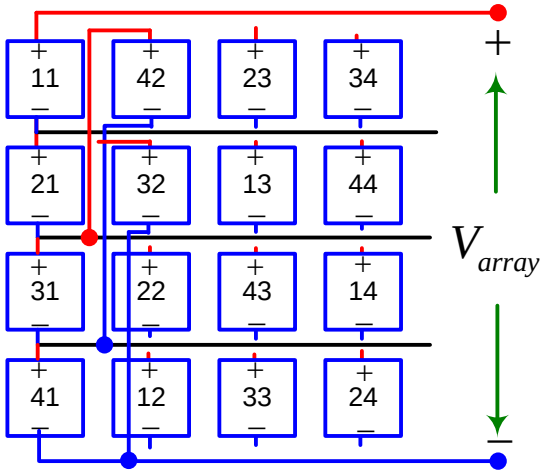

Fig. 2.6 MS Configuration

(e) ***Futoshiki Configuration***

PV array systems, including TCT and Futoshiki designs, as well as the numerous PSCs used to power them, are compared and contrasted [Sahu and Nayak, 2016]. Both types of PV array setups are examined and contrasted to validate their experimental validity. To get the best electric performance metrics, a 64.87 W GMPP is what has been found to work best for a Futoshiki puzzle-based arrangement.

(f) ***Novel Configuration***

By making some adjustments to the standard TCT setup, the authors of [Bana and Saini, 2017] came up with a new arrangement for a PV array of size (4×5) is known as "Novel." We also conduct an experimental evaluation of the "Novel" configuration in comparison to the conventional layouts (SP, BL, HC and TCT), with the optimal value of GMPP set at 1290 W and irradiation levels ranging from 100 to 980 W/m^2.

(g) ***Latin Square Configuration***

In [Pachauri *et al.*, 2018], For the purpose of evaluating player skill with a more organic method, the Latin Square (LS) game employs a variant of the TCT configuration known as LS-TCT as the challenge (i. e. left to right, bottom to top, diagonal pattern). For the LS-TCT configuration depicted in Fig. 2.7, the best results are determined to be 78.7%, 330 W and 2279 W as FF, PL and GMPP respectively, in comparison to the TCT configuration.

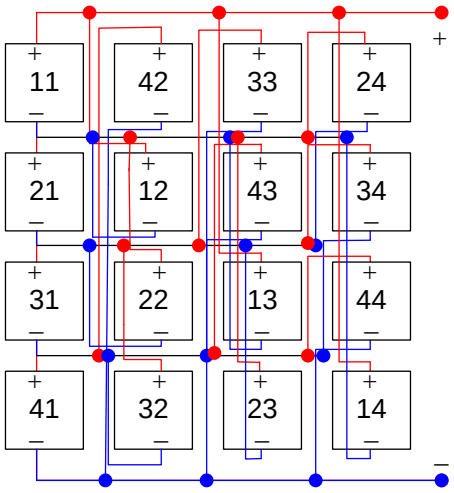

Fig. 2.7 LS-TCT configuration

2.3 SUMMARY

This chapter introduces a cutting-edge methodology for constructing various models of PV array configurations to mitigate the negative effects of partial shading. Every configuration is described and discussed from the perspectives of advantages, shortcomings, and essential aspects. In order to assess the different PV configurations based on topology, modelling, performance, scalability, grid connectivity, etc., a thorough literature review on the subject is conducted. These advanced PV array arrangements can be divided into traditional, hybrid, reconfigurable, and puzzle-based segments. The number of connections between PV modules in an array with ties increased and longer wire needs to give these puzzle-based game configurations a performance edge over more traditional arrangement. As a result of their enhanced capacity to cast a wider net, metaheuristic approaches in the field of concern research have explored uncharted avenues of inquiry.

CHAPTER- 3
PV SYSTEM MODELLING AND ROLE OF SYMMETRIC MATRIX BASED PV ARRAY CONFIGURATION FOR ACHIEVING HIGHER GMPP

3.1 INTRODUCTION

The study of RE based generating is expanding quickly in the modern period due to worries over environmental degradation and the depletion of fossil fuels [Goss *et al.*,2014]. As a result of numerous benefits, the amount of electricity used is increasing rapidly. There is currently no more effective renewable energy system than the PV system. The PV system has broad acceptance due to its many benefits, including no negative environmental impact and little maintenance needs [Kumar *et al.*,2016]. It is extremely difficult to increase the PV array system's electrical power rating while it is shaded (Partially or fully). In this area, the existing literature reports numerous techniques for obtaining the most power. In a shadowed environment, the efficiency of a PV array drops dramatically. Additionally, buildings, clouds, and tree shadow are the main contributors of PSCs. Moreover, the PV cells have been harmed by hotspot conditions. To avoid the same issue, PV cells and bypass diodes are installed in series [Yadav *et al.*,2016; Patel and Agarwal,2008].

3.2 STRATEGIC CONFIGURATION and PV SYSTEM

3.2.1 Solar PV System

Arranging solar PV cells in series and parallel maximizes the power requirement for better rating loads. Its electrical circuit configuration is depicted in Fig. 3.1.

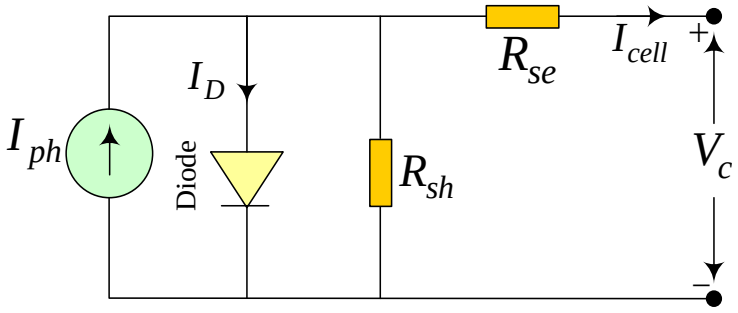

Fig. 3.1 PV cell equivalent electrical circuit

The voltage at the output of an array shown in Fig. 3.1 with the Eq. (1) as

$$V_C = \frac{AkT_c}{e} ln\left(\frac{I_{ph}+I_D-I_{cell}}{I_D}\right) - \frac{R_{se}R_{sh}}{R_{se}+R_{sh}} I_{cell} \quad (1)$$

In this equation, V_C and A represent the voltage and ideality factor of the cell, respectively. T_C is the temperature of the cell, and e is the charge of an electron. In addition, the photo current (I_{ph}) and the saturation current (I_D) are shown as symbols. The series resistance R_{se}, the shunt resistance R_{sh}, and the PV cell current I_{cell} are also indicated.

The properties of commercially available PV modules under common test settings are taken into account in MATLAB/Simulink modeling to investigate PV array systems under PSCs, as shown in Table 3.1.

Table 3.1-Parameters of commercially available PV module

Parameters	Values
V_{oc}	44.2 V
I_{sc}	5.2 A
V_m	35.8 V
I_m	4.75 A
P_m	170 W

3.2.2 The SM-TCT Size 8 Rules of Conduct

The row (p^{th}) and column (q^{th}) of an arrangement for n^{th} element corresponding, n_{pq} is scripted as,

$$n_{pq}, where \begin{cases} p = no.\ of\ row & (p = 1\ to\ 8) \\ q = no.\ of\ column & (q = 1\ to\ 8) \end{cases} \tag{2}$$

(i) Row, column and diagonal wise summation/analysis

The properties of SM matrix (8×8 size) based on the rows-columns and diagonal arrangements are shown in Fig. 3, and are expressed in Eq. (3) – (5) as,

$$\sum_{p=1}^{8} n_{pq} = Aggregate\ for\ p^{th} row, \quad (p = 1\ to\ 8) \tag{3}$$

$$\sum_{q=1}^{8} n_{pq} = Aggregate\ for\ q^{th} column, \quad (q = 1\ to\ 8) \tag{4}$$

$$R_n C_{m-7} = R_{n-1} C_{m-6} = \ldots\ldots\ldots\ldots\ldots R_{n-7} C_m \quad (\text{where, } n,m=8) \tag{5}$$

3.2.3 SM-TCT PV array configuration

In this research, three different dynamic shading instances are studied in relation to pre-existing TCT connections using SM-based electrical connections. If you add up all the numbers in a row or column, you get the same total, so using SM to arrange your numbers ensures that they are easily distinguishable. Each diagonal digit is also repeated itself with the same quantity. Fig. 3.2(a)-(e) illustrates the basic characteristics of an 8×8 SM arrangement.

1	2	3	4	5	6	7	8
2	3	4	5	6	7	8	1
3	4	5	6	7	8	1	2
4	5	6	7	8	1	2	3
5	6	7	8	1	2	3	4
6	7	8	1	2	3	4	5
7	8	1	2	3	4	5	6
8	1	2	3	4	5	6	7

(a) Row-wise summation

1	2	3	4	5	6	7	8
2	3	4	5	6	7	8	1
3	4	5	6	7	8	1	2
4	5	6	7	8	1	2	3
5	6	7	8	1	2	3	4
6	7	8	1	2	3	4	5
7	8	1	2	3	4	5	6
8	1	2	3	4	5	6	7

(b) Column- wise summation

1	2	3	4	5	6	7	8
2	3	4	5	6	7	8	1
3	4	5	6	7	8	1	2
4	5	6	7	8	1	2	3
5	6	7	8	1	2	3	4
6	7	8	1	2	3	4	5
7	8	1	2	3	4	5	6
8	1	2	3	4	5	6	7

(c) Repeated one diagonal digits

	C1	C2	C3	C4	C5	C6	C7	C8
R1	1	2	3	4	5	6	7	8
R2	2	3	4	5	6	7	8	1
R3	3	4	5	6	7	8	1	2
R4	4	5	6	7	8	1	2	3
R5	5	6	7	8	1	2	3	4
R6	6	7	8	1	2	3	4	5
R7	7	8	1	2	3	4	5	6
R8	8	1	2	3	4	5	6	7

(d) Repeated SM sub-matrix

	C1	C2	C3	C4	C5	C6	C7	C8
R1	11	22	33	44	55	66	77	88
R2	21	32	43	54	65	76	87	18
R3	31	42	53	64	75	86	17	28
R4	41	52	63	74	85	16	27	38
R5	51	62	73	84	15	26	37	48
R6	61	72	83	14	25	36	47	58
R7	71	82	13	24	35	46	57	68
R8	81	12	23	34	45	56	67	78

(e) SM-TCT configuration

Fig. 3.2(a)-(e) Symmetric matrix: Properties

The sum of each row and column adds up to 36, as shown in Fig. 3.2(a)–(e). Furthermore, as can be seen in Fig. 3.2(d), there is a recurrence of corresponding matrix elements of size 4×4. Moreover, as is seen in Fig. 3.2, (d), the inverted matrices of size 4×4 are repeated. Thus, the characteristics have been confirmed for SM size (8×8). The first and second digits represent the total number of rows and the total length of the columns in an 8 by 8 PV array, respectively.

Using Fig. 3.3(a)-(b), we can see the process for resetting TCT in SM-TCT links. The strategic configuration redistributes the shadowing effect by spreading it across the modules in an array, reducing the amount of shade cast on PV modules

across rows and columns. which improves the system's overall performance. All of the PV panels in a system follow the same procedure.

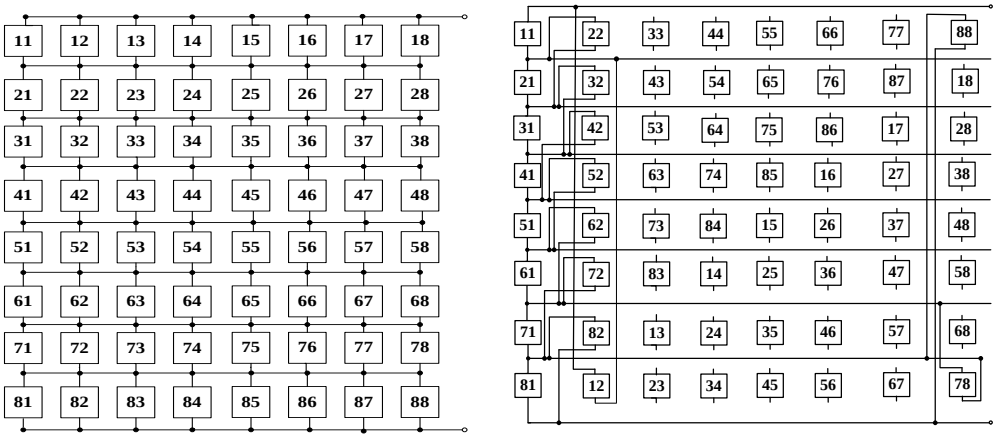

(a) TCT configuration (b) SM-TCT arrangement

Fig. 3.3(a)-(b) Electrical connections of TCT and SM-TCT configuration

3.3 CASE STUDIES AND PERFORMANCE EVALUATION OF SHADED TEXTURES

This in-depth analysis suggests that cases I-III under PSCs are preferable and possibly to happen for intended electrical connections between the two PV modules.

3.3.1 Shading Scenarios

The realistic PSCs (lamp posts, corner and single vertex shapes) are taken into account for in-depth analysis (see Fig. 3.4(a)-(c)).

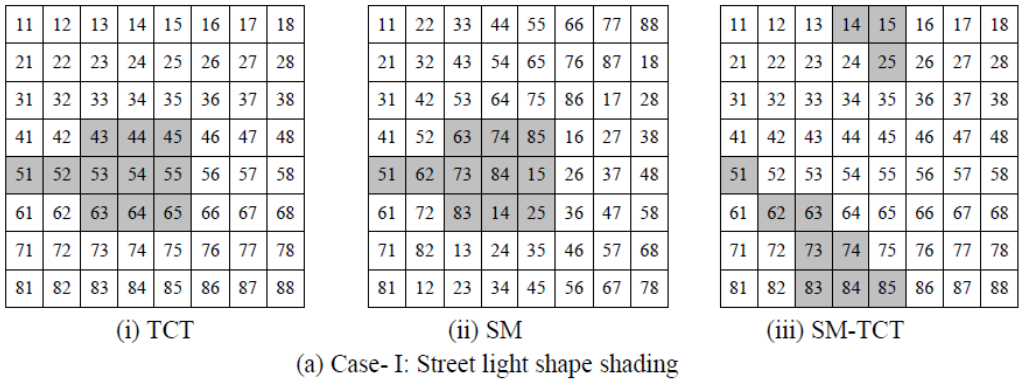

(i) TCT (ii) SM (iii) SM-TCT

(a) Case- I: Street light shape shading

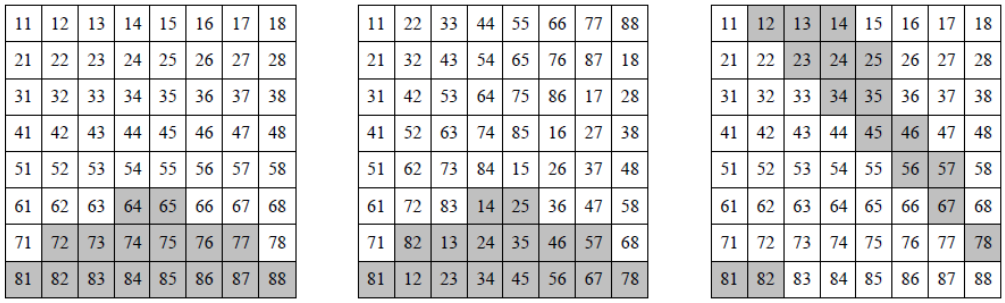

(i) TCT (ii) SM (iii) SM-TCT

(b) Case- II: Triangular or building shape shading

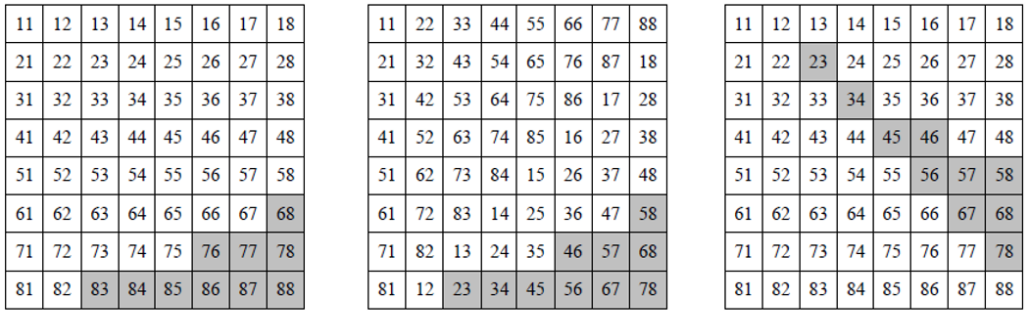

(i) TCT (ii) SM (iii) SM-TCT

(c) Case- III: Single corner shape shading

Fig. 3.4(a)-(c) Special shading cases for performance investigation on 8×8 size PV array

3.3.2 Partial Shading Losses

Power outages occur when the energy output at MPPT from a given PV unit does not match the energy input from the grid. Avoiding the diode requires fooling

the MPP monitoring program into running at the LMPP rather than the GMPP when the PV system is only partly veiled. In order to express the obtained PL,

$$\text{PL} = \text{MP (without shading)} - \text{Global MP (under shading)} \tag{6}$$

3.3.3 Fill Factor

The FF is a measure of the amount of energy that can be extracted from the GMPP in comparison to the product of short circuit (S.C.) current and the open circuit (O.C.) voltage of the PV cell. In addition, Eq. (7) is used to determine FF values from I-V curves as,

$$\text{Fill factor} = \frac{\text{Global Maximum Power}}{\left(\text{V}_{\text{o.c.}}\right)\left(\text{I}_{\text{s.c.}}\right)} \tag{7}$$

3.4 RESULTS and DISCUSSION

Three different types of shading conditions (I, II, and III) are used to evaluate the relative performance of the two PV array connections. The voltage of a PV array can be written in Eq. (6) as:

$$Array\ Voltage = \sum_{i=1}^{i=8} V_{mi} \tag{8}$$

Where,V_{mi} denotes ith row of PV array voltage and under the shading case-I, the current flowing across the rows of the TCT configuration can be calculated with Eq. (9)-(13) as,

$$I_{R1} = I_{R2} = I_{R3} = I_m + I_m + I_m + I_m + I_m + I_m + I_m + I_m = 8 \times I_m \tag{9}$$

$$I_{R4} = I_m + I_m + 0.5 \times I_m + 0.5 \times I_m + 0.5 \times I_m + I_m + I_m + I_m = 6.5 \times I_m \tag{10}$$

$$I_{R5} = 0.5 \times I_m + 0.5 \times I_m + 0.5 \times I_m + 0.5 \times I_m + 0.5 \times I_m + I_m + I_m + I_m = 5.5 \times I_m \quad (11)$$

$$I_{R6} = I_m + I_m + 0.5 \times I_m + 0.5 \times I_m + 0.5 \times I_m + I_m + I_m + I_m = 6.5 \times I_m \quad (12)$$

$$I_{R7} = I_{R8} = I_m + I_m + I_m + I_m + I_m + I_m + I_m + I_m = 8 \times I_m \quad (13)$$

Because of the shading effect, the values of the produced currents in the various rows are not identical to one another. In the P-V curves, multiple power maxima points are shown as LMPP and GMPP. It can be ignored that the marginal row-to-row variation in voltage and instead use Eq. (14) to determine the PV array's output voltage. Providing that no rows are skipped over and all PV modules are exposed to the same amount of light.

$$P_{array} = V_{array} \times 8I_m \quad (14)$$

Each column of an SM-TCT PV array system for PSCs has a current that is calculated and expressed using Eq. (15)-(21).

$$I_{R1} = I_m + I_m + I_m + 0.5 \times I_m + 0.5 \times I_m + I_m + I_m + I_m = 7 \times I_m \quad (15)$$

$$I_{R2} = I_m + I_m + I_m + I_m + 0.5 \times I_m + I_m + I_m + I_m = 7.5 \times I_m \quad (16)$$

$$I_{R3} = I_{R4} = I_m + I_m + I_m + I_m + I_m + I_m + I_m + I_m = 8 \times I_m \quad (17)$$

$$I_{R5} = 0.5 \times I_m + I_m + I_m + I_m + I_m + I_m + I_m + I_m = 7.5 \times I_m \quad (18)$$

$$I_{R6} = I_m + 0.5 \times I_m + 0.5 \times I_m + I_m + I_m + I_m + I_m + I_m = 7 \times I_m \quad (19)$$

$$I_{R7} = I_m + I_m + 0.5 \times I_m + 0.5 \times I_m + I_m + I_m + I_m + I_m = 7 \times I_m \quad (20)$$

$$I_{R8} = I_m + I_m + 0.5 \times I_m + 0.5 \times I_m + 0.5 \times I_m + I_m + I_m + I_m = 6.5 \times I_m \quad (21)$$

SM-TCT system lines have different outcomes but the same GMPPs. All of the discussed shading scenarios verify PE for the SM-TCT scheme. All the mentioned shading scenarios verify that improved PE is achieved for SM-TCT system.

3.4.1 P-V and I-V curves for considered configurations

Fig. 3.5(a)-(c) shows the behaviour of P-V curves for TCT and SM-TCT configurations during PSCs (I-III). Under a single instance of case-I regular shading, the GMP for a standard TCT array layout is 8163 W. Moreover, the SM-TCT panel configuration yields a GMPP that is higher than 9141 W. In Fig. 3.5(a), the periodic shading case-I, the P-V curves for both conventional TCT and the SM-TCT systems that were recommended. Moreover, the GMP array for the strategic SM-TCT scheme was higher than that of conventional TCT system and quantitative outcomes are depicted in Table 3.2.

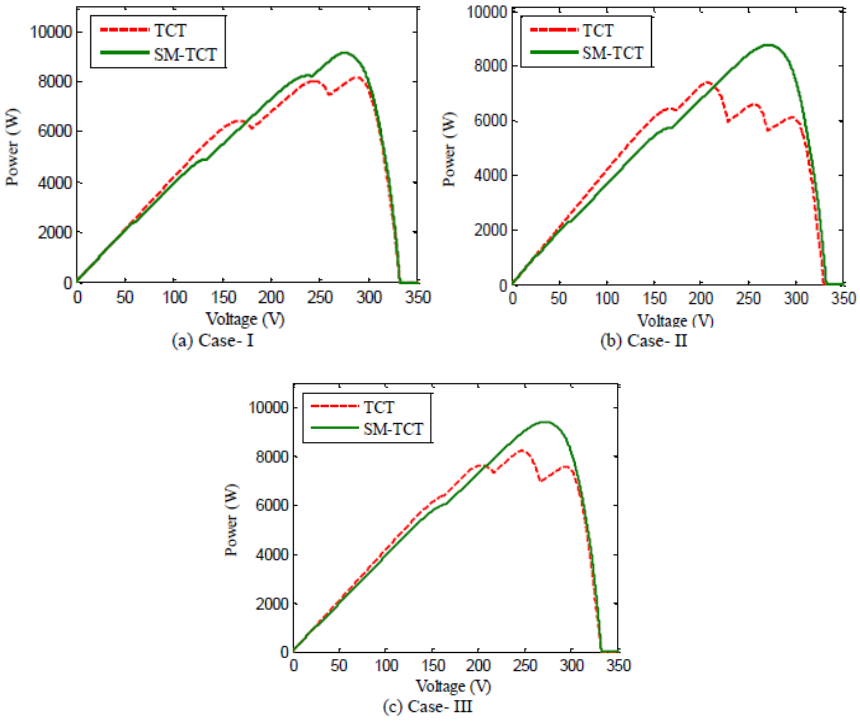

Fig. 3.5(a)-(c). P–V curves for regular shading test cases: I- III

Fig. 3.6(a)-(c) shows how the traditional TCT is underperformed in terms of I-V curves compared to novel SM-TCT PV array in shading scenarios I-III.

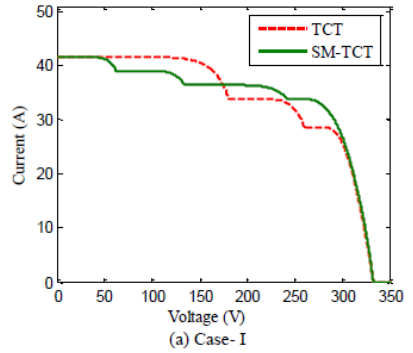

(a) Case- I

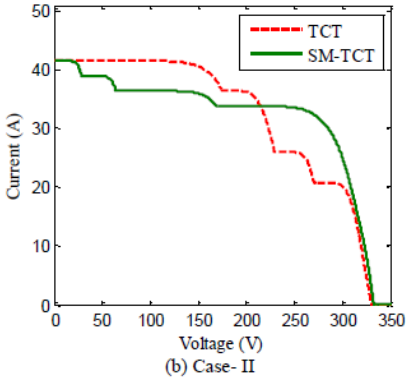

(b) Case- II

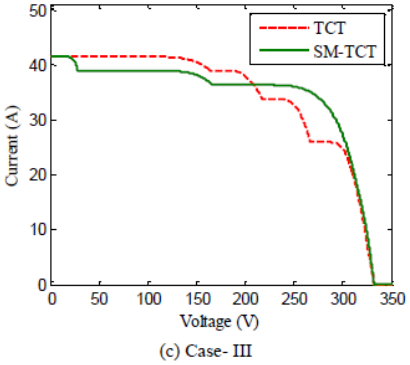

(c) Case- III

Fig. 3.6(a)-(c) I-V curves under shading cases (I-III)

Table 3.2-Quantitative indices of study during PSCs

Performance parameters	Case-I		Case-II		Case-III	
	TCT	SM-TCT	TCT	SM-TCT	TCT	SM-TCT
Power at GMPP (kW)	8.16	9.14	7.382	8.76	8.22	9.41
Voltage at GMPP (kV)	0.288	0.27	0.2072	0.271	0.246	0.272
V_{OC} (V)	332.50	332.50	329.6	332.2	332	332
I_{SC} (A)	41.50	41.50	41.60	41.60	41.5	41.5
PL (kW)	2.27	1.29	3.058	1.671	2.214	1.025
MML (%)	10.14	9.06	16.32	13.73	9.15	7.99
FF	0.59	0.661	0.538	0.634	0.595	0.681
PR	0.781	0.875	0.707	0.839	0.787	0.901
PE (%)	--	10.69	--	15.81	--	12.62

3.4.2. Power Loss

Table 3.2 compiles the results of our evaluations of the losses in the TCT and SM-TCT connections, as well as the power acquired at GMPP, which comes to 10440W when no shading is present. An extensive analysis of the obtained results is also provided in Fig. 3.7.

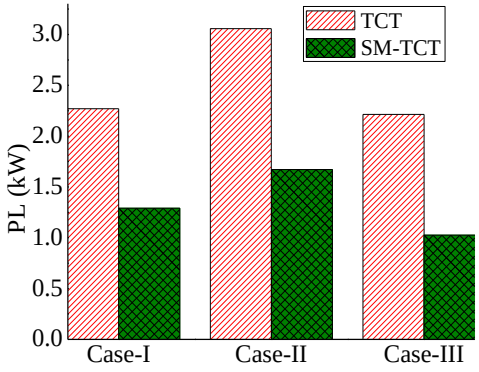

Fig. 3.7 PL analysis under regular shading cases: I-III

3.4.3. Performance Enhancement and Fill Factor

In this section, the performance parameters (% PE and % FF) during the consider shadowing cases are depicted in Fig. 3.8 as,

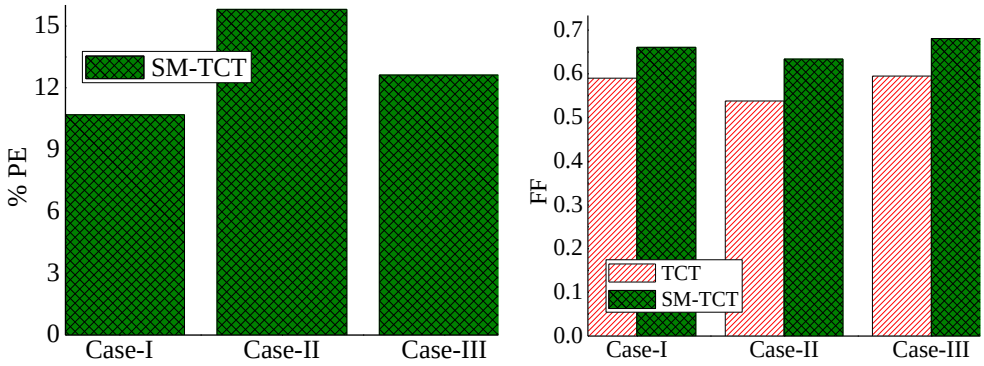

Fig. 3.8 (a) % PE (b) FF under shading cases: I-III

3.4.4. Performance Ratio

The PR's efficacy is estimated for shading situations I–III. Shading-I increases TCT and SM-PR TCT's from 0.781 to 0.875. Table 3.2 and Fig. 3.9 illustrate PR values including both PV array layouts.

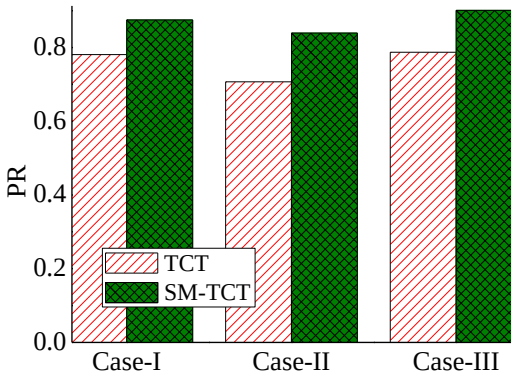

Fig. 3.9 PR under regular shading cases: I-III

3.5 SUMMARY

The thesis employs SM puzzles to compare the existing TCT configuration to three shading situations and found lowest energy loss, maximum global output, and best FF improvement. Extensive testing is done on these configurations using three distinct shadow cases (lamp post, cornered and single vertex shading). In case-II, we have observed highest increment in power at GMPP by 1.378 kW, power loss has been reduced to 1.671 kW in SM-TCT configuration, FF gets incremented to 0.634 from 0.538 % and PE is achieved as 15.81 %. The study is useful overall and can serve as a standard in the area.

CHAPTER- 4
Shape-Do-Ku GAME PUZZLE BASED PV ARRAY RECONFIGURATION FOR HIGHER GMPP

4.1 INTRODUCTION

The revitalized analyst must look at useful RE sources in this era, when the fossil fuel supply is in short supply and severely constricted. RE sources like wind turbines and PV systems are developing, but they each have their own environmental limits that must be taken into account [Premkumar *et al.*,2020]. Regarding the most convenient accessibility of bio-fuel cell power. PV technology has significant challenges as a result of a variety of known and unidentified reasons, such as malfunction and climatic pollutants. In the present day, environmental constraints, such as dust that has formed on the panel surface, are rapidly expanding. Shadows cast on the surface of PV plants may be cast by a number of factors, including passing clouds, nearby trees, and elevated structures, especially in urban areas [Babu *et al.*,2020]. Recent years have seen a surge of interest in studying the effects of modifying the electrical connections between PV modules to increase the efficiency of PV systems [Petronea and Ramos-Pajab,2011]. In contrast to the typical ones, PV module rearrangement techniques are used to improve performance. There are many different ways to arrange PV modules in an array, including in series, in parallel, in SP, in BL, in TCT, and in HC [Wang and Hsu,2010].

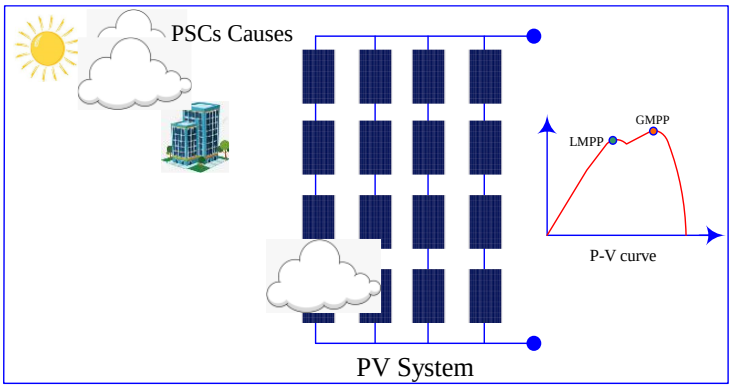

Fig. 4.1 Various Shading Conditions affecting PV performance

4.2 PV SYSTEM TECHNOLOGY and ARRAY

The section that follows elucidates the modelling strategies for PV systems that are assumed in the proposed work:

4.2.1 PV system modeling

PV modules are connected to SP configuration for a significant amount of electricity generation as given in Fig. 4.2.

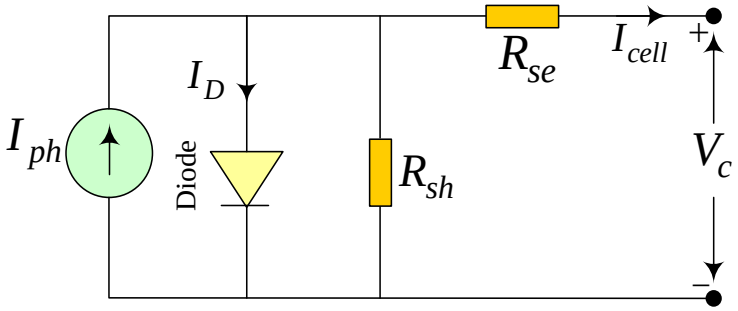

Fig. 4.2 Equivalent circuit of PV cell

The voltage of a solar photovoltaic cell (V_c) is proportional to the transmittable solar current I_{sc} and is thus a function of solar irradiation as depicted in Eq. (1),

$$V_C = \frac{AkT_c}{e} ln\left(\frac{I_{ph}+I_D-I_{cell}}{I_D}\right) - \frac{R_{se}R_{sh}}{R_{se}+R_{sh}} I_{cell} \quad (1)$$

Table 4.1 depicts modelling of PV array systems under PSCs, we consider commercially available PV module specifications at standard test scenarios in MATLAB/Simulink.

Table 4.1-Parameters of commercially available PV module

Parameters	Values
V_{oc}	44.2 V
I_{sc}	5.2 A
V_m	35.8 V
I_m	4.75 A
P_m	170 W

4.2.2 PV array configurations

(a) Conventional Configurations

The various PV array configurations (SP, BL, HC, TCT, hybrid SP-TCT, BL-HC, BL-TCT, and the proposed LS-TCT) are depicted in Fig. 4.3(a)-(h). Conventional SP, BL, and HC configurations for a 4×4 array of PV panels, with conduct measured in relation to GMPP and FF, are shown in Fig. 4.3(a)-(c). TCT arrangement, depicted in Fig. 4.3(d), is obtained by ties connected across individual rows of interconnections to produce high power, and it is used for arrays of size 4×4 of PV panels. It is clear from Fig. 4.3(e)-(g) that the hybrid topology of a PV array is derived from the combination of the existing configurations (SP, BL, and HC topologies).

(b) ***Latin Square puzzle configuration***

In Fig. 4.3(h), we can see the novel LS-TCT array, PV module placements are re-allocated in accordance with a modified TCT while keeping the electrical

interconnections the same. Each PV module's first and second digits serve as row and column indicators in this layout. In the classic game of LS, players try to calculate maximum integer number rows and columns. The Leonard Euler matrix has one symbol per row and column. During PV array reconfiguration under PSCs, the property of a similar problem with more dispersed shading [Madhusudanam *et al.*,2018] is examined. The shade dispersion feature is always different based on a set of integer numbers, making for a challenging game puzzle. As a result, the placement of the LS problem has varied features and offers alternative options for placing integer numbers (1-4). In Fig. 4.3(k), the process for reconfiguring a PV array using an LS problem is displayed.

(c) Su-Do-Ku configuration

When testing PV array reconfigurations under PSCs, this SDK issue was initially presented for shade dispersion [Rani *et al.*,2013]. To rearrange the 4×4 PV array, a set of rules are applied, each of which consists of an integer number (1-4) in each row and column of the matrix. Potential electrical connections and design strategies are shown graphically in Fig. 4.3(i) and 4.3(l).

(d) *Shape-Do-Ku configuration*

There is no technical connection between the SPDK puzzle and the SDK puzzle, but it does exist in a number of different sizes (4×4, 5×5, and 6×6) and exhibits symmetrical properties. However, it is a variant of the LS puzzle, with the only requirement being that each number appear exactly once in every column and every row [Wanko and Nickell,2013]. In this thesis, the PV array is rearranged using an SPDK puzzle of 4×4 squares. The electrical connections are shown in Fig. 4.3(j), and the design process is shown in Fig. 4.3(m).

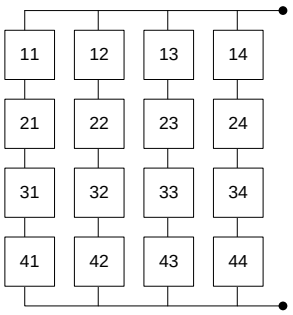

(a) SP

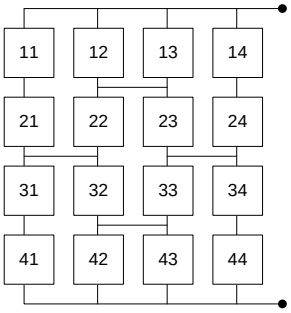

(b) BL

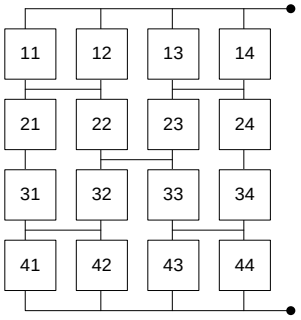

(c) HC

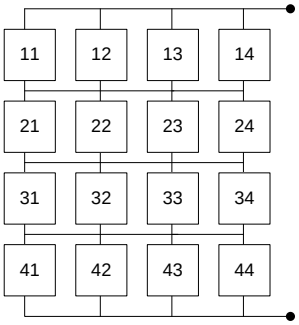

(d) TCT

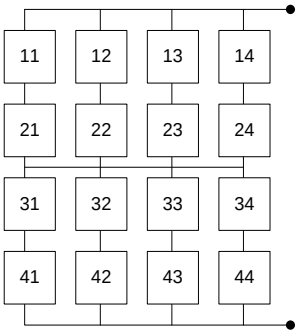

(e) SP-TCT

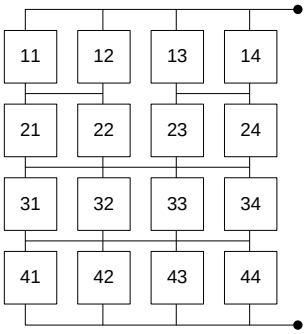

(f) BL-HC

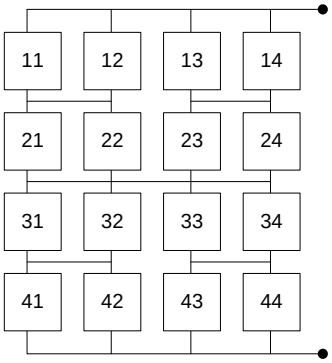

(g) BL-TCT

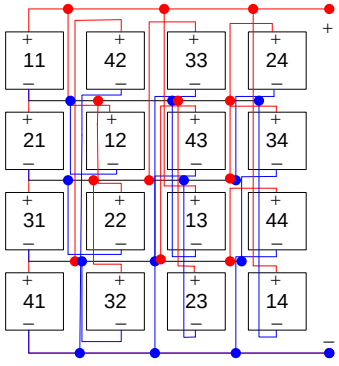

(h) LS-TCT

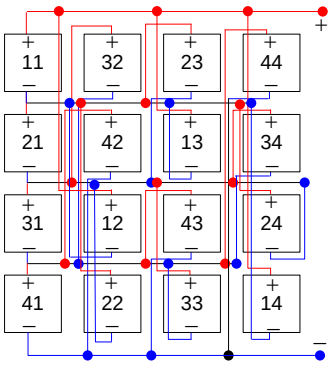

(i) SDK

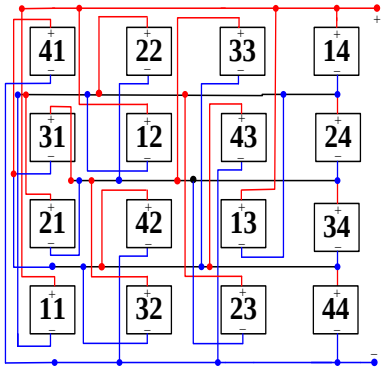

(j) SPDK

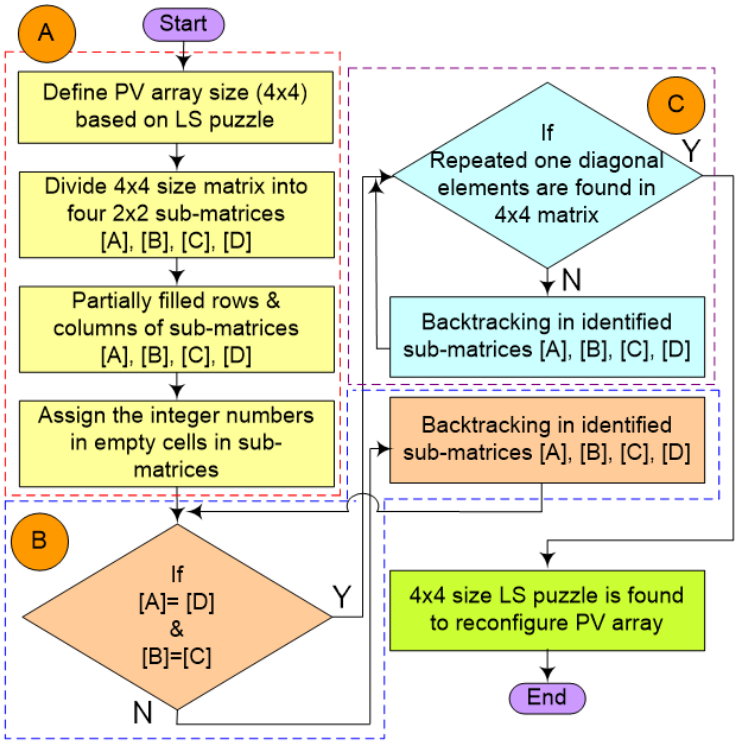

(k) Flow chart for LS methodology to design 4x4 size PV array

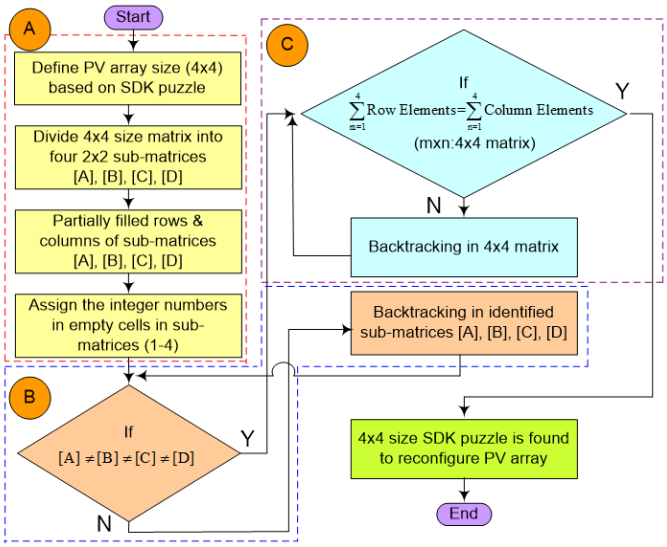

(l) Flow chart for SDK methodology to design 4x4 size PV array

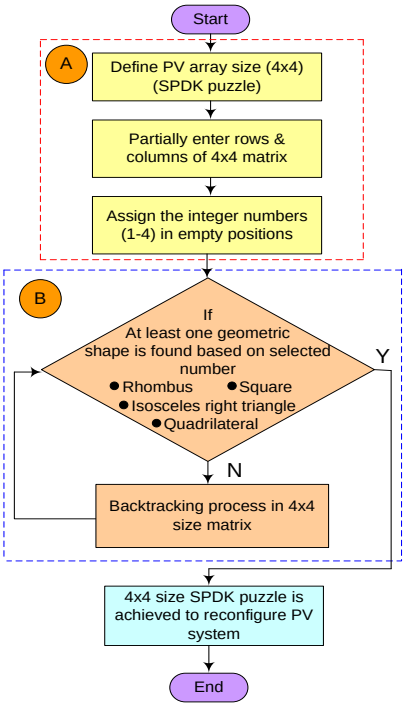

(m) Methodology to design SPDK PV array (4×4 size)

Fig. 4.3(a)-(m) Conventional, hybrid, game puzzle-based configurations and their flow charts

4.3 ANALYSIS OF PERFORMANCE PARAMETERS AND SHADING PATTERNS

Evaluating a technique's performance metrics is essential for demonstrating its superiority. This article serves as a warning that the authors have used a variety of performance metrics to determine whether or not their proposed PV array reconfiguration technique is superior. The subsequent sections provide a thorough examination of these variables:

4.3.1 Performance Parameters

(a) *Power Loss*

Analyzing PV array performance under a variety of shading conditions is depicted in Fig. 4.4. It can be traced back to the difference between GMPP and LMPP, which is at the heart of the deceptive nature of the former. The only thing that affects the performance of a PV array in terms of PL is the interconnections between the modules. Eq. (2) provides an expression for the PL of the PV system.

PL = Power at the standard condition – GMP under diverse PSCs (2)

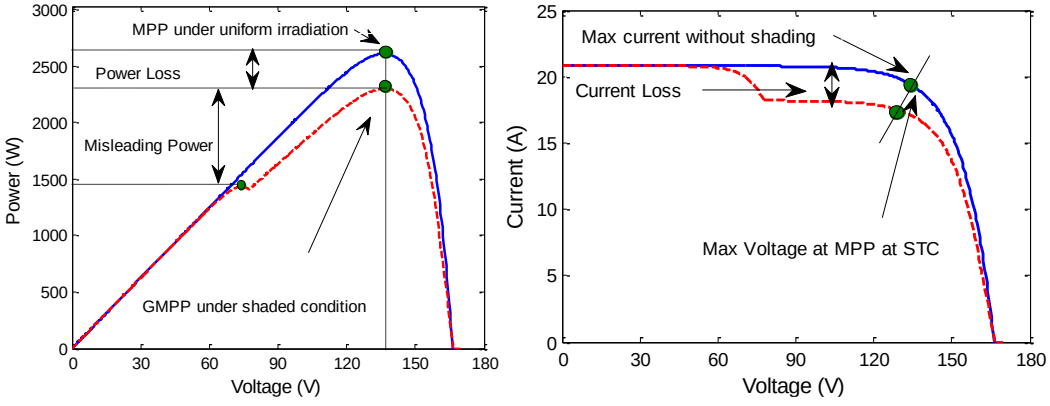

(a) P-V curve (b) I-V curve

Fig. 4.4 (a)-(b) Shading impact on P-V and I-V curves

(b) ***Fill Factor***

As can be seen in Fig. 4, PL has an effect on FF while operating in the presence of PSCs. The P-V and I-V plots confirm that the I_{sc} & V_{oc} have a direct impact on the FF, as predicted by Eq. (3).

$$FF = \frac{P_{GMPP}}{V_{OC} I_{SC}} \tag{3}$$

(c) ***Performance Ratio***

In order to calculate the PV array's PR at STCs, we can use Eq. (4), which states that the PR equals the ratio of the power generated at the GMPP while subject to PSCs and the power generated under normalised conditions.

$$\%PR = \frac{GMPP\ at\ PSCs}{MPP\ at\ s\tan dard\ condition} \times 100 \tag{4}$$

4.3.2 Analysis of Shading Scenarios

The thesis displays eight different configurations, including three examples of each: SP, BL, HC, TCT, BL-HC, SP-TCT, BL-TCT, and LS-TCT. The article uses the shifting of shadows to differentiate between three different types of shading patterns. Radiation doses of 1000 W/m^2 and 500 W/m^2 are among those taken into account.

(a) ***Shading Pattern-1***

There are three distinct shadow-casting scenarios here, depicted in Fig. 4.5 as Cases 1, 2, and 3 as,

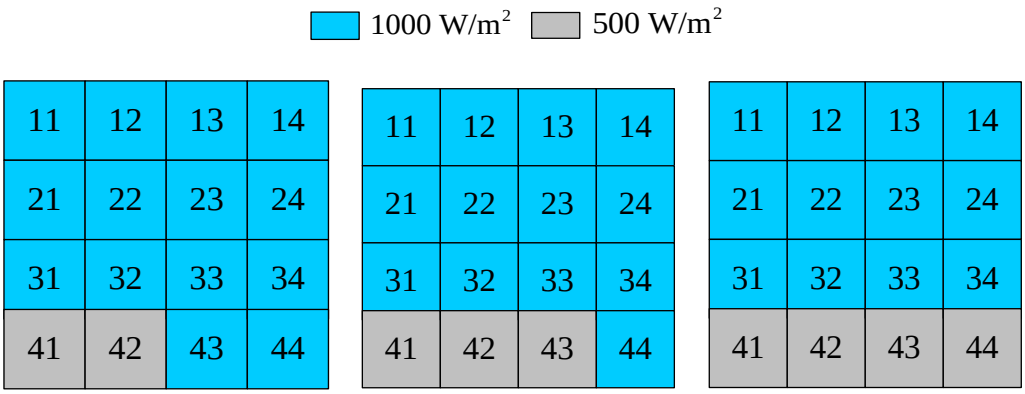

(a) Case-1 (b) Case-2 (c) Case-3

Fig. 4.5(a)-(c) Shading cases 1-3 for pattern-1

An even 1000 W/m^2 of solar radiation is falling on three PV modules in the first, second, and third rows. Two modules in the fourth row get 500 W/m^2 of solar irradiation, while the other two get 1000 W/m^2 of irradiation. Therefore, Eq. (5)-(10) can be used to calculate how much current is generated by a 4×4 PV array in the first, second, third, and fourth rows. Case-1 shading current generation as,

$$I_{R1} = I_{R2} = I_{R3} = 4\left(\frac{S_x}{S_{STC}}\right) I_m = \left(\frac{1000}{1000}\right) I_m + \left(\frac{1000}{1000}\right) I_m + \left(\frac{1000}{1000}\right) I_m + \left(\frac{1000}{1000}\right) I_m = 4I_m \quad (5)$$

$$I_{R4} = \left(\frac{500}{1000}\right) I_m + \left(\frac{500}{1000}\right) I_m + \left(\frac{1000}{1000}\right) I_m + \left(\frac{1000}{1000}\right) I_m = 3I_m \quad (6)$$

Similarly, the current generated under case-2,

$$I_{R1} = I_{R2} = I_{R3} = \left(\frac{1000}{1000}\right) I_m + \left(\frac{1000}{1000}\right) I_m + \left(\frac{1000}{1000}\right) I_m + \left(\frac{1000}{1000}\right) I_m = 4I_m \quad (7)$$

$$I_{R4} = \left(\frac{1000}{1000}\right) I_m + \left(\frac{500}{1000}\right) I_m + \left(\frac{500}{1000}\right) I_m + \left(\frac{500}{1000}\right) I_m = 2.5I_m \quad (8)$$

Moreover, the current generated under shading case- 3 as,

$$I_{R1} = I_{R2} = I_{R3} = \left(\frac{1000}{1000}\right) I_m + \left(\frac{1000}{1000}\right) I_m + \left(\frac{1000}{1000}\right) I_m + \left(\frac{1000}{1000}\right) I_m = 4I_m \quad (9)$$

$$I_{R4} = \left(\frac{500}{1000}\right) I_m + \left(\frac{500}{1000}\right) I_m + \left(\frac{500}{1000}\right) I_m + \left(\frac{500}{1000}\right) I_m = 2I_m \quad (10)$$

(b) Shading Pattern-2

As shown in cases 1–3 of Fig. 4.6, the shadow is likely moving from bottom left to top right, beginning with the bottom two modules,

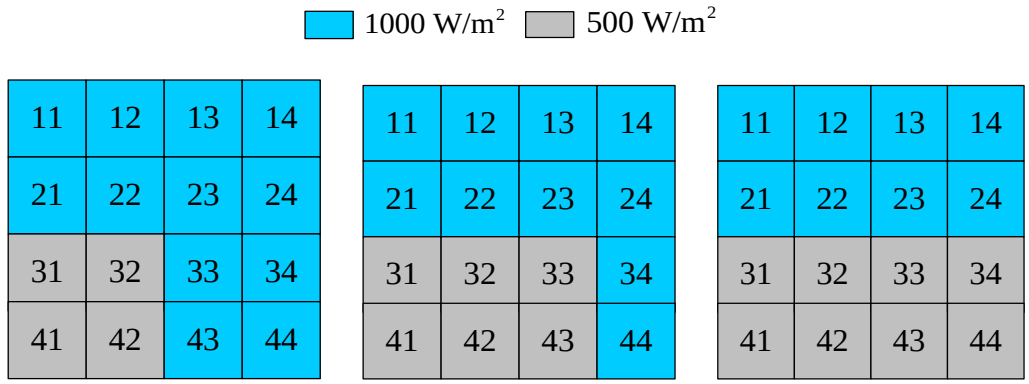

(a) Case-1 (b) Case-2 (c) Case-3

Fig. 4.6(a)-(c) Shading cases 1-3 for pattern-2

Calculations of the induced current in shading scenarios 1, 2, and 3 can be made theoretically and expressed in Eq. (11)- (16) as,

Generated current for case-1:

$$I_{R1} = I_{R2} = \left(\frac{1000}{1000}\right) I_m + \left(\frac{1000}{1000}\right) I_m + \left(\frac{1000}{1000}\right) I_m + \left(\frac{1000}{1000}\right) I_m = 4I_m \quad (11)$$

$$I_{R3} = I_{R4} = 0.5I_m + 0.5I_m + 0.5I_m + I_m = 2.5I_m \quad (12)$$

Generated current for case-2:

$$I_{R1} = I_{R2} = \left(\frac{1000}{1000}\right) I_m + \left(\frac{1000}{1000}\right) I_m + \left(\frac{1000}{1000}\right) I_m + \left(\frac{1000}{1000}\right) I_m = 4I_m \quad (13)$$

$$I_{R3} = I_{R4} = 0.5I_m + 0.5I_m + 0.5I_m + I_m = 2.5I_m \quad (14)$$

Generated current for case-3:

$$I_{R1} = I_{R2} = \left(\frac{1000}{1000}\right) I_m + \left(\frac{1000}{1000}\right) I_m + \left(\frac{1000}{1000}\right) I_m + \left(\frac{1000}{1000}\right) I_m = 4I_m \quad (15)$$

$$I_{R3} = I_{R4} = 0.5I_m + 0.5I_m + 0.5I_m + 0.5I_m = 2I_m \quad (16)$$

(c) Shading Pattern-3

When we compare PV arrays arranged in patterns 1 and 3, we see that as the sun moves higher in the sky, the shadows cast by the arrays move upward. Cases 1-3 in Fig. 4.7 demonstrate the left-to-right shading on PV modules,

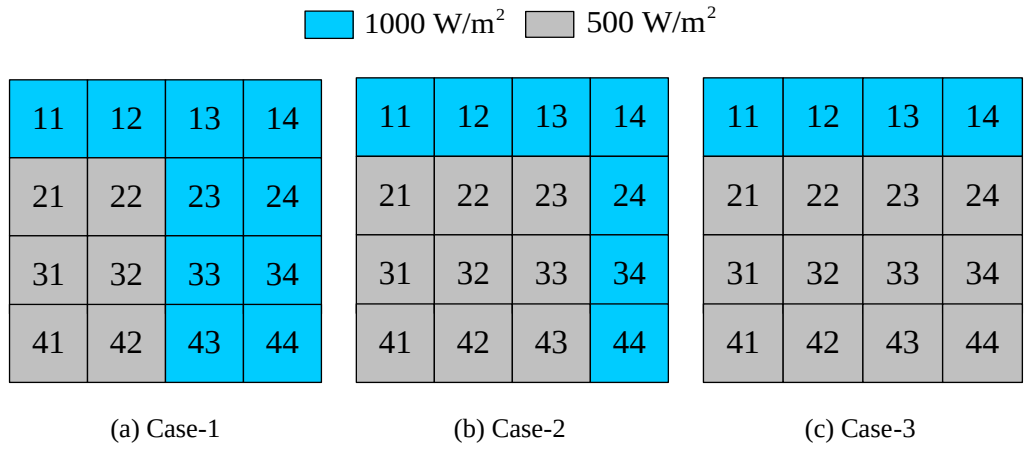

(a) Case-1 (b) Case-2 (c) Case-3

Fig. 4.7(a)-(c) Shading cases 1-3 for pattern-3

Cases 1, 2, and 3 of shading are analyzed theoretically in Eq. (17)-(22) read as,

Generated current for case-1:

$$I_{R1} = \left(\frac{1000}{1000}\right) I_m + \left(\frac{1000}{1000}\right) I_m + \left(\frac{1000}{1000}\right) I_m + \left(\frac{1000}{1000}\right) I_m = 4I_m \quad (17)$$

$$I_{R2} = I_{R3} = I_{R4} = 0.5I_m + 0.5I_m + \left(\frac{1000}{1000}\right) I_m + \left(\frac{1000}{1000}\right) I_m = 3I_m \quad (18)$$

Generated current for case-2:

$$I_{R1} = \left(\frac{1000}{1000}\right) I_m + \left(\frac{1000}{1000}\right) I_m + \left(\frac{1000}{1000}\right) I_m + \left(\frac{1000}{1000}\right) I_m = 4I_m \quad (19)$$

$$I_{R2} = I_{R3} = I_{R4} = 0.5I_m + 0.5I_m + 0.5I_m + \left(\frac{1000}{1000}\right) I_m = 2.5I_m \quad (20)$$

Generated current for case-3:

$$I_{R1} = \left(\frac{1000}{1000}\right) I_m + \left(\frac{1000}{1000}\right) I_m + \left(\frac{1000}{1000}\right) I_m + \left(\frac{1000}{1000}\right) I_m = 4I_m \quad (21)$$

$$I_{R2} = I_{R3} = I_{R4} = 0.5I_m + 0.5I_m + 0.5I_m + 0.5I_m = 2I_m \quad (22)$$

4.4 RESULTS and DISCUSSION

The following studies have been demonstrated on different PV array configurations to estimate the overall performance with the due effect of different PSCs.

4.4.1 P-V and I-V curves at STC

The MATLAB-simulated P-V and I-V curves for a single PV module at STC and insolation levels yielding 2610 W of power are shown in Fig. 4.8 as,

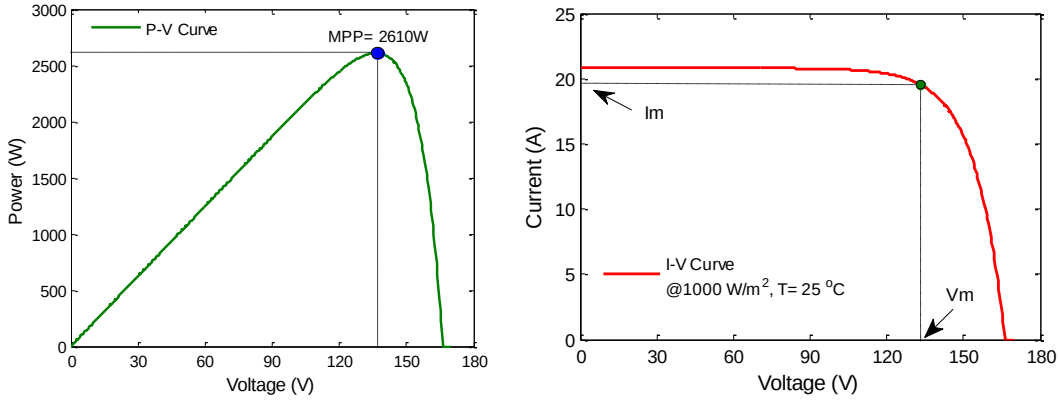

(a) P-V curve (b) I-V curve

Fig. 4.8(a)-(b) P-V and I-V characteristics (STCs)

Table 4.2 displays the current, voltage, and power of LS-TCT connections. In a select few shading situations, LS-TCT configurations can increase their generated

power. By rearranging the modules, the shadowing effect of shading pattern-1 is mitigated across the PV array, resulting in a boost in output.

4.4.2 Effect on PV Array Under Shading Pattern-1

(a) *P-V and I-V curves*

The I-V and P-V curves of all possible PV array topologies under three types of shading patterns are shown and differentiated from bottom to top in Fig. 4.9, with three cases in each pattern (left to right) shown for easy comparison. Figure 4.9(a) shows that the P-V curve has two MPPs, the GMPP and the LMPP, for all topologies. In case "5a," however, where both MPPs are found to be separated from one another and cause a marginal amplification of partial shading effects, the GMPP for LS-TCT is smoother. The resulting GMPP power for the various topologies depicted in Fig. 4.10 is 2053 W, 2134 W, 2091 W, 2169 W, 2169 W, 2118 W, 2118 W, and 2368 W for the conventional (SP, BL, HC, TCT), hybrid (BL-HC, BL-TCT, SP-TCT), and LS-TCT. For the scenario described in Fig. 4.5(b), the P-V curve is displayed in Fig. 4.9(b), and for the scenario described in Fig. 4.5(c), the P-V curve is displayed in Fig. 4.9(c). As can be seen in Fig. 9(c), both the local and global MPP are partitioned from one another in the classical and hybrid topologies, which is relevant to the shading example in Fig. 4.5(c). The GMPP obtained power for cases 5(b) and 5(c) are respectively 1988 W, 1960 W, 1942 W, 1942 W, 1942 W, 1942 W, 1958 W, 2333 W, and 2247 W, as shown in Fig. 4.10.

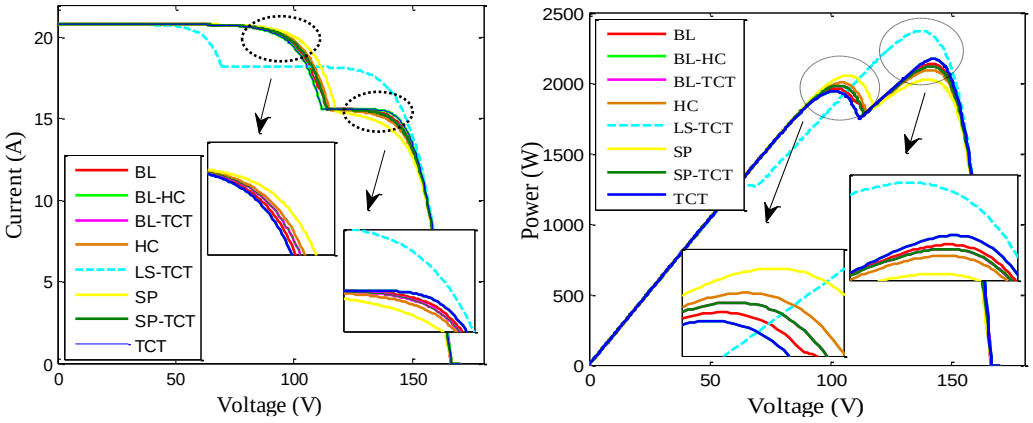

(a) I-V and P-V curves for case-1

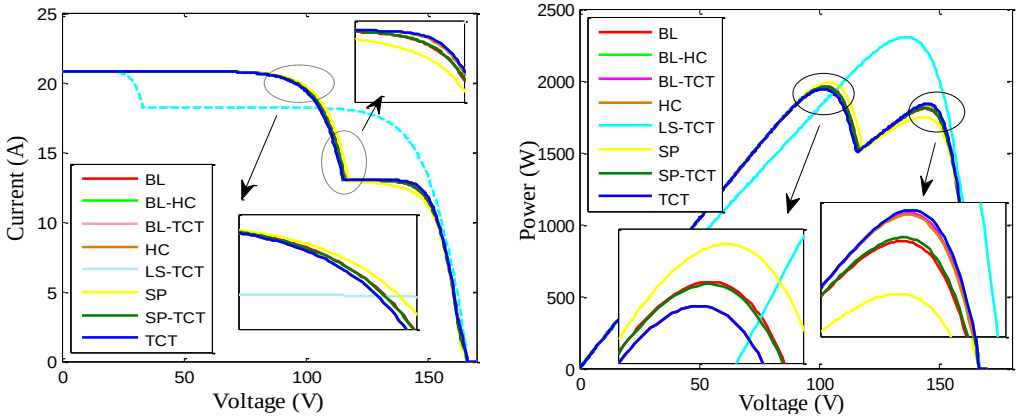

(b) I-V and P-V curves for case-2

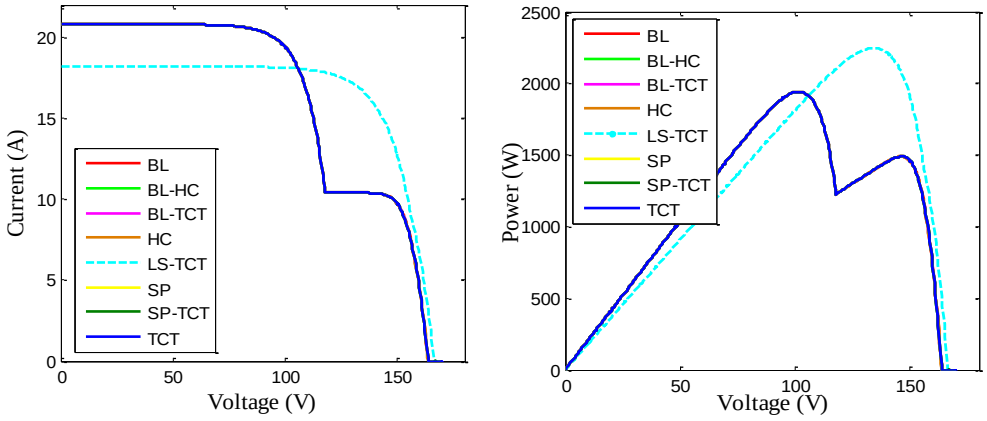

(c) I-V and P-V curves for case-3

Fig. 4.9(a)-(c) I-V and P-V curves under shading pattern-1

Table 4.2-Performance Matrices for each configuration under shading pattern-I

Performance Parameters	**Case-1**							
	SP	**BL**	**HC**	**TCT**	**BL-HC**	**BL-TCT**	**SP-TCT**	**LS-TCT**
V_{oc}(V)	166.1	166.1	166.1	166.1	166.1	166.1	166.1	166.1
I_{sc}(A)	20.8	20.8	20.8	20.8	20.8	20.8	20.8	20.8
V_m (V)	107.3	142.3	141	142.4	142.4	141.9	141.9	127.8
I_m (A)	19.14	15.23	14.83	15.23	15.23	14.93	14.93	17.96
P_{GMPP} (W)	2053	2134	2091	2169	2169	2118	2118	2368
P_{LMPP} (W)	2024	1960	2001	1942	1942	1981	1981	1274
P_L (W)	557	476	519	441	441	492	492	242
FF	0.5944	0.6273	0.6052	0.6277	0.6277	0.6132	0.6132	0.6644
Performance Parameters	**Case-2**							
	SP	**BL**	**HC**	**TCT**	**BL-HC**	**BL-TCT**	**SP-TCT**	**LS-TCT**
V_{oc}(V)	166.1	166.1	166.1	166.1	166.1	166.1	166.1	166.1
I_{sc}(A)	20.8	20.8	20.8	20.8	20.8	20.8	20.8	20.8
V_m (V)	104.5	102.4	101.5	101.5	101.5	101.5	103	136.1
I_m (A)	19.03	19.14	19.14	19.14	19.14	19.14	19.02	16.92
P_{GMPP} (W)	1988	1960	1942	1942	1942	1942	1958	2333
P_{LMPP} (W)	1747	1806	1835	1841	1841	1838	1810	606.7
P_L (W)	622	650	668	668	668	668	652	277
FF	0.5756	0.5673	0.5623	0.5623	0.5623	0.5623	0.567	0.666

Table 4.2 Continue…

Performance Parameters	Case-3							
	SP	**BL**	**HC**	**TCT**	**BL-HC**	**BL-TCT**	**SP-TCT**	**LS-TCT**
V_{oc}(V)	163.6	163.6	163.6	163.6	163.6	163.6	163.6	166.2
I_{sc}(A)	20.8	20.8	20.8	20.8	20.8	20.8	20.8	18.2
V_m (V)	101.5	101.5	101.5	101.5	101.5	101.5	101.5	134.8
I_m (A)	19.14	19.14	19.14	19.14	19.14	19.14	19.14	16.67
P_{GMPP} (W)	1942	1942	1942	1942	1942	1942	1942	2247
P_{LMPP} (W)	1489	1489	1489	1489	1489	1489	1489	0
P_L (W)	668	668	668	668	668	668	668	363
FF	0.5709	0.5709	0.5709	0.5709	0.5709	0.5709	0.5709	0.7429

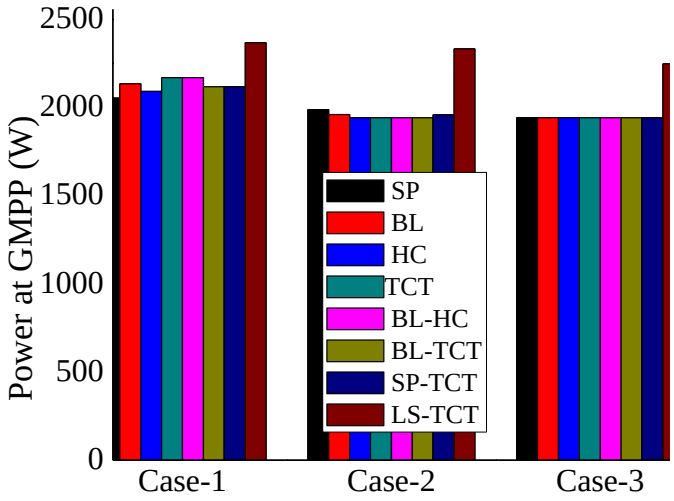

Fig. 4.10 Power at GMPP for cases 1-3 under shading pattern-1

(b) *Power Loss*

When put through the same rigors as shade pattern-1, the LS-TCT puzzle pattern consistently outperforms the SP, BL, HC, TCT, BL-HC, BL-TCT, and SP-TCT variants. Fig. 4.11 is a bar chart depicting the PL, and Table 4.2 is a tabular

representation of the same data. Under all of pattern-1's shading conditions, it has been found that the PL are minimal in the LS-TCT puzzle arrangement.

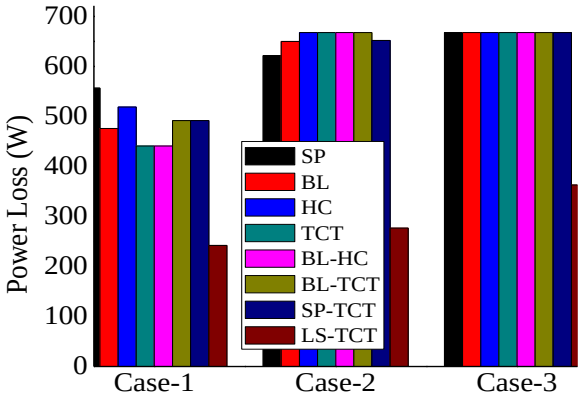

Fig. 4.11 PL for cases 1-3 under shading pattern-1

(c) *Fill Factor*

As shade shifts from one end of the PV Array to the other, it has an amplified effect, resulting in a lower FF. Figure 4.12 is a bar graph formed by the first shading pattern in Fig. 4.5(a)-(c). For each possible arrangement of shading pattern-1, the corresponding FF values are shown in Table 4.2. It can be inferred from the shading pattern-1 that FF for LS-TCT topology is superior.

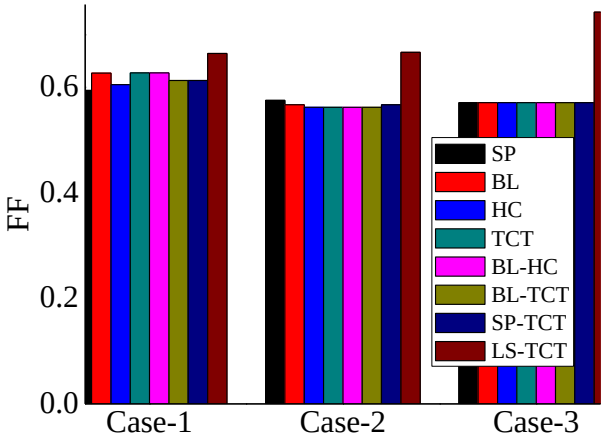

Fig. 4.12. FF for cases 1-3 under shading pattern-1

4.4.3 Impact of Shading Pattern-2 on PV Array

(a) *P-V and I-V curves*

The P-V characteristic for shading pattern 2's cases "1-3" is depicted for a PV array in Fig. 4.13. As an example, consider the situation depicted in Fig. 4.6(a)-(c) on the P-V plot. It appears from the graph that the MPP on a global and regional scale are very different. Cases "1-3" on the P-V curve reveal the increasing impact of shading, which can be interpreted in light of the shade example in Fig. 4.6(a). At GMPP, the obtained power for SP, BL, HC, TCT, BL-HC, BL-TCT, SP-TCT, and LS-TCT connections is 1994 W, 2010 W, 2037 W, 2059 W, 2059 W, and 2108 W, respectively. For the shading scenarios depicted in Fig. 4.13(b) and 4.13(c), the corresponding P-V plot is shown below. Power output at GMPP for examples "2" and "3" is shown in Fig. 4.14 as 1686 W, 1721 W, 1703 W, 1725 W, 1725 W, 2004 W, 1379 W, 1379 W, 1379 W, 1379 W, 1379 W, 1892 W for SP, BL, HC, TCT, BL-HC, BL-TCT, SP-TCT, and LS-TCT, respectively. Table 4.3 displays the results of a comparison of the different PV array framework designs at GMPP based on power and voltage. The result shows that the LS-TCT puzzle pattern generates the most power out of a total of eight different 4×4 topologies. Table 4.3 displays the power, voltage, and current for the LS-TCT topology and are able to increase the array's output in a select few shading scenarios.

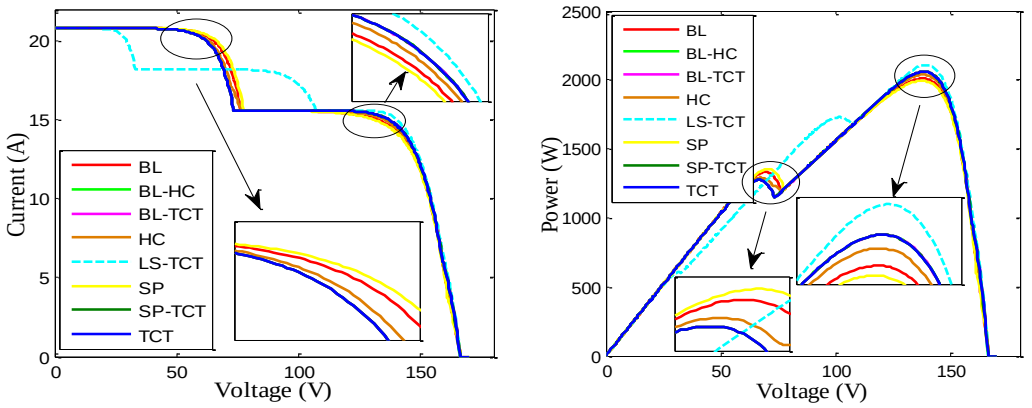

(a) I-V and P-V curves for case-1

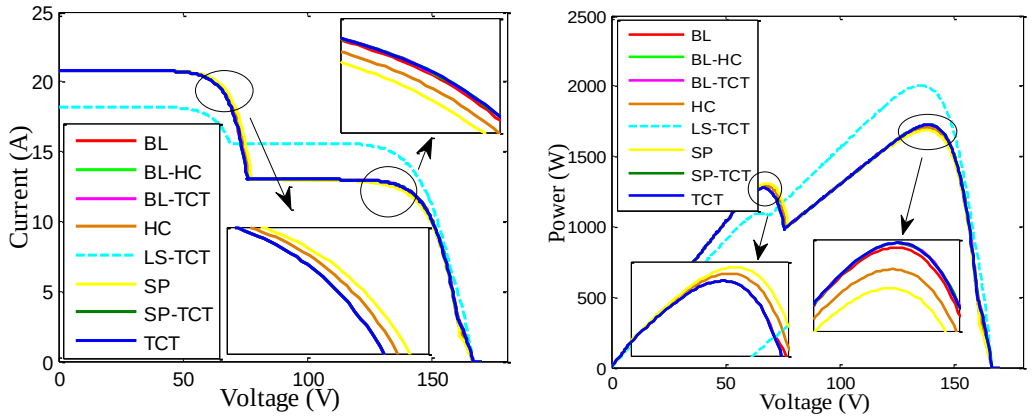

(b) I-V and P-V curves for case-2

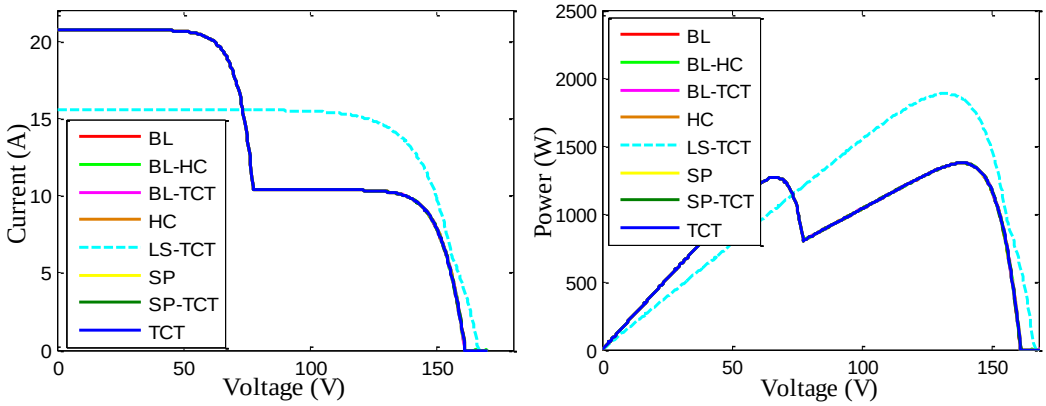

(c) I-V and P-V curves for case-3

Fig. 4.13(a)-(c) I-V and P-V curves under shading pattern-2

Table 4.3-Performance matrices for each topology under shading pattern-2

Performance Parameters	Case-1							
	SP	**BL**	**HC**	**TCT**	**BL-HC**	**BL-TCT**	**SP-TCT**	**LS-TCT**
V_{oc}(V)	166.2	166.2	166.2	166.2	166.2	166.2	166.2	166.2
I_{sc}(A)	20.8	20.8	20.8	20.8	20.8	20.8	20.8	20.8
V_m (V)	137.7	138	138.8	138.5	138.5	138.5	138.5	139.3
I_m (A)	14.48	14.57	14.67	14.86	14.86	14.86	14.86	15.13
P_{GMPP} (W)	1994	2010	2037	2059	2059	2059	2059	2108
P_{LMPP} (W)	1353	1331	1292	1274	1274	1274	1274	1729
P_L (W)	616	600	573	551	551	551	551	502
FF	0.5768	0.5816	0.589	0.5954	0.5954	0.5954	0.5954	0.6097
Performance Parameters	**Case-2**							
	SP	**BL**	**HC**	**TCT**	**BL-HC**	**BL-TCT**	**SP-TCT**	**LS-TCT**
V_{oc}(V)	166.2	166.2	166.2	166.2	166.2	166.2	166.2	166.2
I_{sc}(A)	20.8	20.8	20.8	20.8	20.8	20.8	20.8	18.2
V_m (V)	138.2	138.7	138.2	139	139	139	139	136
I_m (A)	12.2	12.4	12.32	12.4	12.4	12.4	12.4	14.73
P_{GMPP} (W)	1686	1721	1703	1725	1725	1725	1725	2004
P_{LMPP} (W)	1307	1274	1292	1274	1274	1274	1274	1097
P_L (W)	924	889	907	885	885	885	885	606
FF	0.4877	0.4975	0.4925	0.4986	0.4986	0.4986	0.4986	0.6623
Performance Parameters	**Case-3**							
	SP	**BL**	**HC**	**TCT**	**BL-HC**	**BL-TCT**	**SP- TCT**	LS-TCT
V_{oc}(V)	160.7	160.7	160.7	160.7	160.7	160.7	160.7	166
I_{sc}(A)	20.8	20.8	20.8	20.8	20.8	20.8	20.8	15.6
V_m (V)	138.6	138.6	138.6	138.6	138.6	138.6	138.6	131.9
I_m (A)	9.949	9.949	9.949	9.949	9.949	9.949	9.949	14.35
P_{GMPP} (W)	1379	1379	1379	1379	1379	1379	1379	1892
P_{LMPP} (W)	1274	1274	1274	1274	1274	1274	1274	0
P_L (W)	1231	1231	1231	1231	1231	1231	1231	718
FF	0.4125	0.4125	0.4125	0.4125	0.4125	0.4125	0.4125	0.7309

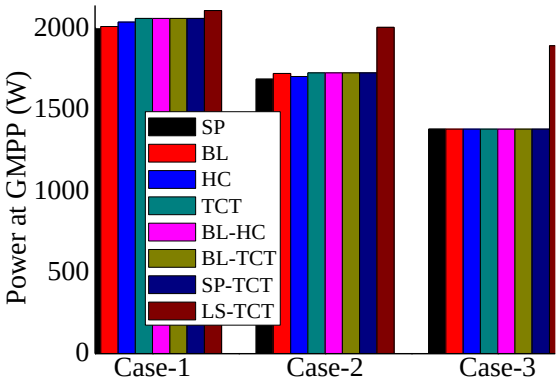

Fig. 4.14 Power at GMPP for cases 1-3 under shading pattern-2

(b) Power Loss

It turns out that the LS-TCT puzzle pattern outperforms the other eight 4×4 topologies in every case of shading pattern-2. Fig. 4.15 is a bar graph depiction of the PL, and Table 4.3 can be used to infer them. The LS-TCT puzzle pattern has the lowest PL across the board.

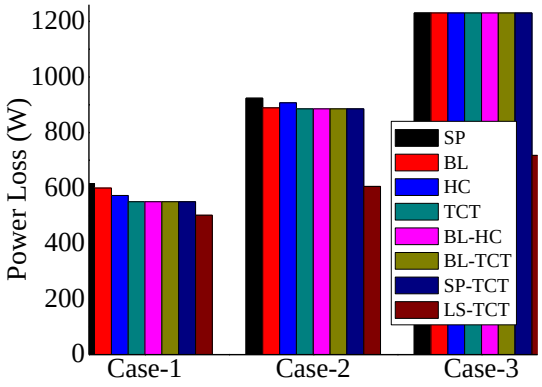

Fig. 4.15 PL for cases 1-3 under shading pattern-2

(c) *Fill Factor*

As shade spreads from one end of a PV Array to the other, it weakens the array as a whole and reduces FF. By using the examples of pattern 2 presented in Fig. 4.6 (a)-(c), it is formed as a bar graph and displayed in Fig. 4.16. Table 4.3 displays its corresponding values for all possible combinations of shading pattern-1. The superiority of FF for the LS-TCT topology in terms of the second shading

pattern is inferred.

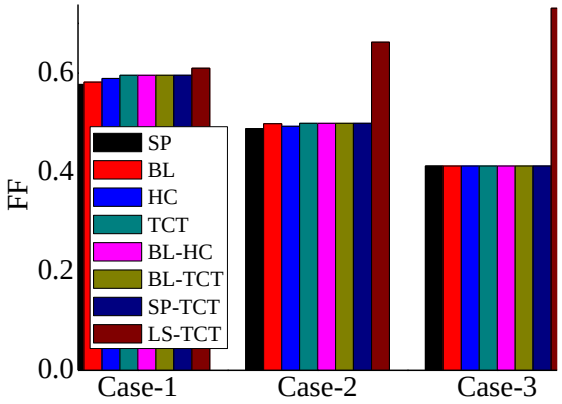

Fig. 4.16 FF for cases 1-3 under shading pattern-2

4.4.4 Effect on PV array under shading pattern-3

(a) *P-V and I-V Curves*

In Fig. 4.17, the performance behaviour of proposed array configurations are investigated with respect to the shading pattern-3 cases "1-3". MPPs are seen on the P–V plot in relation to the shading instance in Fig. 4.7(a) (c). According to the graph, local and global MPP are far apart. As we move from cases "1-3" on the power curve to Fig. 4.7(a), shading's effect increases. GMPP demonstrated 1945 W, 1956 W, 1943 W, 1969 W, 1942 W, 1942 W, 1942 W, and 2004 W for SP, BL, HC, TCT, BL-HC, BL–TCT, SP–TCT, and LS-TCT frameworks. The shading instance of Fig. 4.7(b) (P–V)'s curve is shown in Fig. 4.17. (b). Local and global MPP are far apart, as shown by the graph. At GMPP, SP, BL, HC, TCT, BL-HC, BL–TCT, SP–TCT, and LS-TCT arrangement power is 1615 W, 1613 W, 1626 W, 1628 W, 1626 W, 1626 W, 1613 W, and 1715 W. The shading instance of Fig. 4.7(c) (P–V)'s plot is shown in Fig. 4.17. (c). The power observed at GMPP for this is 1287 W, 1287 W, 1287 W, 1287 W, 1287 W, 1287 W, 1287 W, and 1368 W for SP, BL, HC, TCT, BL-HC, BL–TCT, SP–TCT, and LS-TCT interconnections, as shown in Fig. 4.18 with bar graph representation.

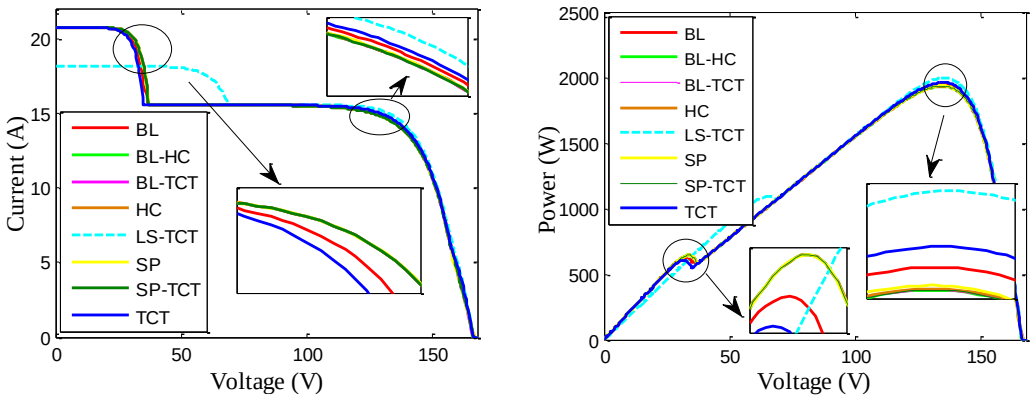

(a) I-V and P-V curves for case-1

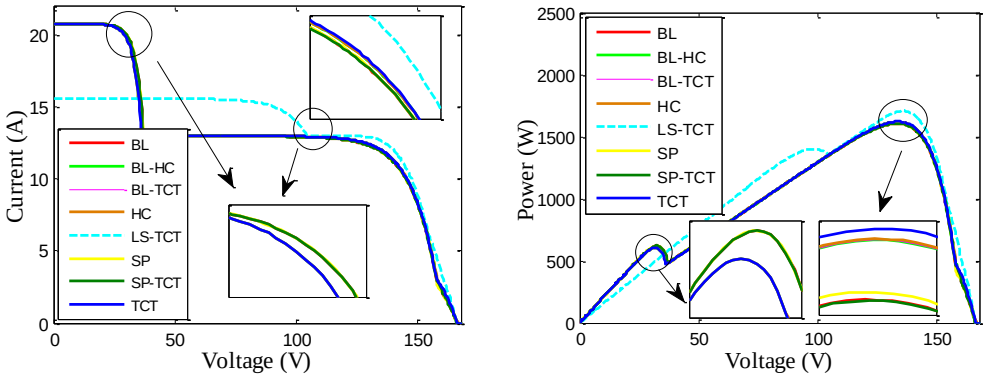

(b) I-V and P-V curves for case-2

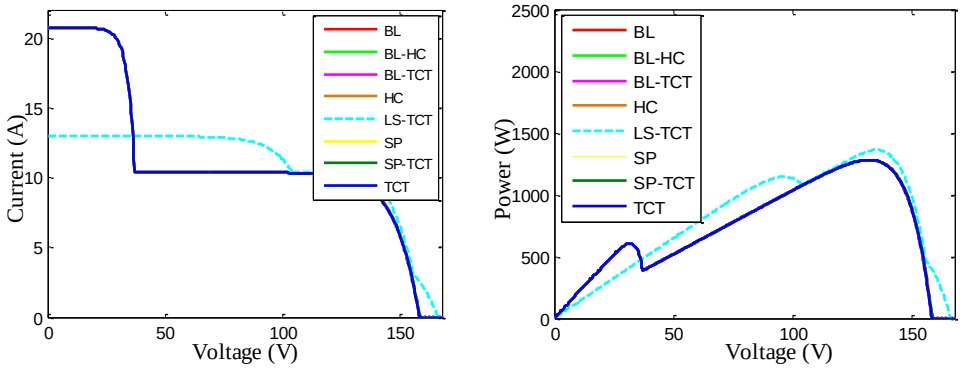

(c) I-V and P-V curves for case-3

Fig. 4.17(a)-(c) I-V and P-V curves under shading pattern-2

Table 4.4 shows LS-TCT arrangement's current, voltage, and power. After reordering modules in LS puzzle pattern, some shading scenarios increase PV array power.

Table 4.4-Performance parameters for configuration experiencing shading pattern-3

Performance Parameters	Case-1							
	SP	**BL**	**HC**	**TCT**	**BL-HC**	**BL-TCT**	**SP-TCT**	**LS-TCT**
V_{oc}(V)	166	166	166	166	166	166	166	166
I_{sc}(A)	20.8	20.8	20.8	20.8	20.8	20.8	20.8	18.2
V_m (V)	134.7	135.2	134.8	135.4	134.8	134.8	134.8	135.3
I_m (A)	14.44	14.47	14.42	14.55	14.41	14.41	14.41	14.81
P_{GMPP} (W)	1945	1956	1943	1969	1942	1942	1942	2004
P_{LMPP} (W)	645.7	622.8	645.7	606.6	645.7	645.7	645.7	1097
P_L (W)	665	654	667	641	668	668	668	606
FF	0.5633	0.5666	0.563	0.5706	0.5626	0.5626	0.5626	0.6632
Performance Parameters	**Case-2**							
	SP	**BL**	**HC**	**TCT**	**BL-HC**	**BL-TCT**	**SP-TCT**	**LS-TCT**
V_{oc}(V)	165.8	165.8	165.8	165.8	165.8	165.8	165.8	165.8
I_{sc}(A)	20.8	20.8	20.8	20.8	20.8	20.8	20.8	15.6
V_m (V)	133.7	133.8	134.1	134.1	134	134	133.9	136
I_m (A)	12.08	12.06	12.13	12.14	12.13	12.13	12.05	12.61
P_{GMPP} (W)	1615	1613	1626	1628	1626	1626	1613	1715
P_{LMPP} (W)	622.8	622.8	606.6	606.6	606.6	606.6	622.8	1407
P_L (W)	995	997	984	982	984	984	997	895
FF	0.4683	0.4679	0.4717	0.4721	0.4713	0.4713	0.4679	0.663
Performance Parameters	**Case-3**							
	SP	**BL**	**HC**	**TCT**	**BL-HC**	**BL-TCT**	**SP-TCT**	**LS-TCT**
V_{oc}(V)	158.3	158.3	158.3	158.3	158.3	158.3	158.3	165.7
I_{sc}(A)	20.08	20.08	20.08	20.08	20.08	20.08	20.08	13
V_m (V)	132.5	132.5	132.5	132.5	132.5	132.5	132.5	135.4
I_m (A)	9.713	9.713	9.713	9.713	9.713	9.713	9.713	10.1
P_{GMPP} (W)	1287	1287	1287	1287	1287	1287	1287	1368
P_{LMPP} (W)	605.9	605.9	605.9	605.9	605.9	605.9	605.9	1148
P_L (W)	1323	1323	1323	1323	1323	1323	1323	1242
FF	0.4049	0.4049	0.4049	0.4049	0.4049	0.4049	0.4049	0.6349

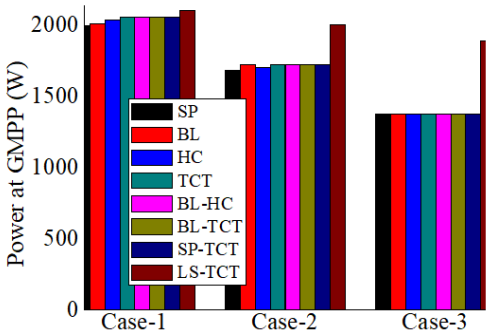

Fig. 4.18 Power at GMPP for cases 1-3 under shading pattern-3

(b) *Power Loss*

The LS-TCT puzzle pattern reveals the highest efficiency in all three cases of shading pattern-3. Bar graph (Fig. 4.19) and tabular form (Table 4.4) are employed to visually and tabularly represent the PL. Furthermore, the LS-TCT puzzle pattern has the lowest PL parameters across all shading conditions for pattern-3.

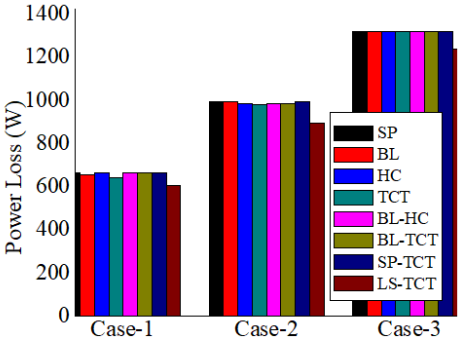

Fig. 4.19 PL for cases 1-3 under shading pattern-3

(c) *Fill Factor*

As the shadow crosses the PV Array from one end to the other, its negative impact grows and the FF drops. Formed as a bar chart by the three shading examples of shading pattern- 3 in Fig. 4.7 (a)-(c), it is displayed in Fig. 4.20. Its values for all of the different shade patterns-3 configurations are shown in Table 4.4. The third shading pattern strongly suggests that FF for LS-TCT topology is the best option.

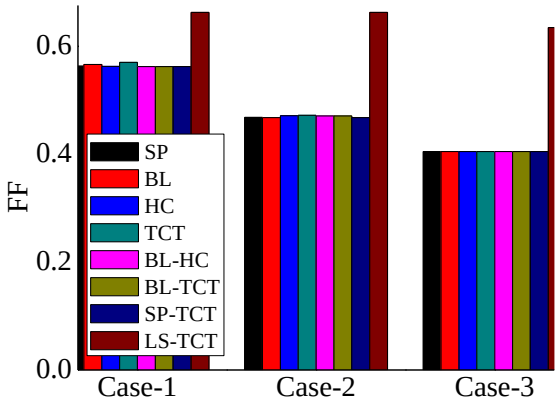

Fig. 4.20 FF for cases 1-3 under shading pattern-3

4.5 RESULTS AND ITS VALIDATION

4.5.1 Analysis of Shading Pattern-4

Complete research into validating the performance of 4×4 sizes of TCT, LS-TCT, SDK, and SPDK configurations is considered under shading pattern-4. As can be seen in Fig. 4.21, the study takes into account irradiation levels of 1000 W/m^2, 500 W/m^2, and 300 W/m^2 in this realistic shading scenario.

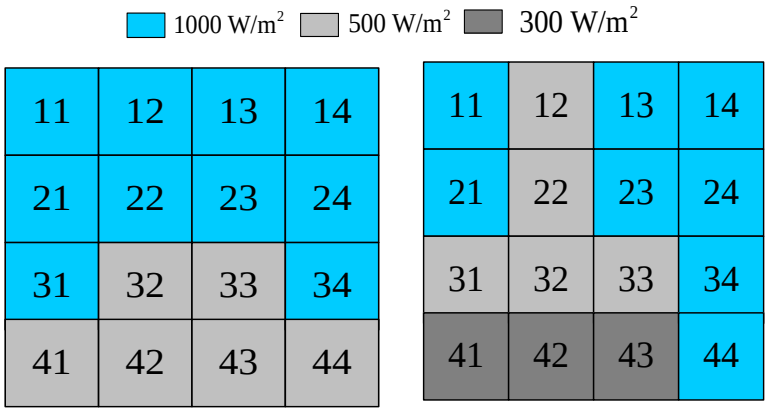

(a) Case-1 (b) Case-2

Fig. 4.21(a)-(c) Shading cases 1-2 for pattern-4

4.5.2 MATLAB /Simulink Analysis: P-V And I-V Characteristics

Under comprehensive analysis of the performance of 4×4 size TCT, SDK, and

SPDK configurations, the MPP can be found at 80W. Fig. 4.22(a)-(b) depicts the results of the investigation that compares the performance of PV array connections in two different shading scenarios (pattern-4). The TCT setup suffered severe PL because of incoherence between the PV module output maximum power and the array's GMPP. In case-I, two non-uniform irradiation conditions (1000 and 500 W/m^2) result in a GMPP of 47.08 W for the TCT arrangement. Additionally, GMPP locations are observed to be 61.77 W, 61.77 W, and 63.89 W under similar sun irradiance conditions for the LS-TCT, SDK, and SPDK configurations, respectively. Based on the highest GMPP and the fewest number of power maxima on P-V curves under PSCs, the performance output of the PV array configurations under consideration is examined.

The lowest equal GMPP values are 54.14 W and the highest PL are observed in TCT and LS-TCT configurations at 25.86 W during a similar shading case-II. The GMMP coordinates for an SDK setup are 61.81 W and those for an SPDK setup are 61.95 W. SPDK has the best GMPP and the lowest PL (18.05 W) in the shading case-I study, in addition to a better FF (0.714).

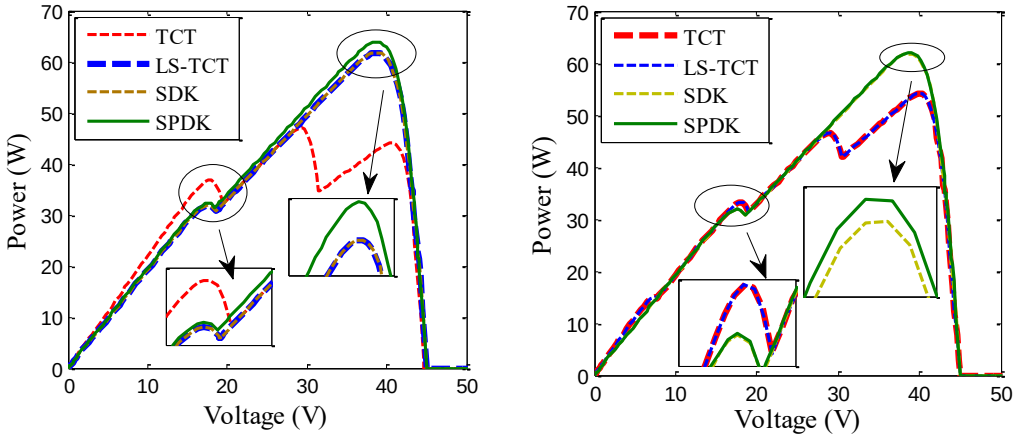

(a) (b)

Fig. 4.22 (a)-(b) P-V characteristics of TCT, LS-TCT, SDK and SPDK systems

Fig. 4.23(a) displays the results of shading case-I testing of the I-V characteristics of TCT, LS-TCT, SDK, and SPDK configurations (pattern-4). In comparison to the SDK, LS-TCT, and TCT configurations, where the maximum current is 1.611 A, 1.611 A, and 1.582 A, respectively. The SPDK configuration produces the highest maximum current (I_m) at 1.652 A. Each of the O.C. voltages (V_{OC}) measures at 44.64 V, 45.028 V, 45.028 V, and 45.028 V.

The values of current under shading case-II (pattern-4), are 1.350 A for TCT, 1.589 A for LS-TCT, 1.350 A for SDK and 1.350 A for SPDK. All PV array configurations show a value of 45.028 V, which is observed to be the case. It proves that uneven solar irradiation is more damaging to S.C. current than V_{OC} .

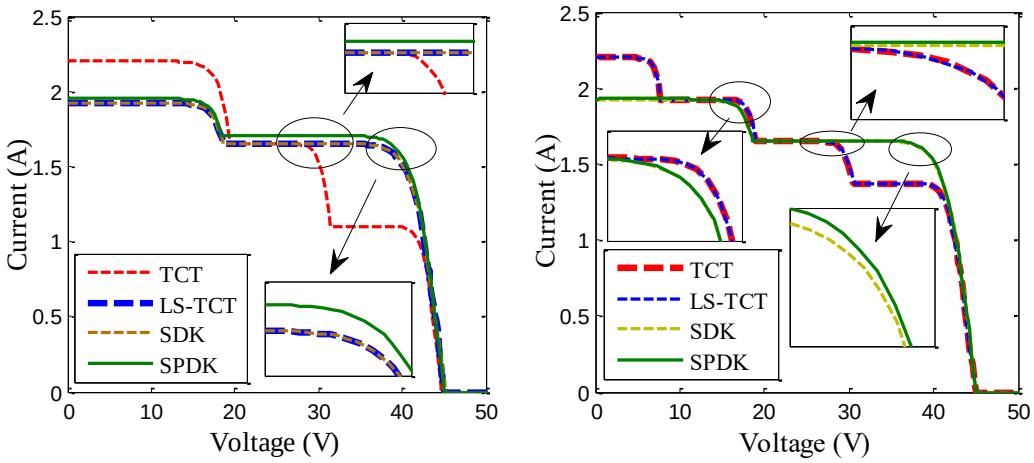

Fig. 4.23 (a)-(b) I-V characteristics of TCT, LS-TCT, SDK and SPDK configurations

Quantitative results from an in-depth investigation of shading's impact on a photovoltaic system are compiled here in Table-4.5 as,

Table 4.5-Performance matrices for shading pattern-4

Performance Parameters	Case-1							
	MATLAB/Simulation study				Experimental study			
	TCT	LS-TCT	SDK	SPDK	TCT	LS-TCT	SDK	SPDK
V_{oc}(V)	44.64	45.028	45.028	45.028	44.88	44.45	44.18	44.65
I_{sc}(A)	2.19	1.92	1.92	1.95	2.202	1.927	1.927	1.977
V_m (V)	29.22	39.03	39.03	38.66	29.32	38.54	38.54	39.29
I_m (A)	1.611	1.582	1.582	1.652	1.561	1.555	1.555	1.584
P_{GMPP} (W)	47.08	61.77	61.77	63.89	45.77	59.95	59.95	62.25
P_{LMPP} (W)	36.68	31.86	31.86	32.34	34.8	29.99	29.99	32.51
P_L (W)	32.92	18.23	18.23	16.11	34.23	20.05	20.05	17.75
FF	0.481	0.714	0.714	0.727	0.708	0.801	0.801	0.807
Performance Parameters	Case-2							
	MATLAB/Simulation study				Experimental study			
	TCT	LS-TCT	SDK	SPDK	TCT	LS-TCT	SDK	SPDK
V_{oc}(V)	45.028	45.028	45.028	45.028	45.03	45.04	45.06	45.09
I_{sc}(A)	2.199	2.199	1.924	1.927	2.22	2.22	1.955	1.968
V_m (V)	40.05	40.05	38.89	38.97	41.11	41.04	38.77	38.47
I_m (A)	1.351	1.351	1.589	1.350	1.279	1.330	1.561	1.610
P_{GMPP} (W)	54.14	54.14	61.81	61.95	52.62	54.69	60.55	61.95
P_{LMPP} (W)	33.26	33.26	31.9	31.9	31.24	32.49	32.49	32.49
P_L (W)	25.86	25.86	18.19	18.05	27.38	25.31	19.45	18.05
FF	0.548	0.543	0.713	0.714	0.526	0.551	0.687	0.6982

4.5.3 Experimental Analysis: P-V And I-V Characteristics

The effectiveness of TCT, LS-TCT, SDK, and SPDK arrangement in a 4×4 array is investigated experimentally. The maximum power point (MPP) is 80W when exposed to ideal/uniform irradiance of 1000 W/m^2. Moreover, similar shade scenarios I and II are used in the present investigation of PV system configurations (pattern-4). The experimental setup is depicted in Fig. 4.24, and its main components are as follows. In order to characterize the PV system, we have (i) sixteen PV modules laid out in a 4×4 matrix, (ii) a resistive load (variable), and (iii) a data logger we developed in-house to record the voltage and current as they occur in real time. This data logger system was built with voltage and current sensors to record and track electrical data in real time. Performance was managed by the Arduino System (ATmega-328 micro-controller). The micro-SD card records the electrical data in real time so it can be analyzed later. The Table-4.6 below details the technical specifications of commercially available solar PV modules and components employed in MATLAB/Simulink simulations and experiments.

Electrical performance of conventional and puzzle-based configurations (TCT, LS-TCT, SDK, and SPDK) are discussed after an extensive experimental study is conducted. Under shading cases I&II, as depicted in Fig. 4.25(a)-(b), P-V curves for all four PV array configurations are obtained.

Table 4.6– Specifications and role of components used in the developed experimental setup.

Section	Components	Specifications	Function/Role
• Solar PV array	• PV module	• PV module max. power: 5 W • I_{sc}: 0.55 A, V_{oc}: 11.25 V • I_m: 0.52 A, V_m: 9.62 V • PV module: 16 (4 × 4 array) • Cell technology: Poly-Si • Manf.: Solar Universe India • Model: SFTI18P5	SP configured PV array (4 × 4) for study under PSCs.
• Electrical Measurements & measuring units (Arduino compatible)	• Voltage Sensor	• Number of voltage sensor: one • Range: 0.02445 - 25 V (DC) • Resolution: 0.00489 • Model: ACS755	After calibration and range extension, voltage sensor module makes it possible to measure voltages of 0–90 V.
	• Current Sensor	• No. of current sensor: one • Range: 0.01 - 30A (DC) • Scale Factor: 100 mV per Amp • Chip: ACS712ELC • Model: ACS-712	Used for PV array current measurement at variable resistance.

	• Arduino Nano	• Microcontroller: ATmega328 • Required supply: +5 V • Digital (I/O) pins: 14 • Analogue (I/P) pins: 8 • Flash memory: 16 KB • Temperature Range: —40 °C-85 °C	Arduino-Nano open-source platform is used. Two analogue pins A_4 and A_5 are used to feed sensor data for electrical performance measurement.
	• Micro SD card with shield	• Working Voltage: 5 V/3.3 V • Size:20 × 28 mm • Interface: SPI • Compatible: Micro SD	Used to record the measured electrical data
	• Personal Computer System	• Windows PC system with Arduino open source.	Required for code writing and uploading to the ATmega328 micro-controller
• Load and solar irradiation measurement	• Variable resistive Load	• Range: 0- 360 Ω, 5 A	Used to characterize the PV system from 0 Ω to maximum required load.
	• Pyranometer	• Sun Irradiation measurementup to 1999 W/m^2 • Resolution: 1 W/m^2	Used for measuring solar irradiation in W/m^2 •

Non-coherence condition between the power maxima point of PV modules in an array causes significant shading losses in the TCT configuration. At non-uniform irradiance levels (1000 W/m^2 and 500 W/m^2), the GMPP of the TCT configuration is 45.77 W in shading case-I. Furthermore, the GMPPs are determined to be 59.95 W for LS-TCT setups, 59.95 W for SDK setups, and 62.25 W for SPDK setups. Performance-wise, SPDK outperforms all other PV configurations when PSCs are used. Under un-even irradiance (1000 W/m^2, 500 W/m^2, and 300 W/m^2), the TCT configuration is seen to have a low value of GMPP as 52.62 W. Different GMPP positions of 54.69 W, 60.55 W, and 61.96 W are observed in LS-TCT, SDK, and SPDK configurations when exposed to the same amount of shading.

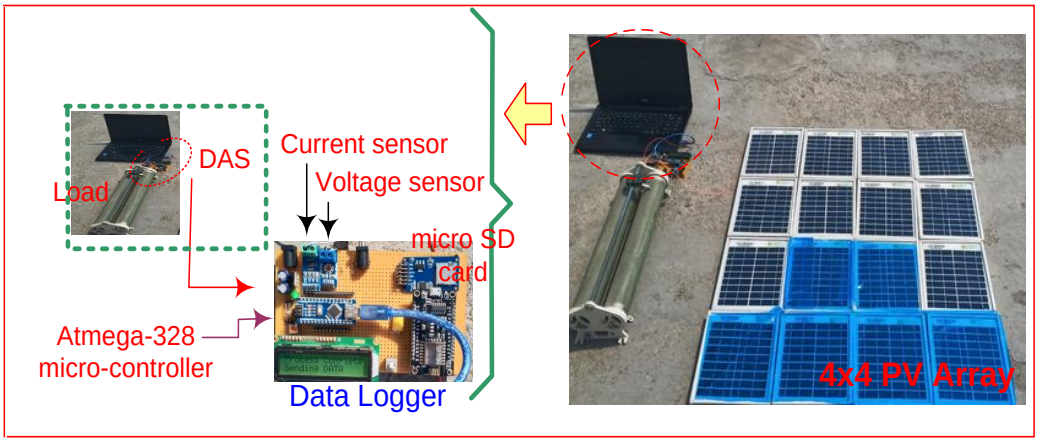

Fig. 4.24 Experimental setup of PV system

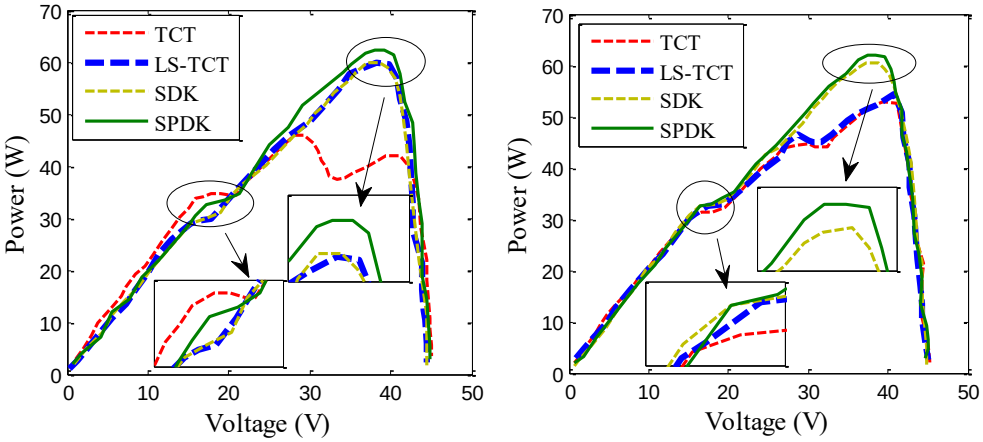

(a) (b)

Fig. 4.25 (a)-(b) P-V characteristics of TCT, LS-TCT, SDK and SPDK configurations

The PV system's S.C. current varies with the amount of available light. During the non-uniform irradiations, Fig. 4.26(a)-(b) displays the performance parameter w.r.t. I-V characteristics of TCT, LS-TCT, SDK, and SPDK configurations. For shading case-I (pattern-4), the S.C. current values are 2.202 A for the TCT configuration, 1.927 A for the LS-TCT configuration, 1.927 A for the SDK configuration, and 1.927 A for the SPDK configuration. SPDK configuration has best performance under distinguish shading scenarios like 1000 W/m^2 and 500 W/m^2, with FF values of 0.708, 0.801, 0.801, and 0.807 respectively.

For the performance analyses, the distinguished irradiance levels (1000 W/m^2, 500 W/m^2, and 300 W/m^2) are taken into consideration for performance assessment. Because of the shading impacts, the S.C. currents are observed as 2.22 A, 2.22 A, 1.955 A, and 1.968 A for the TCT, LS-TCT, SDK, and SPDK configurations respectively. Additionally, the values of FF are studied to be 0.526, 0.551, 0.6873, and 0.6982; the SPDK configuration provides the best results in these cases of varying shading.

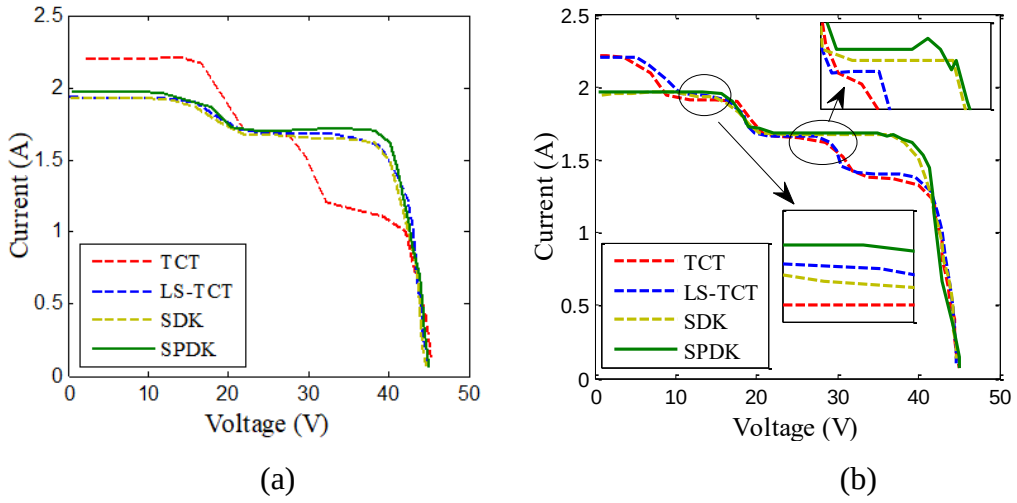

Fig. 4.26 (a)-(b) I-V characteristics of TCT, LS-TCT, SDK and SPDK configurations

(a) Power at GMPP

Fig. 4.27(a)-(b) explored the performance behavior through the Simulink and experimentation studies. During shading cases I-II (pattern-4), the GMPP locations 63.89 W and 61.95 W for the SPDK configuration are found to be higher than those for the considered configurations (TCT, LS-TCT, and SDK) though the MATLAB/Simulink study.

When comparing SPDK configurations to TCT configurations, LS-TCT configurations, and SDK configurations for shading cases I-II (pattern-4), the highest power at GMPP is estimated to be 62.25 W and 61.95 W, respectively. The Global maximum power error is found to be 1.64 W for case I for SPDK configuration, observed under MATLAB/Simulink study and experimental study respectively.

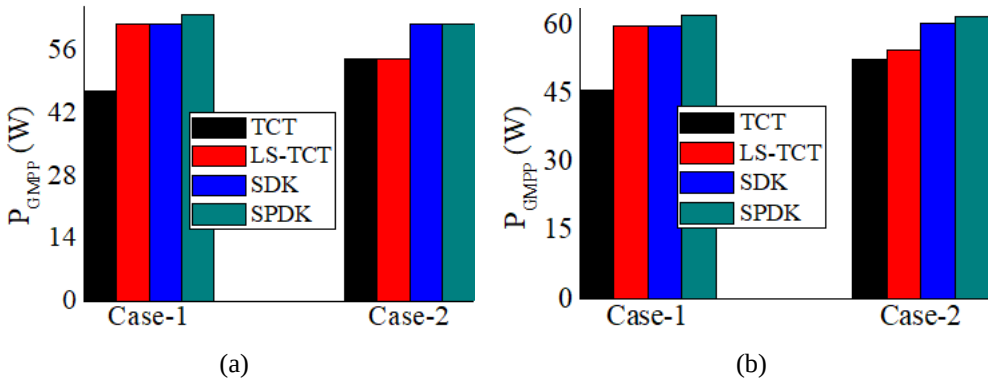

(a) (b)

Fig. 4.27 Power at GMPP for (a) Simulink (b) Experimental analysis

(b) **Power Loss**

For the purposes of PL computations, shading case I and II are considered (pattern-4). Results from both the MATLAB/Simulink modelling and the experimental work are shown in Fig. 4.28(a) and (b). TCT and SPDK configurations experience 32.92 W and 16.11 W, respectively, for the highest and lowest shading case-I, when compared to LS-TCT and SDK configurations. Additionally, when comparing the SPDK configuration to the TCT, LS-TCT, and SDK, the minimum power PL is determined to be 18.05 W for the SPDK.

During shading case I and II, the experimental results show that the PL is minimized for the SPDK configuration, with values of 16.11 W and 18.05 W for the SPDK and LS-TCT and SDK, respectively.

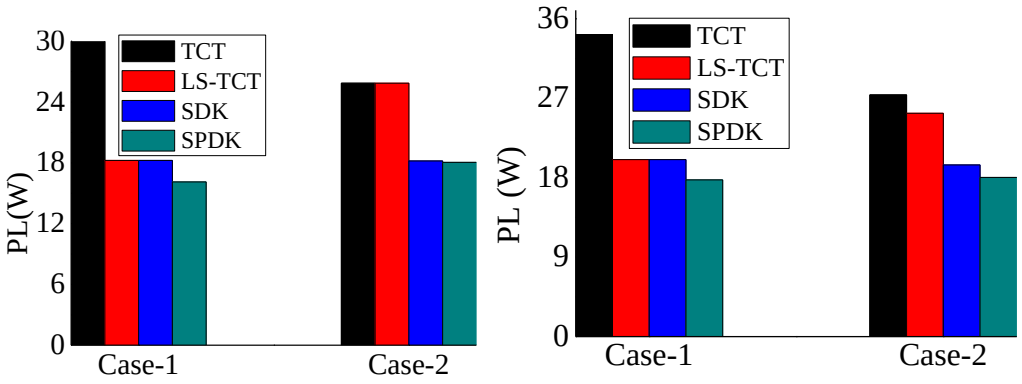

(a) (b)

Fig. 4.28(a) MATLAB/Simulink Study (b) Experimental study

(c) Fill Factor

For the TCT, LS-TCT, SDK, and SPDK configurations, Fig. 4.29 statistically depicts the FF evaluation with dissimilarities observed due to shading cases I-II (pattern-4). SPDK's FF value was improved from 0.727 to 0.714 in MATLAB/Simulink testing. Furthermore, the FF is studied experimentally, with the best values found to be 0.806 and 0.698 for cases I and II of similar shading.

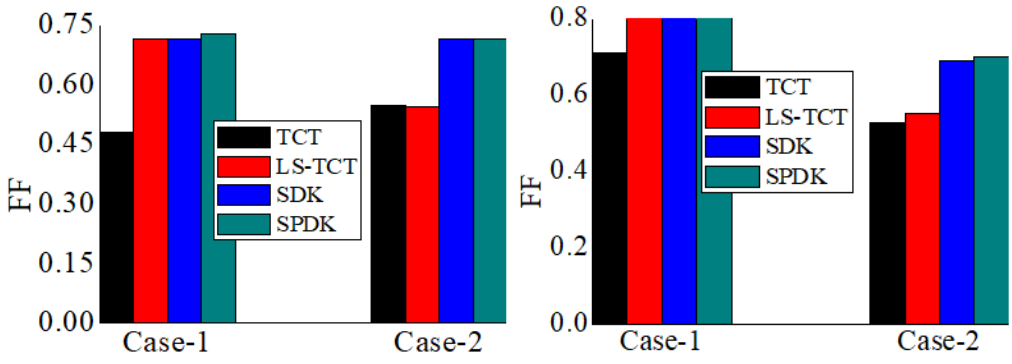

(a) (b)

Fig. 4.29 FF analysis for (a) Simulink (b) Experimental studies

4.6 SUMMARY

In this work, we utilize MATLAB/Simulink models to compare the performance of many different TCT setups, including the SP-TCT, BL-TCT, HC-TCT, BL-HC-TCT, and LS-TCT. Its performance at GMPP, FF, and PL has been evaluated using current, voltage, and power measurements. Due to differences in shading, the LS-TCT had the improved PL and the maximum FF values out of the eight conceivable electrical setups.

- Under shading pattern-1, the most productive puzzle-based LS-TCT configurations achieve a PE of 8.4%, reduce power mismatch losses to 867 W, and boost FF by a maximum of 0.037.

- Compared to TCT (which has higher performance than all other configurations), the LS-TCT configuration's production has the highest PE by 27.11 %, the highest redundancy in mismatch power by 1787 W, and an increased FF of 0.32.

- The puzzle-based configuration proposed in this study has been praised for producing higher extracted output power when testing was conducted using PSCs.

- The best performance is achieved by the proposed SPDK puzzle-based PV array configurations, such as GMPP, PL, and FF. MATLAB/Study: 63.89 W, 16.11 W, 0.727; Experimental Study: 62.25 W, 17.75 W, 0.807; Shading Case 1: (pattern-4).

Experimental research verified the PV system's performance under such shading situations and confirmed the commercial deployment.

CHAPTER- 5

COMPARATIVE STUDY OF SYMMETRIC MATRIX GAME PUZZLE BASED CONFIGURATION FOR HIGHER GMPP

5.1 INTRODUCTION

Due to their numerous benefits, including affordability, reusability, and non-pollution, clean energy sources are becoming increasingly important on a global scale. Solar power is regarded as the principal source of power generation in many home and commercial applications among all RE sources [Gautam and Kaushika,2002; Kaushika and Gautam,2003]. It has been noted that over the previous decade, advances in solar energy technology have been a frequent occurrence. A PV module is ineffective at assisting the high power required load and has a very low efficiency [Karatepe *et al.*, 2007]. As a result, electrical connection methods are preferred to meet larger power demands. PV panel connections are allowable in both parallel and series configurations. The SP, BL, HC, and TCT interconnection schemes are used for the investigation during the PSCs to increase power supply to load [Patel and Agarwal, 2008].

The unique PV array configuration's key features are listed below:

- Using SM-TCT interconnections of PV panels increases shade dispersion over the area covered by the PV array.
- Because of the dramatic reduction in shadow cast on PV modules along any given row, power and voltage are both increased at GMPP compared to TCT, NTCT, and the Shape-do-Ku configurations, as explained by the shade dispersion effect.
- A comprehensive comparison analysis is performed between

MATLAB/Simulink and experimental validation.

- Three realistic PSCs evaluate GMPP positions (voltage and power), FF, and PE performance.

5.2 PV SYSTEM MODELLING AND GAME PUZZLE-BASED CONFIGURATIONS

In the following section, we will discuss the various models used in the process of work planning:

5.2.1 PV System Modelling

In order to supply the demand power to loads, PV array systems are designed by connecting the PV modules in series and/or parallel configurations [Yadav *et al.*, 2017]. The electrical circuit for PV cell is depicted in Fig. 5.1 as,

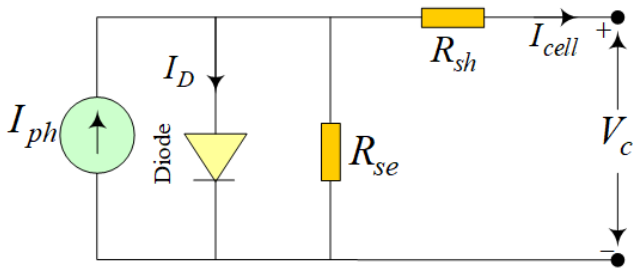

Fig. 5.1 Electrical circuit diagram of a PV cell

The voltage of a PV cell (V_C)is articulated through Eq. (1) as,

$$V_C = \frac{AkT_c}{e} ln\left(\frac{I_{ph}+I_D-I_{cell}}{I_D}\right) - \frac{R_{se}R_{sh}}{R_{se}+R_{sh}} I_{cell} \quad (1)$$

In order to simulate a PV module in MATLAB, you will need to know its technical specifications. Further, 16 individual 5 W commercial PV modules (SFTI18P5: Solar universe India) are utilised in this investigation. Table 5.1 displays the detailed specifications as,

Table 5.1- Specifications of PV modules at 1000W/m^2, 25^{o}C

Parameters	Values (For simulation study)	Values (For experimental study)
V_{oc}	44.2 V	11.25 V
I_{sc}	5.2 A	0.55 A
V_m	35.8 V	9.62 V
I_m	4.75 A	0.52 A
P_m	170 W	5 W

5.2.2 Conventional TCT Configuration

In order to achieve the TCT PV array configuration arrangement, the SP arrangement is modified by establishing cross connections between each row and column of the PV array [Vijayalekshmy *et al.*, 2016]. The voltage from a PV array can be represented graphically as the sum of the voltages from 'n' rows. Therefore, it is written in Eq. (2) using Kirchhoff's voltage law,

$$V_{array} = \sum_{i=1}^{i=n} V_i \tag{2}$$

Eq. (3) expresses Kirchhoff's law, which is used for current analysis at each node point of a PV array as,

$$I_{array} = \sum_{i=1}^{i=4} I_{(j,i)} - I_{(j+1,i)} = 0 \tag{3}$$

In Eq. (4), the current (I_m) generated by the PV modules is proportional to the actual solar irradiance intensity (S_x). This maximum current, I_m is reached at an irradiance of 1000W/m^2 under standard test conditions (S_{STC}) as,

$$I_m = \frac{S_x}{S_{STC}} I_{max} \quad (4)$$

Here, we propose an innovative, less complicated plan for swapping out the PV modules normally used in conventional TCT. When there is a lot of shade, it casts a wider shadow over the PV modules. Acceptance of the suggested PV module replacement scheme is straightforward regardless of the size of the array [Vijayalekshmy *et al.*, 2016]. As can be seen in Fig. 5.2, the first column element from the traditional TCT layout is preserved in the similar column in the new, proposed NTCT layout.

Elements from the first column in the traditional TCT layout of the PV array are maintained in the same position in the proposed NTCT layout. The preferred setup switches the PV modules from the first row of the traditional TCT configuration to the diagonal positions. It's a complete reorganisation of all PV modules after the first row. If you use the Zig-Zag method, PV modules may be rearranged in any row or column for the same result. This system uses 4×4 size PV module arrays, as recommended. The photovoltaic cells shown in the first and third columns have been rotated through 180 degrees to form a clockwise pattern, while those in the second column have been flipped through 180 degrees to form a anticlockwise pattern. Whereas in traditional TCT configurations the PV modules were placed sequentially between the cells, in NTCT they are interspersed at random. If a PV cell is damaged beyond repair, the next cell in the module is activated. According to the suggested plan for rearranging PV modules, the 2×2

modules should be placed where the 3×2 modules are currently standing. The same has been allotted to the subsequent location after that one. When it comes to setting up your [Vijayalekshmy *et al.*,2016] is shown in Fig.5.3 as,

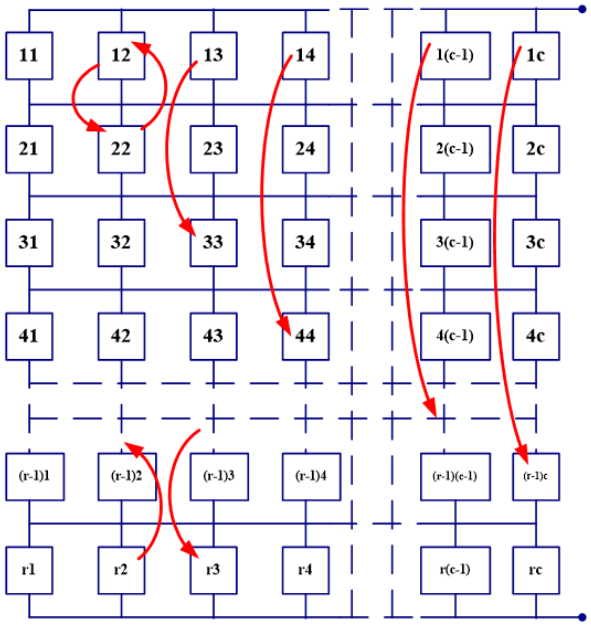

Fig. 5.2 Zig-Zag arrangement for NTCT configuration [Vijayalekshmy *et al.*,2016]

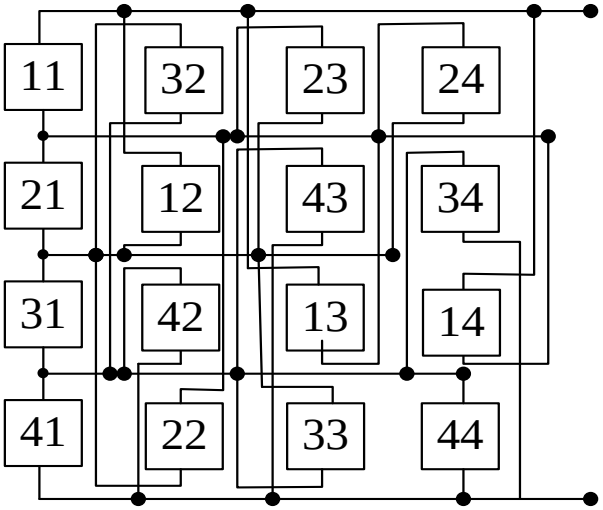

Fig. 5.3 PV module arrangement of NTCT configuration

5.2.3 Shape-Do-Ku Configuration

The Shape-do-Ku puzzle is presented in several symmetrical grid sizes, from 4×4 to 5×5 to 6×6. In comparison to SDK puzzles, SPDK puzzles share the same characteristic of not having any extra outlined regions (like the 3×2 boxes in a 6×6 Su-do-Ku puzzle). Thus, it can be concluded that the Shape-do-Ku puzzle is not technically similar to the Su-do-Ku puzzle but rather is a variant of the Latin square puzzles, in which the only requirement is that each number appears at least once in each row and each column [Wanko and Nickell,2013]. The electrical PV array layout inspired by the Shape-do-Ku puzzle game, in a 4×4 configuration is depicted in Fig.5.4 as,

41	22	33	14
31	12	43	24
21	42	13	34
11	32	23	44

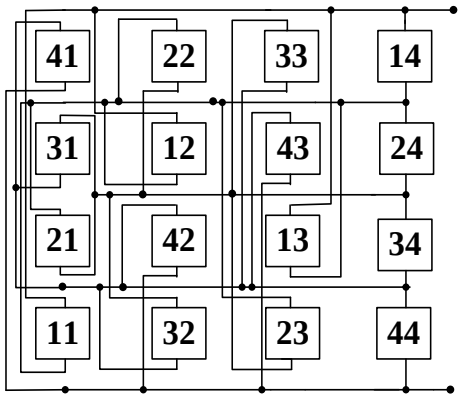

(a) SPDK puzzle (b) Arrangement of SPDK configuration

Fig. 5.4(a)-(b) Reconfiguration methodology of Shape-do-Ku PV array configuration

5.2.4 SM-TCT Configuration

To define SM, we can say that it is a rational cyclic arrangement of integers in a matrix. The sum of the integers in any two adjacent rows or columns in this matrix remains constant. Furthermore, either element of the diagonal is repeated within itself. All the properties of the 4×4 size SM are shown in Fig.5.5(a)-(d) as,

1	2	3	4
2	3	4	1
3	4	1	2
4	1	2	3

(a) Row property

1	2	3	4
2	3	4	1
3	4	1	2
4	1	2	3

(b) Column property

1	2	3	4
2	3	4	1
3	4	1	2
4	1	2	3

(c) Single diagonal property

	C1	C2	C3	C4
R1	1	2	3	4
R2	2	3	4	1
R3	3	4	1	2
R4	4	1	2	3

(d) Repeated sub-matrix elements

Fig. 5.5(a)-(d) SM properties

In accordance with SM properties, it is found that the sum of each row's and column's elements is 10. As can be seen in Fig.5.5(d), there is also a pattern of sub-matrices that are square and repeat every two rows and two columns. When referring to a 4×4 size PV array, Each PV module has two digits: one for rows and one for columns.

In Fig.5.6, the PV module positions are shifted with the help of the suggested SM-TCT arrangement, without any alteration to the electrical interconnections of the PV panels under PSCs.

11	22	33	44
21	32	43	14
31	42	13	24
41	12	23	34

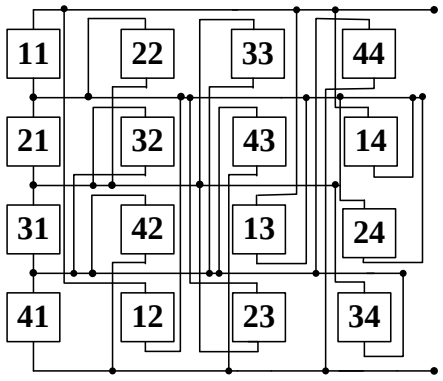

(a) SM based arrangement (b) Arrangement of SM-TCT configuration

Fig. 5.6(a)-(b) Reconfiguration methodology of SM-TCT array configuration

For the placement of elements in the order of (j × k), nth element can be stored corresponding to jth row and kth column, n_{jk} can be written as shown in Eq. (5).

$$n_{ik}, where \begin{cases} j = no.\ of\ row & (j = 1,\ 2, \ldots 4) \\ k = no.\ of\ column & (k = 1,\ 2, \ldots 4) \end{cases} \tag{5}$$

(i) Summation: Row elements

The formulas for four distinct cases of row-wise summing are given in Fig.5.4(a) and implemented through Eq. (6) as,

$$\sum_{k=1}^{k=4} n_{jk} = Summation\ for\ j^{th} row\left(j = 1,2,3,4\right) \tag{6}$$

(ii) Summation: Column elements

The formulas for four distinct cases of column-wise summing are presented in Fig. 4(b) and implemented through Eq. (7). For achieving the SM-TCT configuration, Eq. (5)– (7) are referred.

$$\sum_{j=1}^{j=4} n_{jk} = Summation\ for\ k^{th} column\ (k = 1,2,3,4) \tag{7}$$

5.3 PERFORMANCE PARAMETERS AND COMPARATIVE SHADE STUDY

As a result of PSCs, each PV module in an array has a unique MPP. To further improve the system's efficiency, bypass diodes are used to divert the power produced by PV modules that are partially shaded. Because of the shading effect, the MPP tracking algorithm is always mislead by the presence of LMPP and GMPP. It is possible to monitor performance parameter PSCs with the help of P-V and I-V curves, as shown in Fig. 5.7.

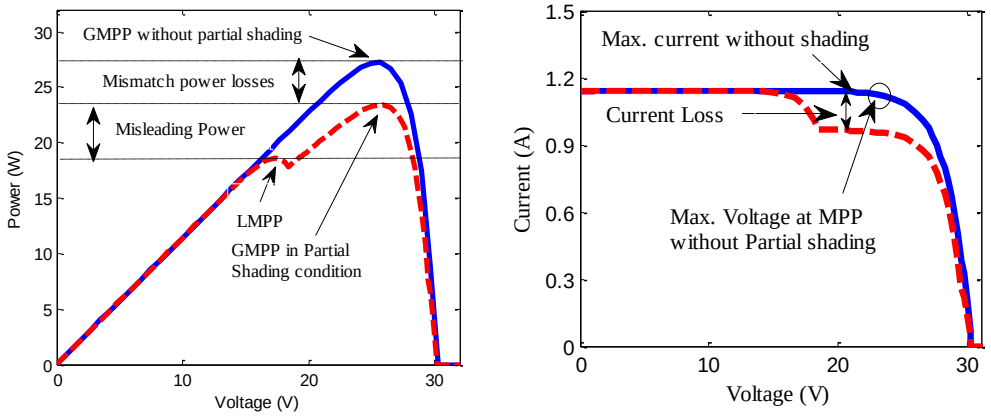

(a) P-V characteristics (b) I-V characteristics

Fig. 5.7(a)-(b) P-V and I-V characteristics

GMPP refers to the maximum power output that can be generated from a PV module when subjected to constant solar radiation levels under PSCs. PL is defined by Eq. (8) as the ratio of the maximum power produced by the array without shading effect to the power generated under PSCs.,

PL= GMP under uniform irradiation – GMP under non-uniform irradiation (8)

5.3.1 Fill Factor

The P-V and I-V curves are used to calculate S.C. current and O. C. voltage at no load. This significant decline in GMPP under PSCs is attributed to the PL that occurs as a result of shading, which also has an effect on the FF value. Eq. (9) can be used for FF evaluation as,

$$FF = \frac{V_{mpp}\, I_{mpp}}{V_{oc}\, I_{SC}} \tag{9}$$

5.3.2 Analysis of Shading Patterns

This manuscript examines three elementary PSCs. [Vijayalekshmy *et al.*, 2016] illustrates the partial shading cases that are more appropriate and possibly appear in a PV array (4×4 size) in Fig.5.8(a)-(c). Individual PV module solar irradiance levels are taken into account in the MATLAB/Simulink model's shading test cases for TCT, NTCT, Shape-do-Ku, and SM-TCT configurations. Both the 1000 W/m^2 and the 500 W/m^2 irradiation levels are taken into account in the MATLAB/Simulink analysis. Furthermore, irradiation levels are measured, including 790 W/m^2 (uniform) and 460 W/m^2 (shaded), for in-depth analysis during experimental study.

11	12	13	14
21	22	23	24
31	32	33	34
41	42	43	44

(i) TCT

11	32	23	24
21	12	43	34
31	42	13	14
41	22	33	44

(ii) NTCT

41	22	33	14
31	12	43	24
21	42	13	34
11	32	23	44

(iii) Shape-do-Ku

11	22	33	44
21	32	43	14
31	42	13	24
41	12	23	34

(iv) SM-TCT

(a) Case- I: Double row shading

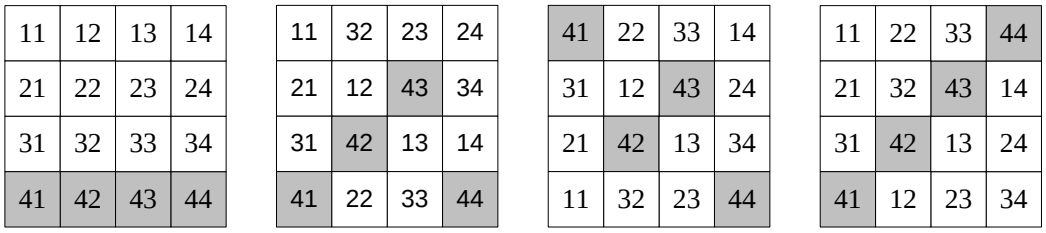

(i) TCT (ii) NTCT (iii) Shape-do-Ku (iv) SM-TCT

(b) Case- II: Single row shading

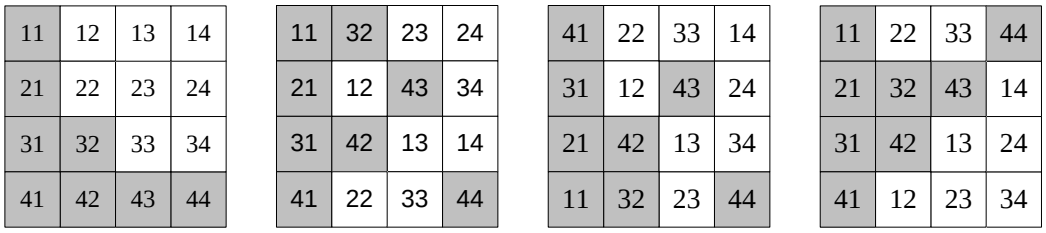

(i) TCT (ii) NTCT (iii) Shape-do-Ku (iv) SM-TCT

(c) Case- III: Oblique shading

Fig. 5.8(a)-(c) Various types shading patterns for performance investigation of PV array

5.4 RESULTS AND DISCUSSION

This study examines the optimal PV array layout in three distinct shading scenarios. TCT, NTCT, SPDK and SM-TCT arrangements of a PV array are analysed, both in reference to their behavioural performance and efficiency, using MATLAB simulation and experimental data. Based on the current flowing through individual row in an array, the general vicinity of the GMPP can be calculated using the formula given in Eq. (10).,

$$I_{R(i)} = \sum_{k=1}^{4} K_{j,k} I_{j,k} \tag{10}$$

In Eq. (11), $K_{j,k}$ depicts solar irradiance for the panels denoted as (j,k).

$$K_{j,k} = \frac{G_{j,k}}{G_{ST}} \tag{11}$$

Where, $G_{j,k}$, the solar irradiance of the PV module is denoted j,k and $i_{j,k}$ is referred to as the generated current by the $(\mathrm{j},\mathrm{k})^{\mathrm{th}}$ module. Generated current from all the PV modules under STC is supposed to be I_m. Therefore, theoretical aspect of generated currents in TCT arrangement within shade case- I as depicted through Eq. (12)-(13) as,

$$I_{R1} = I_{R2} = \left(\frac{1000}{1000}\right) I_m + \left(\frac{1000}{1000}\right) I_m + \left(\frac{1000}{1000}\right) I_m + \left(\frac{1000}{1000}\right) I_m = 4I_m \quad (12)$$

$$I_{R3} = I_{R4} = \left(\frac{500}{1000}\right) I_m + \left(\frac{500}{1000}\right) I_m + \left(\frac{500}{1000}\right) I_m + \left(\frac{500}{1000}\right) I_m = 2I_m \quad (13)$$

Therefore, due to PSCs, row-generated current is not constant. Without taking into account the minute discrepancies between the voltage measured across individual row and the voltage measured across the PV array, is expressed as $V_{array} = 4 \times V_n$. Moreover, the PV array generated power is given in Eq. (14) as,

$$P_{array} = V_{array} \times 4I_m \quad (14)$$

Given that there is no shading of any PV modules and that no rows are ignored in favor of others. For shading case-I, we can express each row's PV array current using Eq. (15)-(24), which we do for the NTCT, Shape-do-Ku, and SM-TCT configurations, respectively.

$$I_{R1} = I_m + 0.5I_m + I_m + I_m = 3.5I_m \quad (15)$$

$$I_{R2} = 0.5I_m + I_m + 0.5I_m + 0.5I_m = 2.5I_m \quad (16)$$

$$I_{R3} = I_m + 0.5I_m + I_m + I_m = 3.5I_m \quad (17)$$

$$I_{R4} = 0.5I_m + I_m + 0.5I_m + 0.5I_m = 2.5I_m \quad (18)$$

The row generated current of Shape-do-Ku configuration is given as,

$$I_{R1} = I_{R2} = 0.5I_m + I_m + 0.5I_m + I_m = 3I_m \quad (19)$$

$$I_{R3} = I_{R4} = I_m + 0.5I_m + I_m + 0.5I_m = 3I_m \quad (20)$$

The row generated current of SM-TCT configuration is given as,

$$I_{R1} = I_m + I_m + 0.5I_m + 0.5I_m = 3I_m \quad (21)$$

$$I_{R2} = I_m + 0.5I_m + 0.5I_m + I_m = 3I_m \quad (22)$$

$$I_{R3} = 0.5I_m + 0.5I_m + I_m + I_m = 3I_m \quad (23)$$

$$I_{R4} = 0.5I_m + I_m + I_m + 0.5I_m = 3I_m \quad (24)$$

PE validation in all permitted NTCT, SPDK, and SM-TCT based arrangement is successful within all three shading test conditions. To arrive at the precise evaluations, we first acquire their MATLAB simulation and experimental study simulation answers. The row current and voltage produced by the TCT, NTCT, SPDK and SM-TCT arrangements in the three different shade scenarios PSCs are used to calculate theoretical power.

5.4.1 Analysis of P-V and I-V Characteristics using MATLAB/Simulink

The effectiveness of TCT, NTCT, Shape-do-Ku and the SM-TCT combinations are all carefully examined. MPP is found to be 2720W under ideal conditions. The behavior of the derived P-V curves for PV array topologies under shading scenarios I to III is shown in Fig. 5.9(a) - (c). Large shading losses are experienced by the TCT arrangement because of the incongruity between the maximum power of the modules and the GMPP of the PV array. To put it another way, the GMPP of the TCT configuration in shading case I is 1452W at both the 1000 W/m^2 and 500 W/m^2 irradiation intensities. On the other hand, we find that the GMPPs for the NTCT, SPDK and SM-TCT arrangements are 1781W, 1831W and 1983W. P-V curve smoothness under shading conditions evaluates PV array configurations.

During the shading case-II, the TCT arrangements poor performance in terms of power is most noticeable at GMPP, where it registers at 2025 W. The GMPP locations for the NTCT, the Shape-do-Ku and the SM-TCT configurations are 2209 W, 2209 W and 2349 W for the same weather conditions (1000 W/m^2, 500 W/m^2). Multiple maximum points on P-V characteristics are used to evaluate the power observed at higher GMPP. Under the shading case-III, power at GMPPs for the TCT, NTCT, Shape-do-Ku, and SM-TCT configurations are observed as 1601 W, 1832 W, 1832 W and 1982 W respectively. Among all of the examined PV arrays, the SM-TCT configuration's shade dispersion (SD) feature allows it to produce the most power at GMPP.

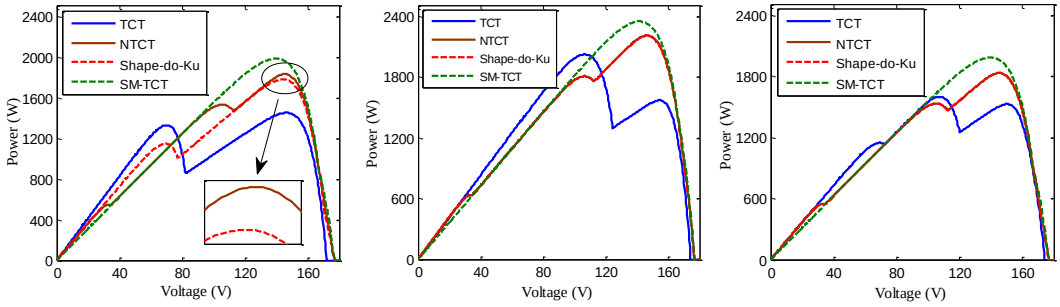

(a) Case-I (b) Case-II (c) Case-III

Fig. 5.9(a)-(c) P–V curves under PSCs.

Fig. 5.10(a)-(c) shows the I-V characteristics of the TCT, NTCT, SPDK, and SM-TCT arrangements for the three different shadowing scenarios of the PV array. Comparing the SM-TCT arrangement to the classical TCT layout, the I-V characteristic is stable. Once all PSCs have been taken into account, it is discovered that the achieved S.C. current of the SM-TCT is lower than that of other setups. All PV array configurations, including 20.8 A, 18.2 A, 18.2 A and 15.6 A have S.C. current values that are observed for case-I.

In the shading instance II, it is seen that the SM-TCT arrangement's I-V

characteristic exhibits smooth behavior, resulting in S.C. current and O.C. voltage of 20.8 A and 171.7 V, respectively. For the TCT, NTCT, and Shape-do-Ku configurations, the values of S.C. current were found to be 20.8 A, 20.8 A and 18.2 A respectively. Due to the impact of shade, NTCT and Shape-do-Ku have more variation. Under shade case-III, SM-TCT based I-V characteristics are smoother than TCT, NTCT, and SPDK configurations. For each setup, the S. C. current is measured and recorded as 18.2, 18.2, 18.2, and 15.6 A, respectively.

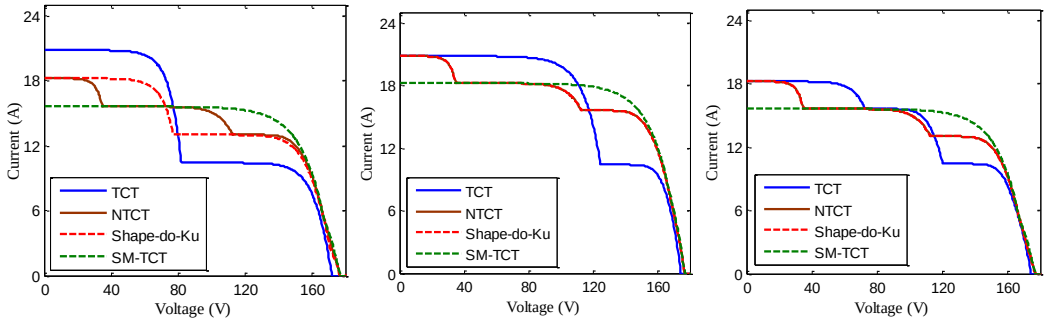

(a) Case-I (b) Case-II (c) Case-III

Fig. 5.10(a)-(c). I–V curves under PSCs

5.4.2 P-V and I-V characteristics: Experimental Analysis

In this experiment, a comparison is carried out for TCT, NTCT, SPDK, and SM-TCT arrangements. Maximum output of 62.39 W is reached under optimal/uniform irradiation conditions (790 W/m^2). Comparable shading cases (I, II, and III) are used to organise the investigation into PV system configurations. Fig. 5.11 depicts the experimental setup. In this experiment, a 4×4 PV array system, a variable load resistance, and a data logger are the main components (self-designed). A data recorder system with voltage and current sensors recorded current and voltage throughout the experiment. The performance of the system was managed by the open-source Arduino system (ATmega-328 microcontroller), and data was stored in micro-SD card to extend the deep understanding.

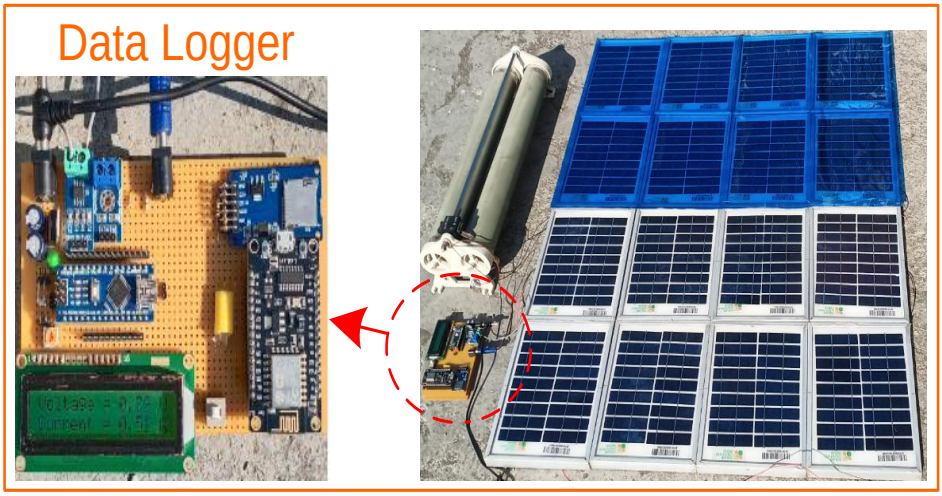

Fig. 5.11. Hardware implementation of PV system

After extensive shadow study, the electrical efficiency of the TCT, NTCT, SPDK, and SM-TCT combinations is assessed. Fig. 5.12(a)-(c) these are the P-V curves for all four PV topologies were produced under shading instances I to III. Power-peak locations on different PV modules that don't line up with one another in an array is causing a significant number of shading losses in the TCT configuration. At distinct irradiation levels of 790 W/m^2 and 410 W/m^2, the GMPP of the TCT setup in shading case-I is 38.24 W. Additionally, for the NTCT, SPDK, and SM-TCT configurations, respectively, the GMPPs are found to be 45.43 W, 44.55 W, and 48.68 W. PV array configurations under PSCs are evaluated by P-V curve smoothness.

The TCT configuration has a low power level at GMPP of 45.47 W for shading case-II. Furthermore, GMPP locations for NTCT, SPDK, and SM-TCT setups with similar non-uniform irradiation conditions (1000 W/m^2, and 500 W/m^2) are different, being 52.48 W, 52.48 W, and 55.46 W respectively. To evaluate the effectiveness of the TCT, NTCT, Shape-do-Ku, and SM-TCT configurations, case-III of oblique-based shading is taken into consideration. Power at GMPP is

calculated from various maximum points on P-V characteristics. For all of the PV array arrangements that were taken into consideration, power at GMPPs was observed at 39.56 W, 45.43 W, 45.43 W, and 48.68 W, respectively.

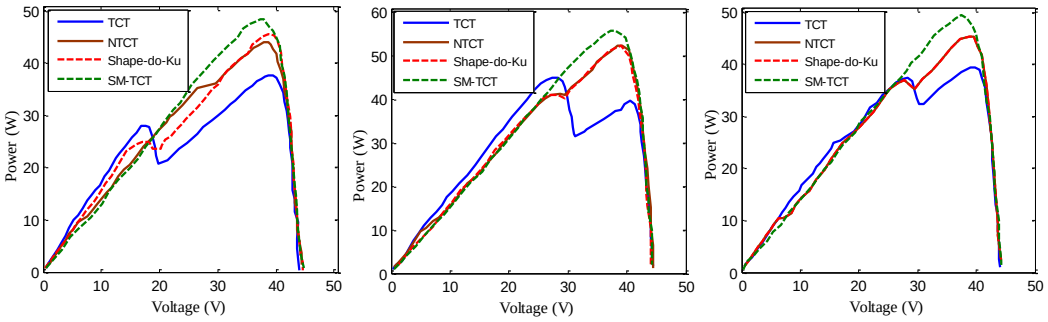

(a) Case-I (b) Case-II (c) Case-III

Fig. 5.12(a)-(c). P–V curves under PSCs

Effect of irradiation level on solar PV system S.C. current. when the amounts of irradiance are not uniform. Fig. 5.13(a)-(c) depicts the I-V characteristics of the TCT, NTCT, Shape-do-Ku, and SM-TCT arrangements for the three different PV array shading scenarios that are being investigated. In contrast to the standard TCT arrangement, the I-V characteristic of the SM-TCT arrangement exhibits no fluctuations for shading case-I. GMPP power is determined using P-V characteristics' highest points. All PV array configurations have observed S.C. current values of 1.737 A, 1.556 A, 1.556 A, and 1.375 A, respectively.

The I-V curves for SM-TCT arrangement has been found to be smoother under shadowing case-II compared to other PV array arrangements. S.C. current and O.C. voltage measurements yield readings of 1.737 A and 44.2 V, respectively. For the TCT, NTCT, and SPDK configurations, the values of S.C. current are determined to be 1.737 A, 1.737 A, and 1.556 A, respectively. Due to the impact of shade, NTCT and Shape-do-Ku have more variation. In contrast to TCT, NTCT, and Shape-do-Ku configurations, the nature of I-V characteristic of SM-TCT is

observed to be smooth in shading cases-III. All PV array configurations S. C. currents are evaluated, and the results are 1.55 A, 1.54 A, 1.54 A and 1.37 A respectively.

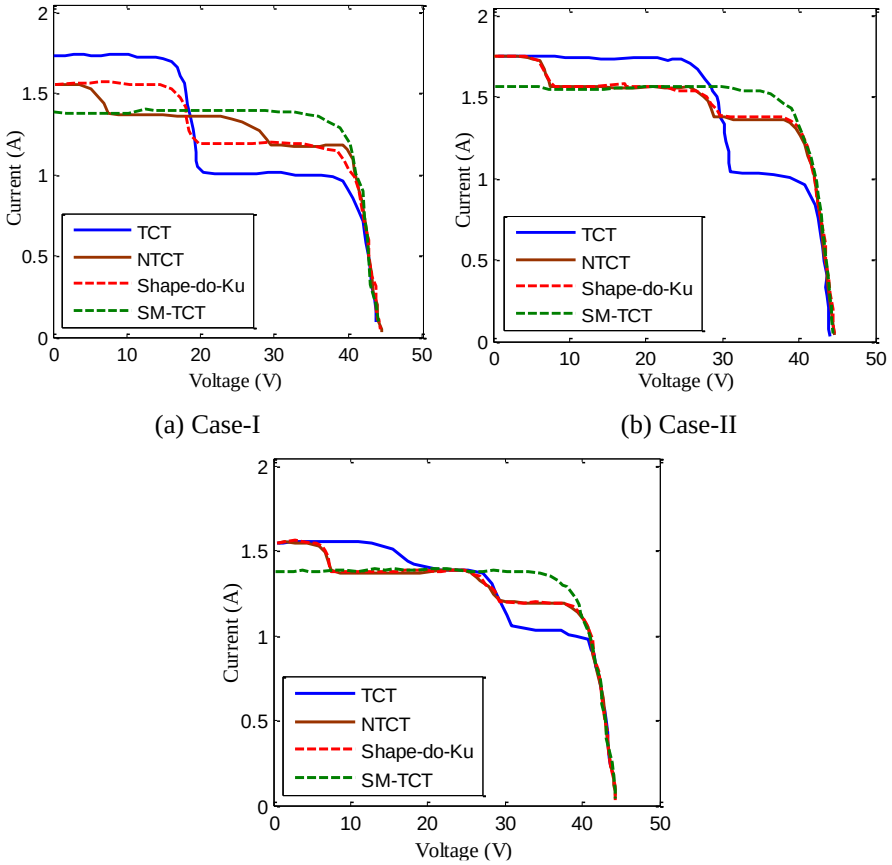

(a) Case-I (b) Case-II

(c) Case -III

Fig. 5.13(a)-(c). I–V curves under PSCs

Both simulated and experimental studies are assessed in terms of P-V and I-V curves to identify the impact of shading cases I-III. Tables 5.2 and 5.3 display the MATLAB/Simulink and experimental study outcomes, respectively.

Table 5.2-Quantitative analysis (MATLAB/Simulink) under PSCs

Performance Parameters	**Case-I**				**Case-II**				**Case-II**			
	TCT	**NTCT**	**SPDK**	**SM-TCT**	**TCT**	**NTCT**	**SPDK**	**SM-TCT**	**TCT**	**NTCT**	**SPDK**	**SM-TCT**
V_{oc}(V)	171.7	176.1	176.1	176.1	174.1	176.5	176.5	176.5	173.9	176.1	176.1	176.1
I_{sc}(A)	20.8	18.2	18.2	15.6	20.8	20.8	20.8	18.2	18.2	18.2	18.2	15.6
V_{GMPP} (V)	147.3	145.3	146.4	140.2	106.7	147.7	147.7	142.3	107.7	145.8	145.8	141
P_{GMPP} (W)	1452	1781	1831	1983	2025	2209	2209	2349	1601	1832	1832	1982
PL (W)	1268	939	889	737	695	511	511	311	1119	888	888	738
PL (%)	46.61	34.52	32.68	27.09	25.55	18.78	18.78	11.43	41.13	32.64	32.64	27.13
FF (%)	40.65	55.56	57.12	72.18	55.91	60.17	60.17	73.12	50.58	57.16	57.16	72.14
PE (%)	--	18.47	20.69	26.77	--	8.32	8.32	13.79	--	12.60	12.60	19.22
Best configuration	**SM-TCT**				**SM-TCT**				**SM-TCT**			

Table 5.3-Experimental study based quantitative analysis of PV array configurations under three PSCs

Performance Parameters	Case-I				Case-II				Case-II			
	TCT	**NTCT**	**Shape-do-ku**	**SM-TCT**	**TCT**	**NTCT**	**Shape-do-ku**	**SM-TCT**	**TCT**	**NTCT**	**Shape-do-ku**	**SM-TCT**
V_{oc}(V)	43.8	44.5	44.5	44.5	44.2	44.5	44.5	44.5	44.2	44.5	44.5	44.5
I_{sc}(A)	1.737	1.556	1.556	1.375	1.737	1.737	1.737	1.556	1.55	1.54	1.54	1.375
V_{GMPP} (V)	39.34	38.7	38.64	37.68	27.91	38.95	38.95	37.68	40.07	38.76	38.76	37.68
P_{GMPP} (W)	38.24	45.43	44.55	48.68	45.47	52.48	52.48	55.46	39.56	45.43	45.43	48.68
PL (W)	24.15	16.96	17.84	13.71	16.92	9.91	9.91	6.93	22.83	16.96	16.96	13.71
PL (%)	38.70	27.18	28.59	21.97	27.11	15.88	15.88	11.10	36.59	27.18	27.18	21.97
FF (%)	50.26	65.61	64.33	79.55	59.22	67.89	67.89	80.09	57.74	66.29	66.29	79.55
PE (%)	--	15.82	14.16	21.44	--	13.35	13.35	21.97	--	12.92	12.92	18.73
Best Configuration	**SM-TCT**				**SM-TCT**				**SM-TCT**			

5.4.3 Power and voltage at GMPP

In Fig. 5.14, shows the assessment of the GMPP's obtained power. MATLAB/Simulink measured the greatest power at GMPP as 1983 W, 2349 W, and 1982 W for SM-TCT setups under shading instances I–III. Additionally, during the experimental study, improved GMPP is obtained for SM-TCT as 48.68 W, 55.46 W and 48.68 W for SM-TCT is comp--red to classical TCT, NTCT, and Shape-do-Ku configurations, respectively.

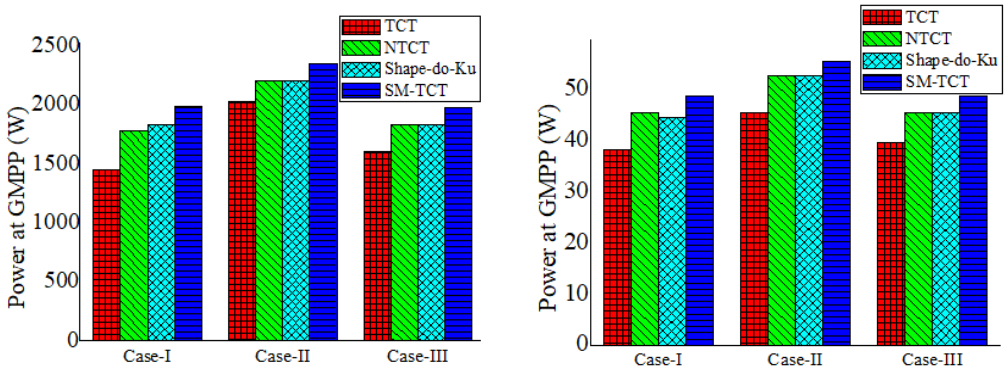

(a) (b)

Fig. 5.14(a)-(b) Power at GMPP (a) Simulink (b) experimental study

Among the most crucial parameters for getting power to the load side is the voltage at GMPP. Voltage at GMPP for TCT, NTCT, Shape-do-Ku, and SM-TCT configurations under shading case-I (147.3 V, 145.3 W, 146.4 V, and 140.2 V), case-II (106.7 V, 147.7 V, 147.7 V, and 142.3 V), and case-III (147.3 V, 145.3 W, 146.4 V, and 140.2 V) are all different (107.7 V, 145.8 V, 145.8 and 141 V).

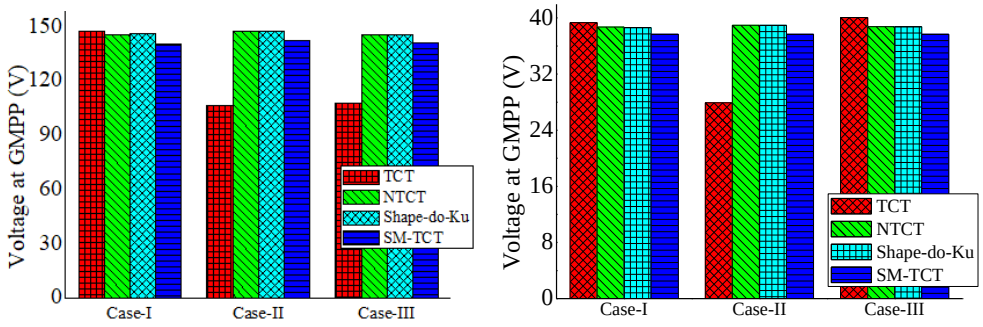

(a) (b)

Fig. 5.15 Voltage at GMPP (a) Simulation (b) Experimental analysis

Differences in voltage at GMPP between the TCT, NTCT, SPDK, and SM-TCT frameworks were observed during the experiment conducted under shading case-I (39.34 V, 38.7 V, 38.64 V and 37.68 V), case-II (27.91 V, 38.95 V, 38.95 V

and 37.68 V) and case-III (40.07 V, 38.76 V, 38.76 V and 37.68 V). For critical performance assessment, Fig.5.15 displays a bar chart showing the voltage at GMPP.

5.4.4 Power Loss

Low PL due to the shading effect on PV systems (TCT, NTCT, SPDK, and SM-TCT) are assessed though the MATLAB/Simulink study. Under shading cases I–III, the SM–TCT configuration is achieved to have the lowest PL at 27.09 %, 11.43 %, and 27.1 %, respectively.

Experimentally, PL observation shows that SM-TCT has the highest values of 21.97 %, 11.10 %, and 21.97 % in all-there-shading cases with similar brightness levels. Through the use of a bar chart, we can see that the PL are lower for the SM-TCT configuration in Fig. 5.16.

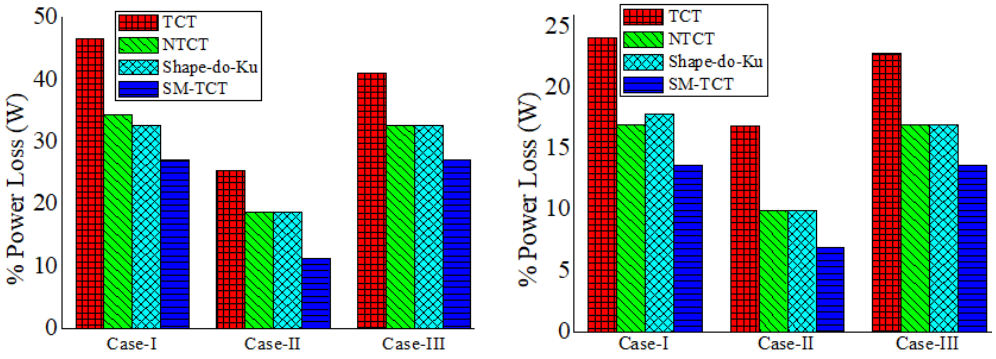

(a) MATLAB/Simulink study (b) Experimental study

Fig. 5.16 (a)-(b). Power Loss

5.4.5 Fill factor

Fig.5.17 is a bar chart contrasting the FF across the various shading instances for the TCT, NTCT, SDK, and SM-TCT configurations. An enhanced FF of 72.18

percent, 73.1 percent, and 72.14 percent was obtained for the SM-TCT in the MATLAB/Simulink investigation of shading examples I, II, and III, respectively. Evaluation of FF shows that SM-TCT achieves the highest values, 79.55 %, 80.09 %, and 79.55 %, respectively, in experimental study under similar shading cases.

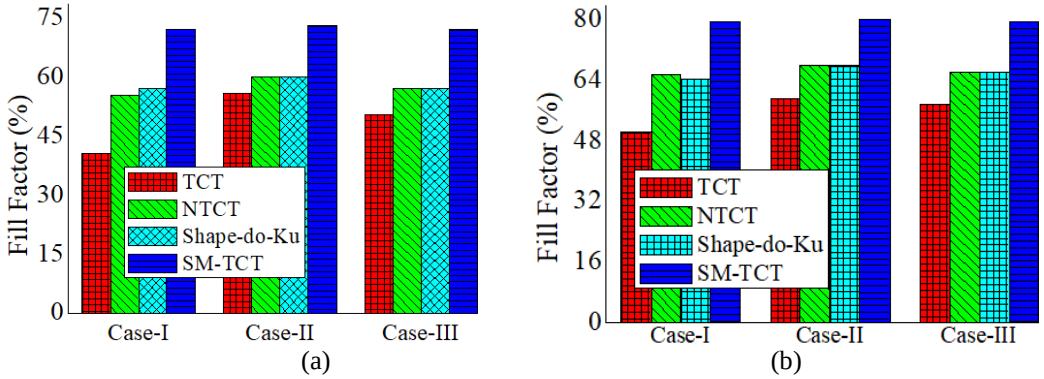

Fig. 5.17 FF analysis under PSCs (a) Simulink study (b) Experimental study

5.4.6 Performance Enhancement

Eq. (25) can be used to calculate PE, which is represented as boost in power output from the rearranged PV array caused by the spread of shade. It can be written as

$$PE = \frac{GMPP_{SM\text{-}TCT} - GMPP_{TCT}}{GMPP_{SM\text{-}TCT}} \quad (25)$$

Experimental research and MATLAB/Simulink are used to evaluate PE. In all three shading scenarios, the SM-TCT configuration achieves the highest PE compared to the TCT baseline (26.77 %, 13.79 %, and 19.22 %, respectively). Additionally, 21.44 %, 21.97 %, and 18.73 % PE were recorded during the experimental study. As can be seen in Fig. 5.18, a bar chart is used to illustrate PE.

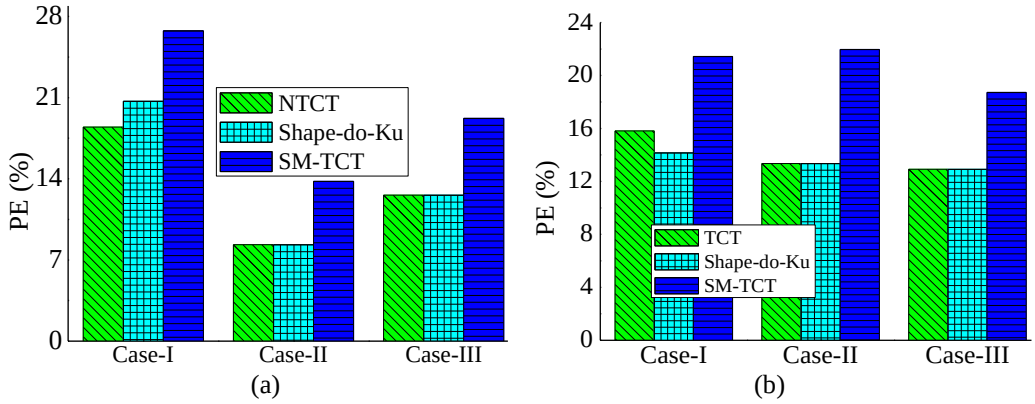

Fig. 5.18 PE analysis under PSCs (a) Simulink study (b) experimental study

5.5 SUMMARY

In this study, the performance of traditional TCT, NTCT with innovative realistic PSCs were used to analyse both Shape-do-Ku and SM-TCT configurations and compared. Any size of PV array can employ the method as a simplified reconfiguration strategy, and performance-related critical metrics like PL, PE, and FF were thoroughly compared in both practical and MATLAB/Simulink investigations. As a result, the design of large PV farms benefits greatly from the suggested reconfiguration method for PV modules. When findings are analysed, the innovative SM-TCT arrangement has fewer power maximum points. The following are the main findings of both studies:

- For case-I, MATLAB/Simulation research conducted under the shade case-I indicated that the optimal performance values for the SM-TCT configuration were 1983 W, 0.72 W, 26.77 %, and 737 W, respectively. Similar performance metrics are noticed and discovered as 48.68 W, 0.79, 21.44 %, and 13.71W during experimental validation.
- Overall, MATLAB/Simulink and experimental experiments using shading scenarios II & III have shown that SM-TCT has the best values.

CHAPTER- 6
EXPERIMENTAL VALIDATION: DPVM-SEC BASED METHODOLOGY TO RECONFIGURE PV ARRAY

6.1 INTRODUCTION

RE is energy that comes from finite resources that can be replenished within a human time frame. Solar, tidal, wave, wind, biomass, and thermal power are all readily available and can be harnessed in nearly any location [Yadav *et al.*,2016]. They are practically endless. Additionally, they have little to no effect on the ecosystem or the climate. The sun's strength is limited by the fact that it is absent at night or when there are more clouds in the sky. Additionally, PSCs become problematic when trying to improvise the efficacy or output of Solar PV array [Kumar *et al.*,2015].

For a variety of causes, PV modules are partially shadowed, including the shadows cast by tall buildings, dry leaves, telecom towers, and more [Singh *et al.*,2021; Anand *et al.*,2020]. The PV panels' derived power decreases with respect to partial shadowing situations. The customization of PV modules employing diverse arrangements, such as Bridge-link (BL), SP, TCT, and honey-comb (HC) game problem dependent setups, can achieve maximum power point tracking (MPPT) [Bleicher *et al.*,2020].

6.2 PV SYSTEM TECHNOLOGY

6.2.1 Development of Photovoltaic System Layout

PV panel voltage is expressed in Eq. (1) and an electrical equivalent circuit is represented in Fig. 6.1,

$$V_C = \frac{AkT_c}{e} ln\left(\frac{I_{ph}+I_{DS}-I_{cell}}{I_{DS}}\right) - \frac{R_s R_{sh}}{R_s+R_{sh}} I_{cell} \quad (1)$$

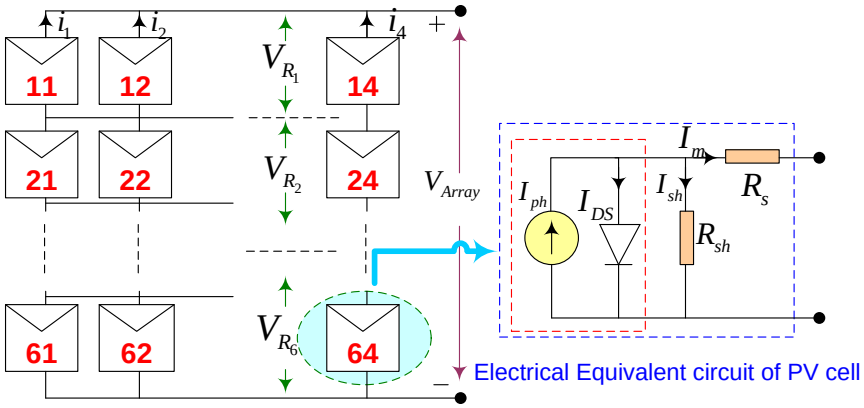

Fig. 6.1 Arrangement in modules of PV array and equivalent circuit

6.2.2 Development of DAS and Experimental Set-up

This experimental setup has been established for comprehensive performance analysis of PV systems operating under PSCs. Under variable resistive load and in a variety of shading conditions, a PV system (6×4) is integrated with a real-time voltage-current data acquisition system (DAS) and experimental setup is depicted in Fig. 6.2 as,

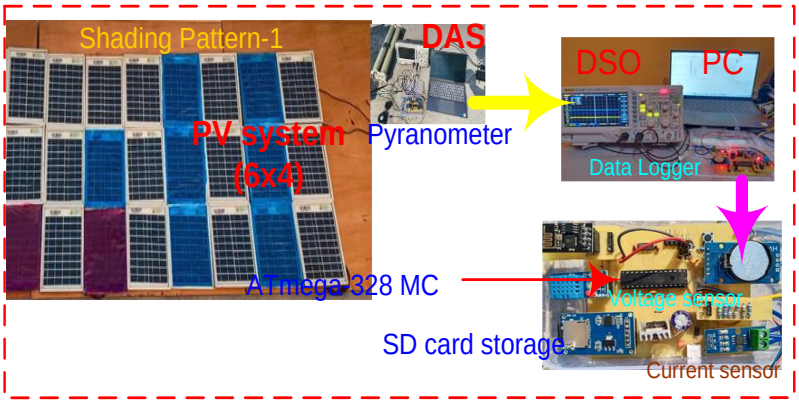

Fig. 6.2 Experimental Setup

To establish a data logger system for a study of electricity's behavior in a shaded setting. Analog sensors (voltage and current) are built into the ATmega-328 microcontroller architecture, allowing for continuous data retrieval. Additionally, the system incorporates a micro-SD card assembly for storing electrical performance for later P-V and I-V characterization analysis. Signal flow diagram of DAS and its wiring configurations elucidate its operation through Fig. 6.3-6.4 as,

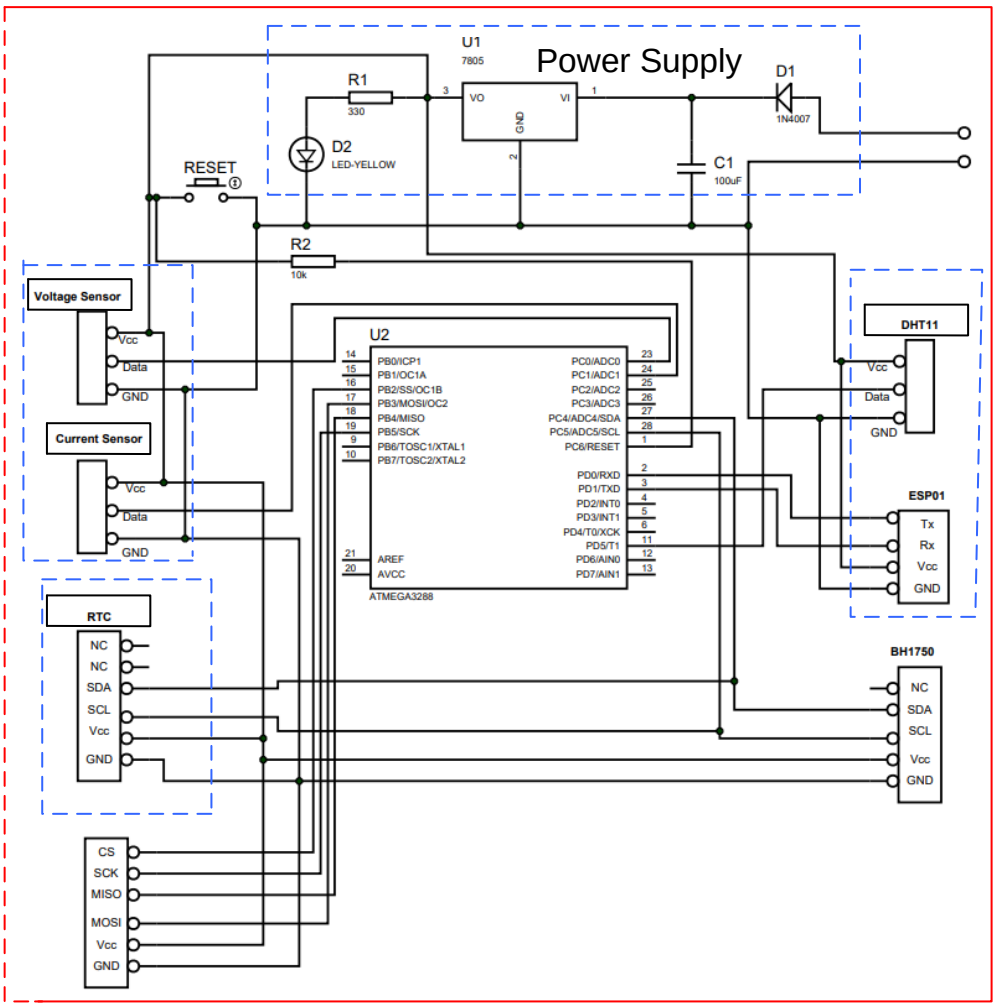

Fig. 6.3 Wiring arrangement of DAS for real time electrical parameters

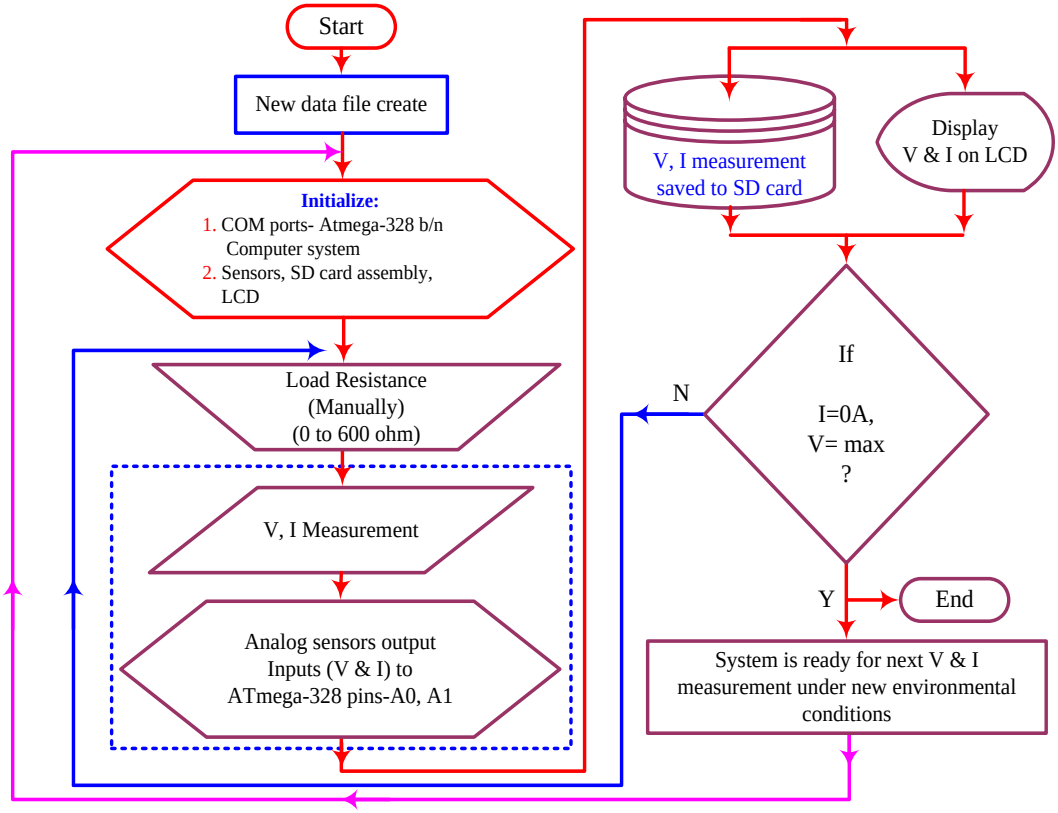

Fig. 6.4 Flow chart to describe the operation of data logger system

6.2.3 Conventional PV Array Arrangements

When PV arrays are connected in series, they are able to generate a substantial amount of energy, which increases the panels' potential. By connecting PV modules in parallel, current can be increased. A straightforward method exists for reorganizing the SP array. TCT configurations, which include cross-tied connections in the parallel strings, are an enhanced form of SP configuration. Because of these changes, mismatch losses caused by PSCs in TCT arrangements are significantly lower than in SP arrangements. Fig. 6.5 depicts the SP and TCT arrangements as,

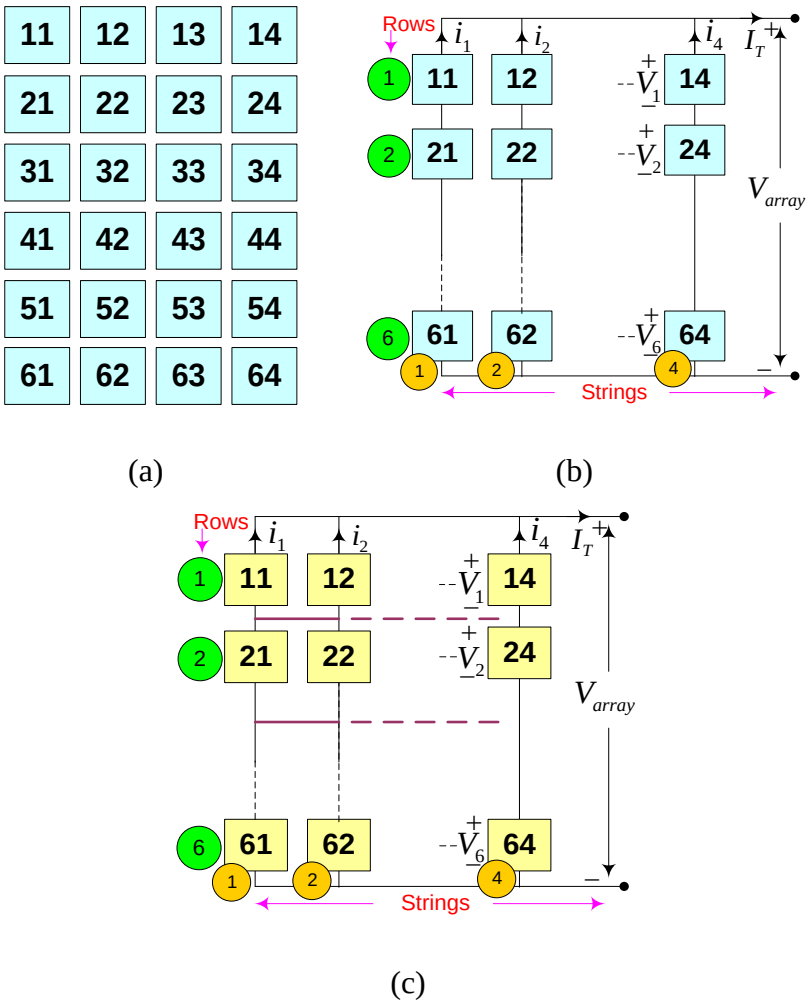

Fig. 6.5(a) Nomenclature of PV system: 6×4 size (b) SP (c) TCT configurations

6.2.4 DPVM-SEC methodology for PV array reconfiguration

Mathematical modelling is provided in Eq. (2) and PV array layout using DPVM-SEC to maximize shade dispersion factor is shown in Table-6.1. The locations of PV arrays according to their naming conventions are shown in Fig. 6.6(a)-(c). In addition, a 6×4 puzzle game is being developed to aid in the reorganization of PV arrays. The puzzle is solved by looking at the integer values

in columns from 1 to 6 and using a seed value-based strategy. To calculate the necessary seed value, we can use the formula,

$$\varphi = \frac{Number\ of\ rows}{2} = \frac{6}{2} = 3 \tag{2}$$

Table 6.1-Placement of integer number to design puzzle for PV array reconfiguration

Column-1	Column-2	Column-3	Column-4
1	1+3=4	(4+3)-6=1	1+3=4
2	2+3=5	(5+3)-6=2	2+3=5
3	3+3=6	(6+3)-6=3	3+3=6
4	(4+3)-6=1	1+3=4	(4+3)-6=1
5	(5+3)-6=2	2+3=5	(5+3)-6=2
6	(6+3)-6=3	3+3=6	(6+3)-6=3

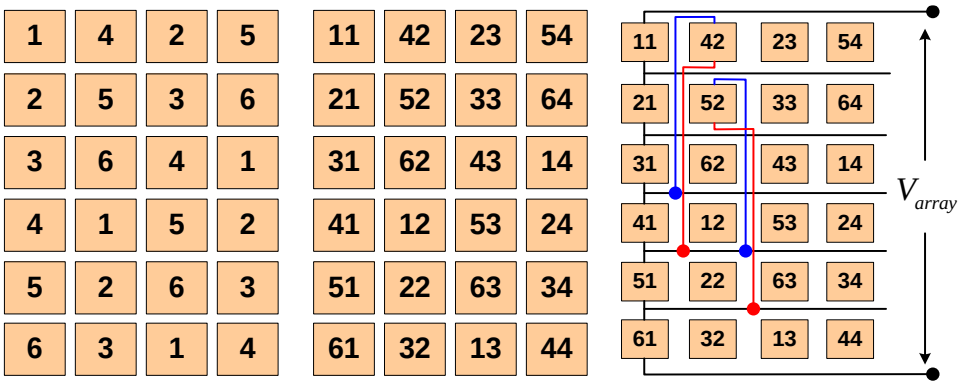

(a) (b) (c)

Fig. 6.6 DPVM-SEC based PV array configurations

6.3 SHADING TRENDS ANALYSIS AND PERFORMANCE PARAMETERS

In this comprehensive analysis of PSCs' impact on PV performance, we take two shading scenarios and a range of sun irradiance levels into account such as

900 W/m^2, 750 W/m^2, 550 W/m^2, 350 W/m^2 and 150 W/m^2. The examined shadow scenarios are shown in Fig. 6.7 as follows,

(a) I (b) II

Fig. 6.7 shading scenarios I-II

Analysis of the shading scenario I row-wise current (SP configuration) theoretically is given in Eq. (3)-(6) as,

$$I_{R1} = I_{R2} = I_{R3} = 0.9I_m + 0.9I_m + 0.9I_m + 0.9I_m = 3.6I_m \quad (3)$$

$$I_{R4} = 0.9I_m + 0.9I_m + 0.55I_m + 0.55I_m = 2.9I_m \quad (4)$$

$$I_{R5} = 0.9I_m + 0.55I_m + 0.55I_m + 0.55I_m = 2.55I_m \quad (5)$$

$$I_{R6} = 0.15I_m + 0.15I_m + 0.55I_m + 0.55I_m = 1.80I_m \quad (6)$$

Analysis of the shading scenario II row-wise current (SP configuration) theoretically is given in Eq. (7)-(9) as,

$$I_{R1} = I_{R2} = 0.9I_m + 0.35I_m + 0.55I_m + 0.55I_m = 2.35I_m \quad (7)$$

$$I_{R3} = I_{R4} = 0.9I_m + 0.9I_m + 0.9I_m + 0.9I_m = 3.6I_m \quad (8)$$

$$I_{R5} = I_{R6} = 0.75I_m + 0.9I_m + 0.35I_m + 0.35I_m = 3.6I_m \quad (9)$$

6.3.1 Power And Voltage at GMPP

Measured in terms of the peak power seen in the P-V characteristics under the shadowing conditions, GMPP output power is the standard for defining power output. Additionally, the voltage at GMPP is the unit of measurement for the potential achieved there.

6.3.2 Power Loss and Fill Factor

If you compare the global power index with the power peak with uniform shadowing, you get PL. In addition, determining FF is a great indicator of the efficiency of PV arrays as it shows how well they perform. In Eq. (10) and (11), we can see the PL and FF as,

$$PL = P_{Ideal\ \text{Irradiation}} - P_{GMPP} \tag{10}$$

$$\%FF = \frac{P_{GMPP}}{V_{OC} I_{SC}} \times 100 \tag{11}$$

6.3.3 Execution Ratio

In a shaded environment, this is the percentage of the PV system's rated power capacity that is actually being delivered to the load side as the power at GMPP. It can be written like in Eq. (12):

$$\%ER = \frac{P_{GMPP}}{P_{Rated}} \times 100 \tag{12}$$

6.3.4 Power Gain

The proposed PV module configuration improves upon the power output of the standard PV module system. The equation for this is:

$$\%\,\mathrm{PG} = \frac{P_{\mathrm{Re}\,configured\ \mathrm{array}} - P_{Conventional\ \mathrm{array}}}{P_{Conventional\ \mathrm{array}}} \times 100 \tag{13}$$

6.4 RESULTS AND DISCUSSION

6.4.1 I-V And P-V Curves during ideal conditions

The maximum power and voltage were measured at 120.1 W and 58.09 V, respectively, when exposed to optimal solar irradiation. The optimal performance, as shown in Fig. 6.8, is useful for figuring out the PL, FF, and PG analysis.

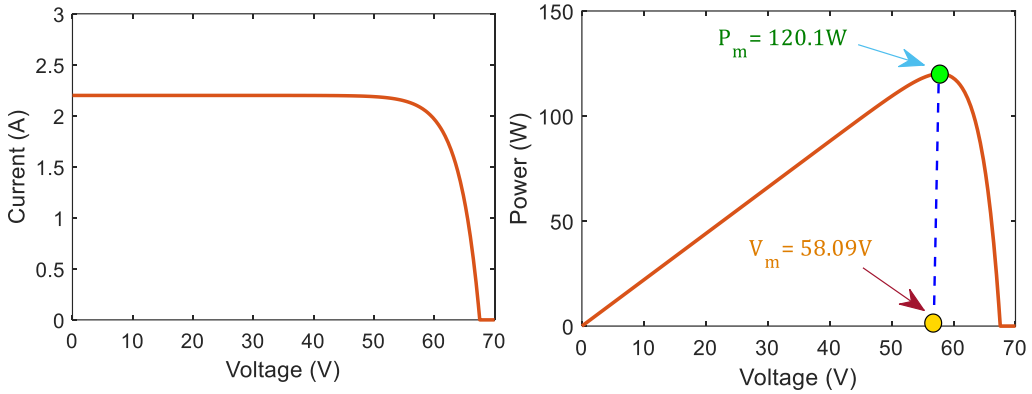

(a) (b)

Fig. 6.8 (a) I-V (b) P-V curves during ideal conditions

6.4.2 I-V and P-V curves under shading scenario I-II

The DPVM-SEC configuration, which outperforms the SP and TCT configurations, produces energy and potential at GMPP of 79.81 W and 77.39 V, respectively, during shading situations I to II. It is determined that the highest current in the SP and TCT-based PV systems is 1.33 A and 1.34 A in the DPVM-SEC method.

The P-V and I-V curves for the first two shading cases are displayed in Fig. 6.9 and 6.10. Additionally, Table-6.1 evaluates and presents the numerical performance outcomes as follows:

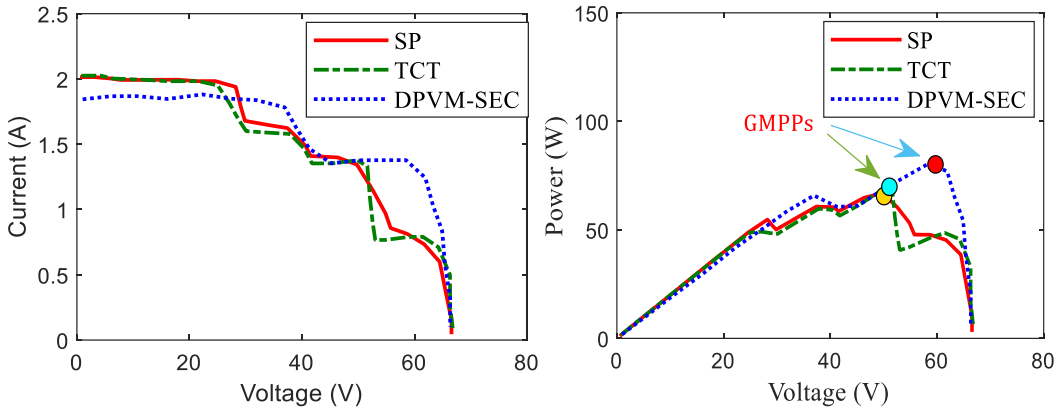

(a) (b)

Fig. 6.9(a) I-V (b) P-V Characteristics during shadow scenario- I

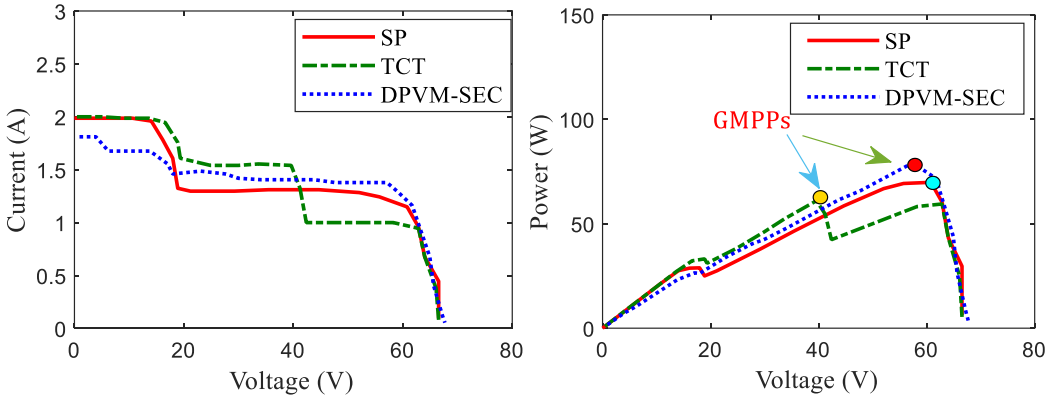

(a) (b)

Fig. 6.10 (a) I-V (b) P-V Characteristics during shading scenario -II

The performance results from the experimental analysis are examined and shown in Table 6.2 as follows:

Table 6.2-The quantitative outcomes of PV systems under PSCs

Performance Indices	Case-I			Case-II		
	SP	**TCT**	**DPVM-SEC**	**SP**	**TCT**	**DPVM-SEC**
V_{oc}(V)	67.19	67.11	67.07	66.82	66.81	66.78
I_{sc}(A)	2.03	2.03	1.842	1.97	1.97	1.78
V_m (V)	50.9	50.05	59.66	59.62	57.96	57.73
I_m (A)	1.27	1.37	1.33	0.964	1.23	1.34
P_m (W)	65.1	68.79	79.81	57.53	71.84	77.39
PL(W)	55	51.31	40.29	62.57	48.26	42.71
FF (%)	49.73	50.49	64.60	43.7	54.58	65.11
ER (%)	54.20	57.27	66.45	47.90	59.81	64.43
PG (%) w.r.t SP	-	5.66	22.59	-	24.82	34.52

6.4.3 Power and Voltage at GMPP

The GMPP positions for shadow scenarios I and II are determined. Higher power outputs at GMPP (79.81 W and 77.39 W, respectively) are achieved with the DPVM-SEC method compared to the more common PV panel topologies (SP and TCT) when I and II shading events occur. In addition, the DPVM-SEC suggestions for designing solar panel frameworks for partial-shading occurrences I-II found a voltage of 59.66 V and 57.73 V at GMPP, respectively. For an illustration of the current and potential at GMPP, see Fig. 6.11(a)- (b).

6.4.4 Fill Factor and Power Loss analysis

Using vital assessment, we can determine the FF and PL for levels I and II of shading. Higher FF values of 64.60 and 65.11 % are achieved using the DPVM-SEC method under shading incidences I and II in comparison to the standard SP and TCT PV panel designs. When considering shading incidences, I and II, it was

also found that the PL for the DPVM-SEC methodology used to design the solar panel framework was lower, coming in at 40.29 W and 42.71 W, respectively. For a static presentation of FF and PL, see Fig. 6.12(a)-(b):

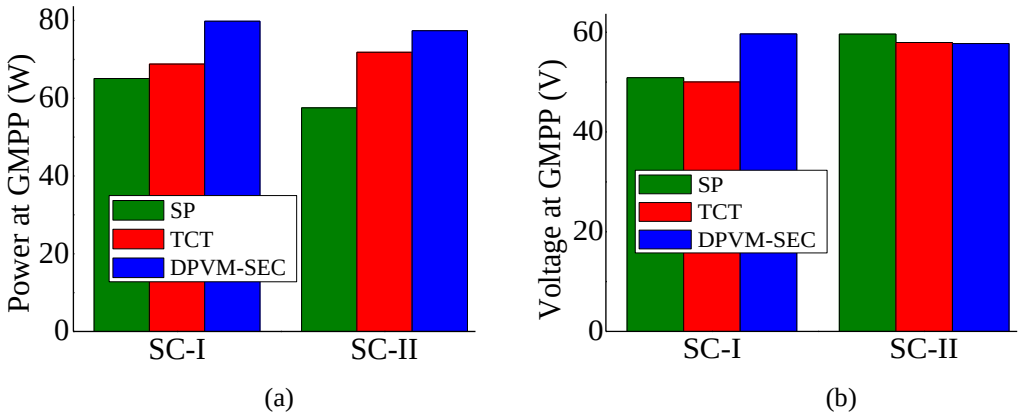

Fig. 6.11(a) Power (b) voltage at GMPP

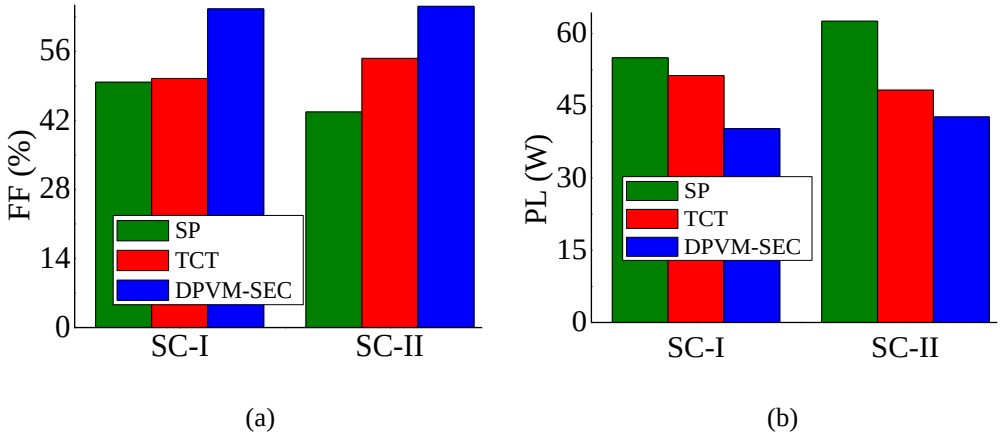

Fig. 6.12 (a) FF (b) PL study

6.4.5 ER And PG Analysis

Vital analysis calculates shading conditions I-II ER and PG values. The DPVM-SEC technique increases ER by 66.45 % and 64.43 % in shaded SP and TCT PV panel configurations. DPVM- SEC's PG for solar panel framework design was 22.59 % and 34.52 %, respectively. Fig. 6.13(a)-(b) shows GMPP's power and voltage.

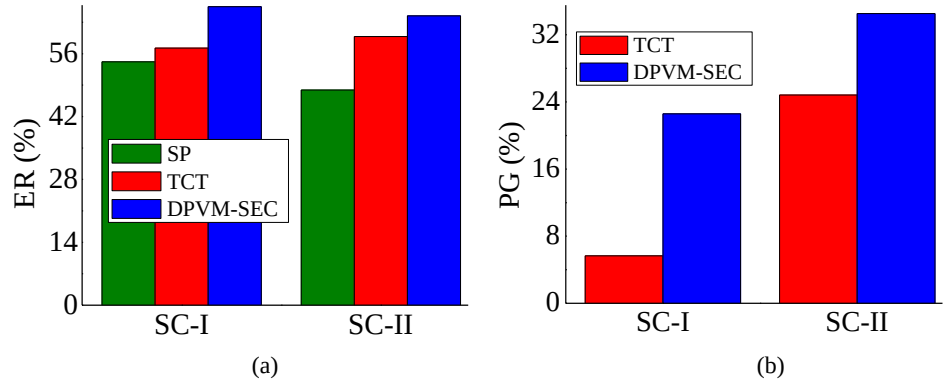

Fig. 6.13 (a) ER (b) PG analysis

6.5 SUMMARY

The results of the study were instrumental in reevaluating and redeveloping the methods found to mitigate partial shading. The DPVM-SEC methodology for pinpointing the optimal panel location within a solar panel was validated as a trustworthy means of boosting PV system dependability, even in partially shaded environments. As for the study's major findings, they are as depicted through:

- The power at GMPP was found to be greater in shadowing conditions I-II, coming in at 79.81 W and 77.39 W, respectively. This is in contrast to more traditional configurations such as SP (65.1 W and 57.53 W) and TCT (68.79 W and 71.84 W), which both had a lower power output.
- PV accuracy can also be evaluated in the presence of such shading conditions using FF attributes. According to the evaluated shadowing scenario, the DPVM-SEC configuration's FF factors are 64.60 and 65.11%.
- Reorganizing a PV module's structure with the DPVM-SEC method reduces power losses to 40.29 W and 42.71 W, respectively, in both shading cases.
- P-V and I-V characterization is utilized in testing the developed DAS to demonstrate its accuracy in comparison to conventional measurement techniques.

CHAPTER- 7
EXPERIMENTAL VALIDATION: MAGIC SQUARE BASED PV ARRAY RECONFIGURATION FOR HIGHER GMPP UNDER PSCs

7.1 INTRODUCTION

The massive power crisis encourages the development of sustainable energy systems, such as those based on solar, tides, geothermal, wind, and biofuels, among others [**Pareek and Dahiya, 2016**]. Research into solar-powered systems is sped up by the debilitating carbon deposits and environmental hazards [**Vijayalekshmy *et al.*,2016**]. In urban areas today, the installation of PV power generating systems to provide electricity for domestic and commercial uses is growing exponentially. Numerous factors influence the assessment of PV systems. One of the biggest challenges for designers and installers to overcome is shade. Specifics of the job are listed below are:

- To investigate the array's efficacy, we consider a few different shading test scenarios.
- The game-puzzle based PV array rearrangement that has been described is used to create and evaluate both the SP and TCT configurations for PV array systems.
- In order to analyze the four PSCs, the P-V and I-V characteristics are implemented, and the performance characteristics that are determined as a result are compared.

7.2 SOLAR PV TECHNOLOGY

7.2.1 PV Modelling

When solar photovoltaic cells are connected in series and parallel, they produce more usable power, making them ideal for use in higher-rated loads. A diagram of the electrically organized circuit layout of a solar PV cell can be found in fig. 7.1.

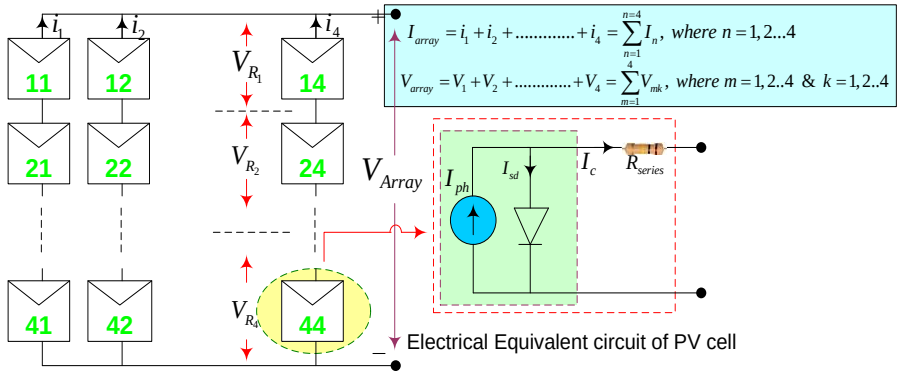

Fig. 7.1 Development of PV array (4×4 size) and PV cell equivalent electrical circuit

The voltage at the output of an array shown in Fig. 7.3 can be demonstrated with the Eq. (1) as

$$V_C = \frac{AkT_c}{e} ln\left(\frac{I_{ph}+I_o-I_c}{I_o}\right) - R_{series}I_c \quad (1)$$

Where, V_C and A are used to reflect the cell voltage and ideality factor respectively. T_C stands for cell temperature and e electron charge. Moreover, I_{ph} and I_o are represented as photo current and saturation current respectively. In addition, R_{series} and I_C stand for the series resistance and PV cell current.

7.2.2 Conventional PV Array Configurations

In the SP topology, finite numbers of modules, arranged in PV array strings

(single) to enhance the voltage level. Parallel arrangement of PV strings in array is directly responsible to elevate the current rating. Furthermore, cross-tied connections are arranged to modify the SP connections and new developed PV array model is called as TCT. The conventional SP and TCT are electrically connected as 4×4 size PV array depicted in Fig. 7.2.

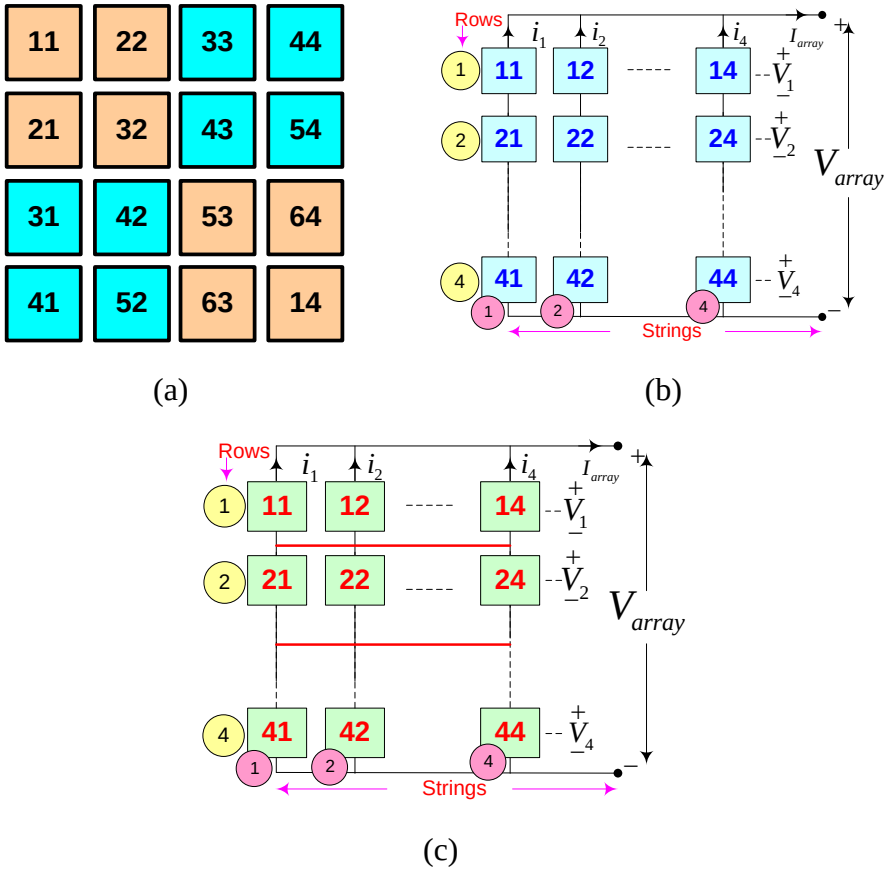

Fig. 7.2 (a) Nomenclature of 4×4 size array (b) SP (c) TCT topologies

7.2.3 Game Puzzle Based: Magic Square Configurations

The proposed game puzzle is dependent upon a particular ordering of integers from 1-4. In this study, MS based puzzle is taken into account for

consideration of extensive study about the GMPP locations, PL analysis, and % PE under shading scenarios. Furthermore, the methodology to obtain the MS puzzle with the equality summation properties e. g. row, column and diagonal are given in Fig. 7.4. The nomenclature and electrical arrangements of modules are explored about to design MS puzzle (4×4 size) based PV array system. The generalized flow chart-based algorithm is given as,

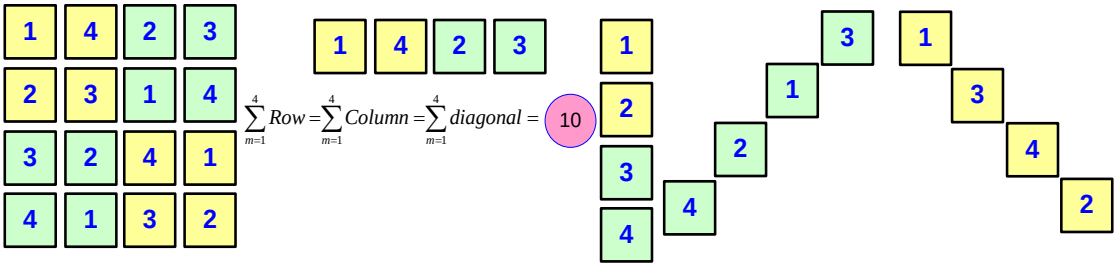

(a) Number placement of MS puzzle with summation properties

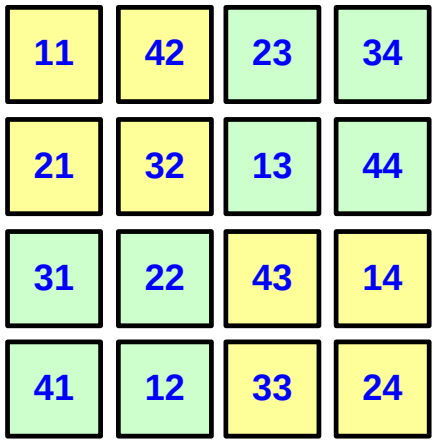

(b) Nomenclature of PV modules

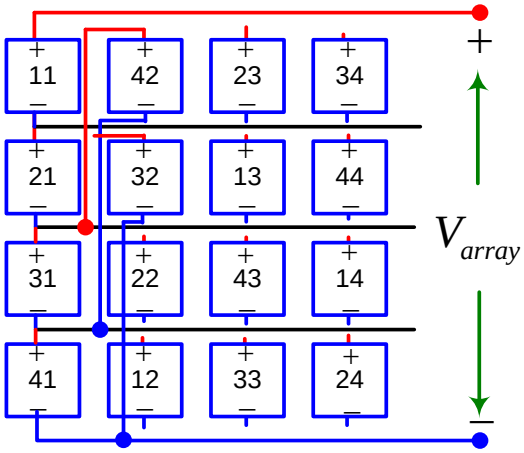

(c) Electrical arrangement of PV array

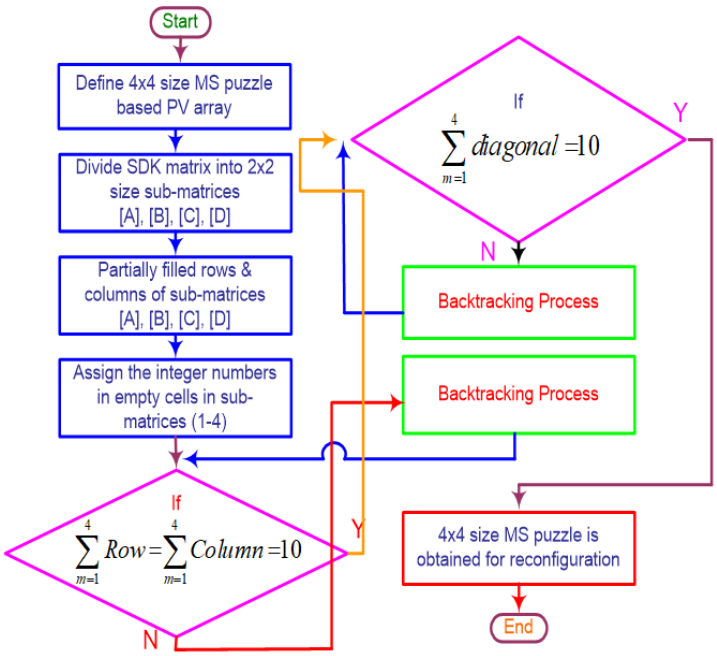

(d) Flow chart operation

Fig. 7.3 Methodology of attaining (4×4 Size) MS puzzle for PV array reconfiguration

7.2.4 Experimental Set-up

The proposed experimental setup is intended to carry out an in-depth performance evaluation of PV system which are operating in PSCs. In order to accommodate circumstances involving variable resistive loads, the PV system (4×4) has been integrated with a voltage-current measurement unit as well as a varying load (DAS). The experimental work bench is depicted in Fig. 7.5. For the purpose of developing the data logger system, analogue sensors, including voltage and current, are connected with the microcontroller system. This allows for the evaluation of electrical performance under shadowing conditions as well as the collection of real-time data. As a further phase that needs to be looked into, the system is also connected to the micro-SD card assembly so that the performance characteristics for P-V and I-V characterization can be stored there. In order to

better illustrate the function, Fig. 7.6-7.7 show the wiring configuration for the DAS as well as the flow of data.

Fig. 7.4 Experimental Setup

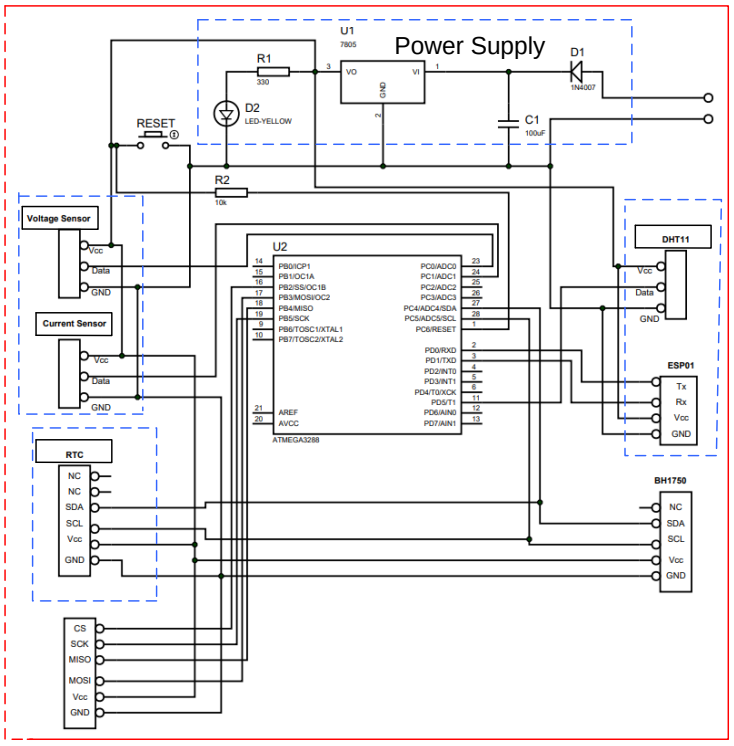

Fig. 7.5 Wiring arrangement of DAS for real time measurement

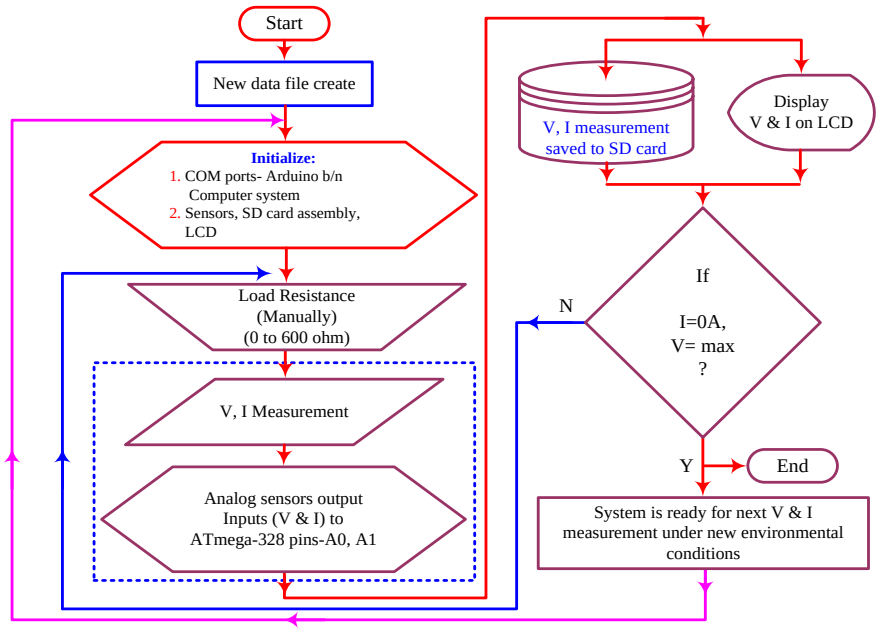

Fig. 7.6 Flow chart to describe the operation of data logger system

7.3 PERFORMANCE PARAMETERS AND SHADING SCENARIOS

Each module in an array has its own power maxima (LMPP and GMPP) on the P-V graph because of PSCs. Due to the abundance of GMPP and LMPP in the current shading environment, it is feasible to deceive the MPPT method into believing that it is unable to supply the load with any more power. To infer performance characteristics, the shape of the I-V as well as the P-V characteristics is shown here.

7.3.1 Power and Voltage at GMPP

Within these shady conditions, the maximum power possible (P_{GMPP}) is the last value on the P-V graph. Additionally, V_{GMPP} is an abbreviation for the voltage that is measured at GMPP.

7.3.2 Fill Factor

When determining the performance efficacy of a P-V system, the FF is the metric that is used. and can be expressed as follows by Eq. (2):

$$\%FF = \left(\frac{P_{GMPP}}{V_{OC} \times I_{SC}}\right) \times 100 \quad (2)$$

7.3.3 Power Loss

PL can be evaluated through the disparity between the power at GMPP and the power at its ideal value. The identification of PL is demonstrated in Eq. (3) as,

$$PL = P_{ideal} - P_{GMPP} \quad (3)$$

7.3.4 Execution Ratio

Eq. (4) expresses ER as a ratio in between power at GMPP and the power rating output of a PV plant system.

$$\%ER = \left(\frac{Power\ at\ GMPP}{Rated\ power\ capacity}\right) \times 100 \quad (4)$$

7.3.5 Power Enhancement

PE refers to the advanced PV configuration's increased power compared to the traditional setup. According to Eq. (5), we can write the PE as a percentage:

$$\%ER = \left(\frac{P_{advanced\ PV\ array} - P_{SP}}{P_{SP}}\right) \times 100 \quad (5)$$

7.3.6 Shading Scenarios I-II

For efficient performance investigation of PV systems in reference to FF, PL, % ER, and GMPP locations under two shading scenarios. These following

shading circumstances have been used in this investigation, as illustrated in Fig. 7.8-7.9:

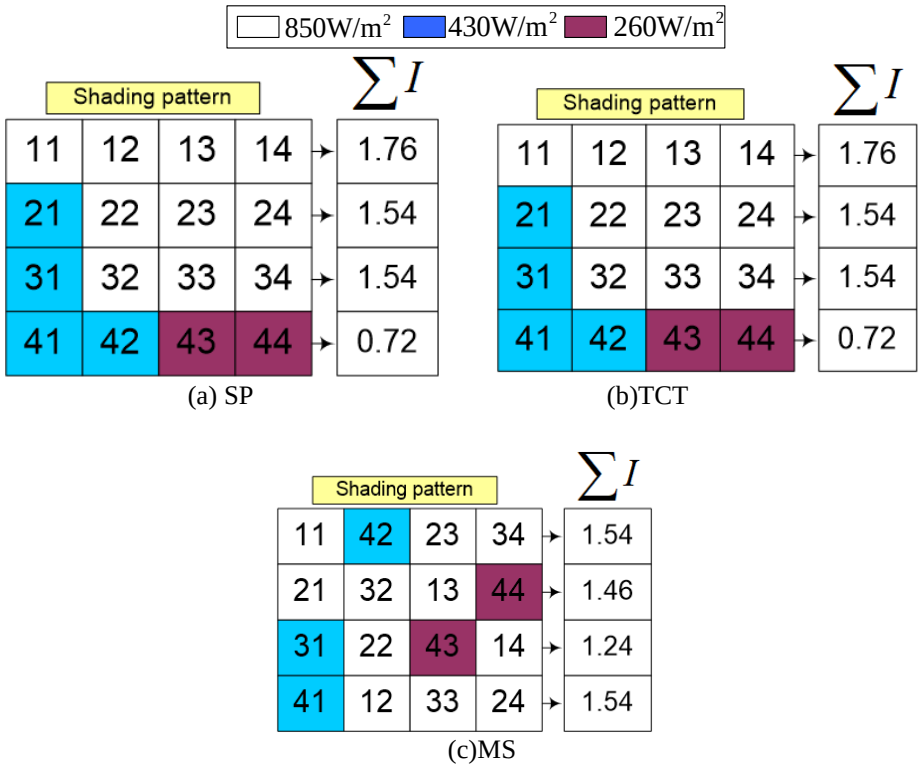

Fig. 7.7 Shade profiles based on reconfigured PV array

Row-by-row analysis of SP-based PV array configurations for theoretically estimating produced current is depicted in Eq. (6)-(8) under the shading case I is given as,

$$I_{R1} = 0.85I_m + 0.85I_m + 0.85I_m + 0.85I_m = 3.4I_m \quad (6)$$

$$I_{R2} = I_{R3} = 0.43I_m + 0.85I_m + 0.85I_m + 0.85I_m = 3.4I_m \quad (7)$$

$$I_{R4} = 0.43I_m + 0.43I_m + 0.26I_m + 0.26I_m = 3.4I_m \quad (8)$$

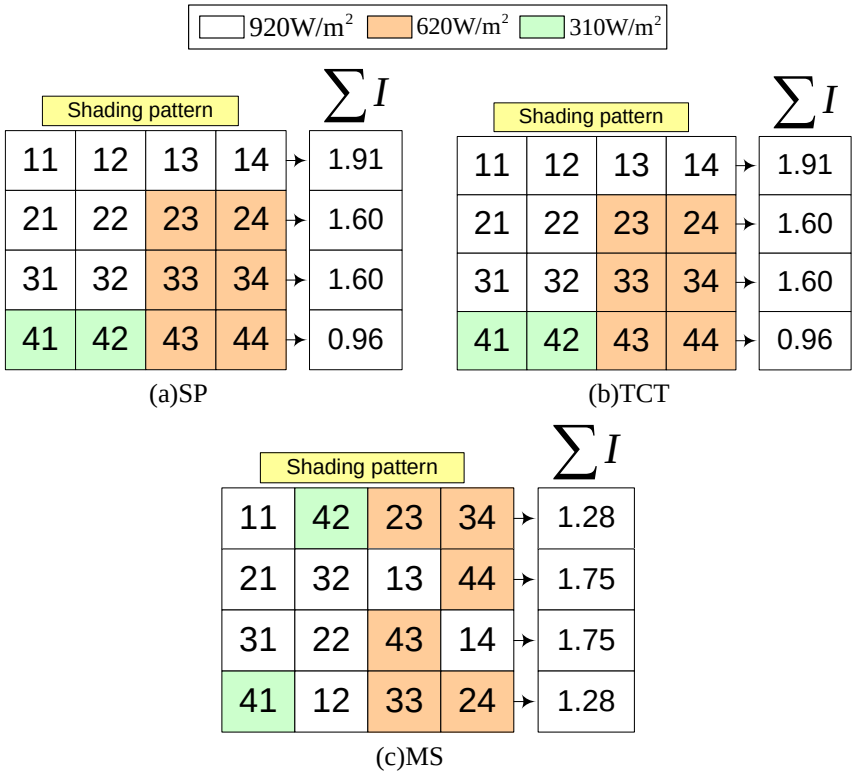

Fig. 7.8 Shade profiles based on redesign PV array

Under the shadowing situation II, the following equation provides a theoretical evaluation of the row-wise current generation by SP-based PV array designs: (9)-(11).

$$I_{R1} = 0.92I_m + 0.92I_m + 0.92I_m + 0.92I_m = 3.68I_m \quad (9)$$

$$I_{R2} = I_{R3} = 0.92I_m + 0.92I_m + 0.62I_m + 0.62I_m = 3.08I_m \quad (10)$$

$$I_{R4} = 0.31I_m + 0.31I_m + 0.62I_m + 0.62I_m = 1.86I_m \quad (11)$$

For shading condition, I and II, an analysis very similar to the one described above can be carried out to determine the current for an MS-based PV array theoretically.

7.4 RESULTS AND DISCUSSION

The implications of these shading schemes on performance for various array configurations are investigated in the following research.

7.4.1 P-V and I-V curve at STCs

According to simulation study, the maximum power and voltage of an array system at STC (standard test conditions) are 80.09 W and 35.55 V, respectively as shown in Fig. 7.10.

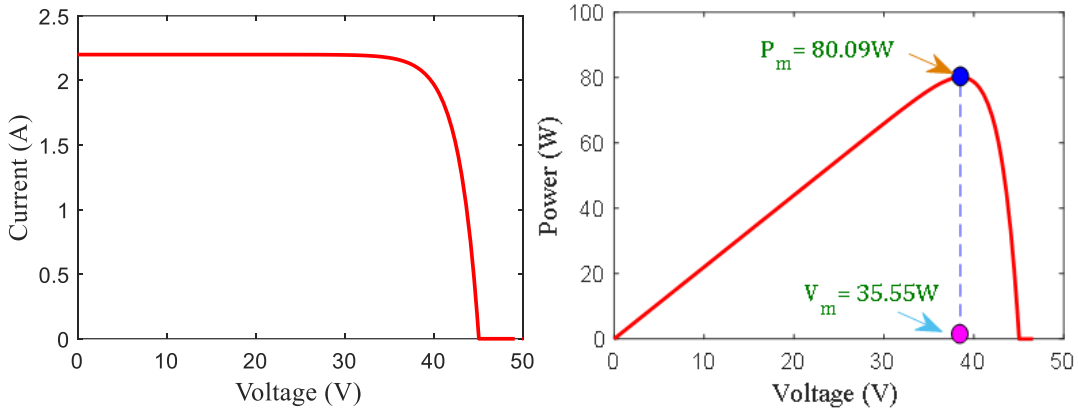

Fig. 7.9(a) I-V and (b) P-V curve at ideal conditions

7.4.2 MATLAB/Simulink Study: Shading Scenario I and II I-V and P-V Curves

As depicted through Fig. 7.11, the I-V characteristics of the MS design are much smoother than those of the SP and TCT designs (a). For SP, TCT, and MS, the S.C. current was observed to be 1.87 A, 1.87 A, and 1.63 A, respectively. The SP and TCT arrangement suffer significant shading losses because there is a discrepancy between the GMPP of the array and the peak power of the module. The GMMP position is found to be higher under shading scenario-I, at 49.05 W, than the SP and TCT arrangements, which are, respectively, 43.4 W and 43.9 W.

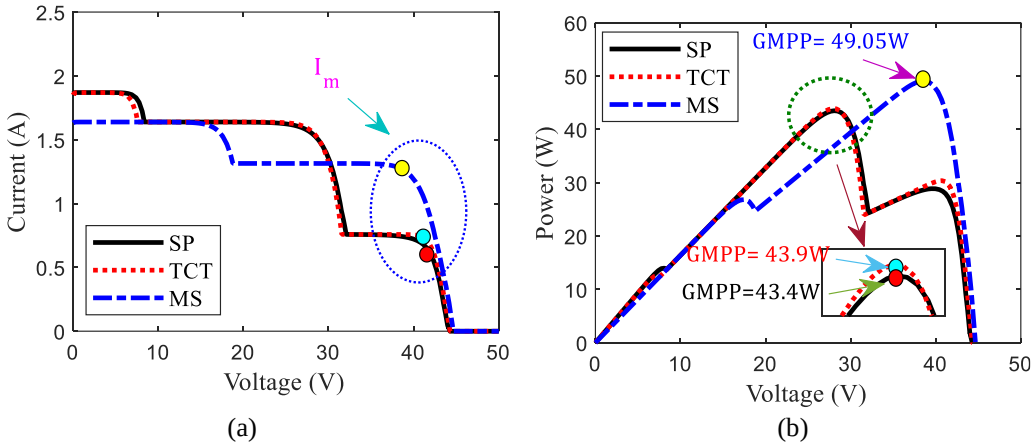

(a) (b)

Fig. 7.10 (a)-(b) I-V and P-V characteristics under PSC-I

TCT and SP in comparison to MS configurations show reliable behaviour through I-V characteristics of MS in shading scenarios II. A comprehensive comparison of the SP, TCT, and MS array models efficacy revealed that SP and TCT have low power performance of 45.76 W and 46.12 W, respectively, compared to MS's 51.35 W. In Fig. 7.12, we see the I-V and P-V curves for case II of the shading analysis.

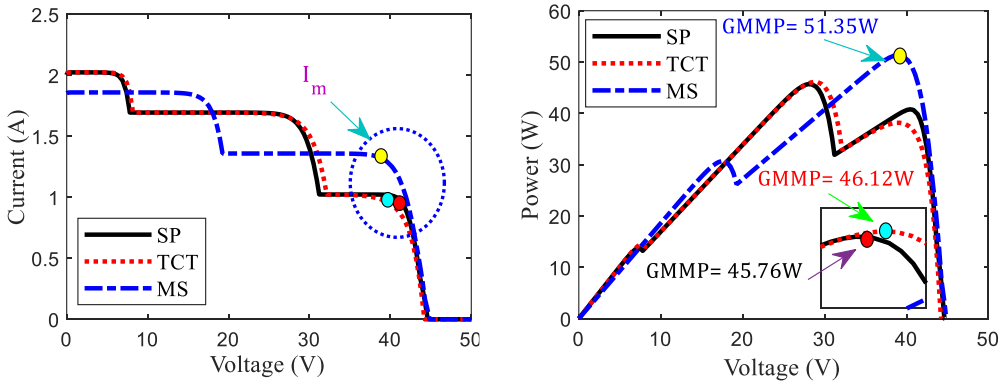

(a) (b)

Fig. 7.11 (a) I-V and (b) P-V curves under PSC-II

The assessment outcomes obtained through MATLAB/Simulink study are depicted in Table-7.1. The obtained performance indices are identified through shadow scenarios I-II as,

Table-7.1 Quantitative performance indices during MATLAB/Simulink study

Performance Indices	Shading Pattern-I			Shading Pattern-II		
	SP	**TCT**	**MS**	**SP**	**TCT**	**MS**
$\mathbf{V_{oc}}$**(V)**	43.8	44	44.4	43.6	43.6	43.7
$\mathbf{I_{sc}}$**(A)**	1.87	1.87	1.63	2.02	2.02	1.85
$\mathbf{V_{GMPP}}$ **(V)**	28.05	28.31	38.82	27.91	28.73	39.12
$\mathbf{I_m}$ **(A)**	1.54	1.55	1.26	1.63	1.60	1.31
$\mathbf{P_{GMPP}}$ **(W)**	43.4	43.9	49.05	45.76	46.12	51.35
PL(**W**)	36.69	36.19	31.04	34.33	33.97	28.74
FF (%)	53.0	53.3	67.8	52.0	52.4	63.5
ER (%)	54.18	54.81	61.24	57.13	57.85	64.11
PE (%) w.r.t SP	-	1.15	13.01	-	0.78	12.21

7.4.3 Experimental Validation: I-V And P-V Plots through Shadow Scenario-I

An experimental investigation was done on 4×4 size SP, TCT and MS arrangement-based PV systems. Power at GMPP is calculated as 80.09 W under standard solar irradiation of 1000 W/m^2. The significance of shading is shown through electrical parameters performance for all configurations i.e., SP, TCT and MS considered shown in Table-7.2. Under shading scenarios, as depicted in Fig.7.13 of cases I, power maxima at MPP for SP, TCT and MS is observed as 42.38 W, 42.65 W and 46.01 W respectively. MS configuration experiences smoother I-V characteristics with value of S.C. current as 1.60 A compared to TCT and SP, under extensive examination in shading scenario-I.

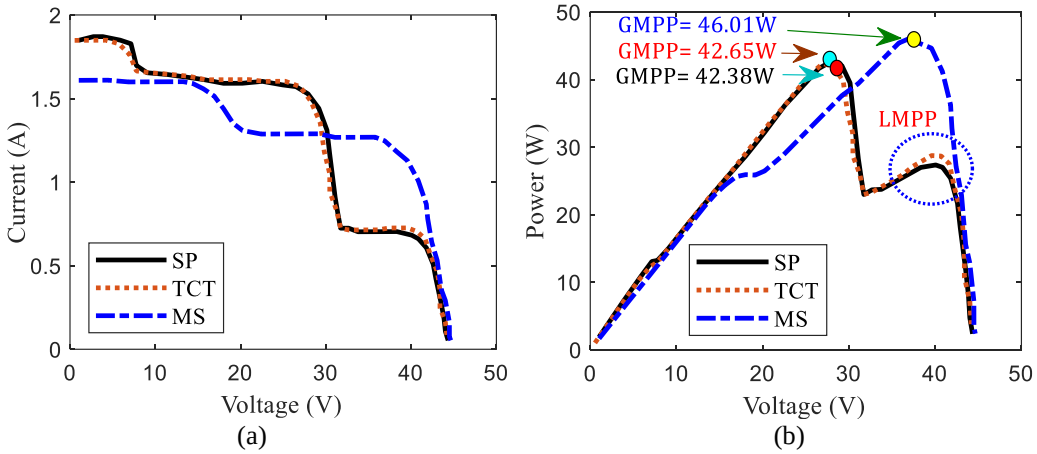

Fig. 7.12(a) I-V and (b) P-V plots under shading scenario-I

The assessment outcomes obtained through experimentation study are depicted in Table-7.2. The obtained performance indices are identified during the shading scenarios-I as,

Table-7.2 Quantitative performance indices during experimental study

Performance Indices	**Shading Pattern-I**		
	SP	**TCT**	**MS**
V_{oc}(V)	42.8	43.2	43.3
I_{sc}(A)	1.84	1.84	1.60
V_{GMPP} (V)	26.97	27.92	36.89
I_m (A)	1.571	1.527	1.24
P_{GMPP} (W)	42.38	42.65	46.01
PL(W)	37.71	37.44	34.08
FF (%)	53.8	53.6	66.4
ER (%)	52.91	53.25	57.44
PE (%) w.r.t SP	-	0.63	8.56

7.4.4 Power at GMPP

Power assessment results are depicted through Fig. 15. While doing

MATLAB/Simulink study shown in Fig. 7.15(a), it has been found out that MS topology with two shadowing scenarios I-II has highest power maxima at GMPP noted as 49.05 W and 51.35 W respectively. In addition to this, when same MS arrangement undergoes electrical analysis experimentally under shadowing scenarios-I as depicted in Fig. 7.15(b) denoted power at GMPP as 46.01 W superior than TCT and SP as 42.65 W and 42.38 W as referred in Table-2. The Global maximum power error is found be 3.04 W for shading pattern-I compared against MATLAB simulation with experimental analysis.

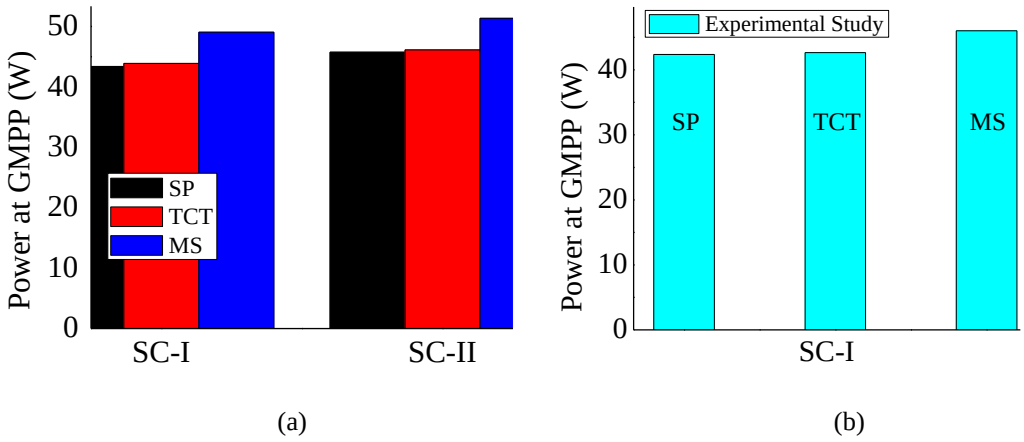

Fig. 7.13 Power at GMPP (a) Simulation (b) Experimental analysis

7.4.5 Fill Factor

MS in comparison with TCT and SP configuration, differences are observed in the FF among the three as represented in Fig. 7.16(a). During MATLAB/Simulink study represented in shading scenarios I-II, shows high improvement in shading efficacy (FF) with MS as 67.8 % and 63.5 % referred to Table-1 while TCT and SP stays at 53.3 % and 53.0 % for case-I and 52.4 % and 52 % for shading case-II respectively. An experimental study was also conducted simultaneously for shading case-I, to validate MS array's performance. As a result of study conducted, MS array % FF is found to be 66.4 % represented as bar chart

in Fig..7.16 (b).

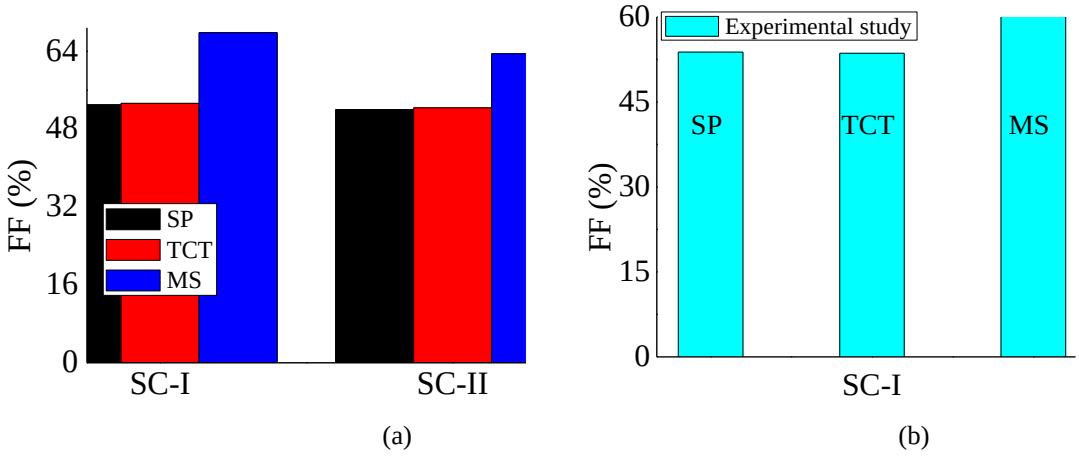

Fig. 7.14 FF for (a) MATLAB/Simulink study (b) Experimental study

7.4.6 Power Loss

PL owing to shading given by diverse sources on PV systems such as SP, TCT, and MS game puzzle-based arrangements are evaluated in the experimental analysis study and MATLAB/Simulink study. The MS model offers minimum losses in power of 31.04 W and 28.74 W referred to Table-7.1 under cases-I and II respectively. Bar chart analysis revealed through Fig. 7.17(a)-(b) represents MS arrangement. According to experimental analysis, MS has highest losses of 34.08 W during case-I as shown in Table-7.2 after performance validation is shown through Fig. 7.17(b).

7.4.7 Execution Ratio and Power Enhancement

On comparing the experimental study with MATLAB/Simulink study, validated ER for MS is superior for both the shading cases of TCT and SP, resulting in performance enhancement as shown in Fig. 7.18(a). Under shadowing conditions, I-II, ER % for MS is noticed to be much enhanced as 61.24 % and 64.11 % compared to conventional configurations as TCT (54.81 % and 57.85 %) and SP

(54.18 % and 57.13 %) as referred to Table-7.1.

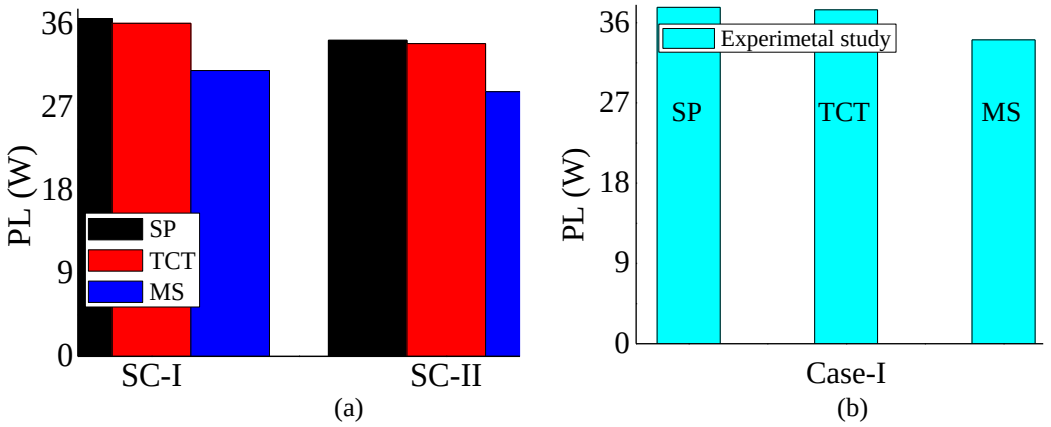

Fig. 7.15 PL for (a) MATLAB/Simulink study (b) Experimental study

In experimental analysis, ER for MS is represented as bar chart depicting in Fig. 7.18(b) has higher value as 57.44 % (referred to Table-2), when investigated against SP and TCT.

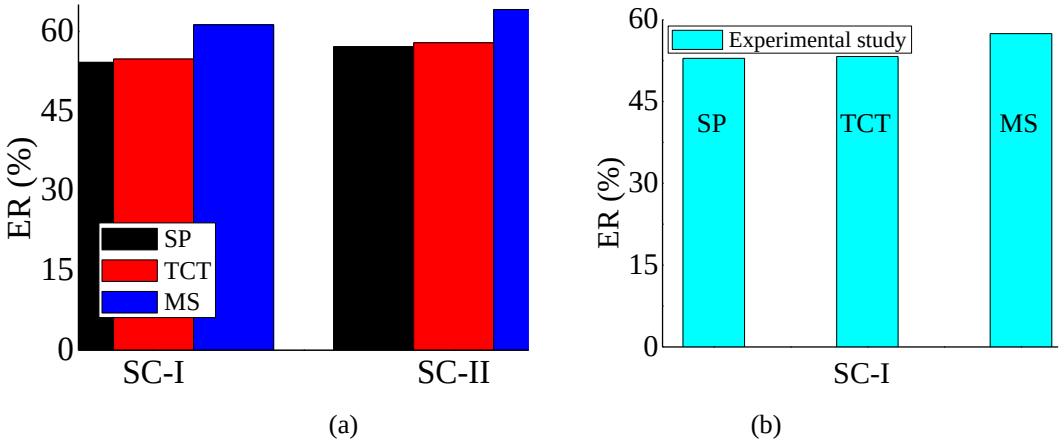

Fig. 7.16 ER under (a) Simulation (b) Experimental analysis

The performance improvement in relation to the SP array configuration is

depicted in a bar graph throughout Fig. 7.19 and is summarized in Table-7.1. The PE is raised in cases I and II from 1.15 % in TCT to 13.01 % in MS and also from 0.78 % in TCT to 12.21 % in MS, respectively. Furthermore, when experimentally analyzed results in an increase of 0.63 % in TCT to 8.56 % in MS w.r.t SP as referred to Table-2 and represented by Fig. 7.19(b).

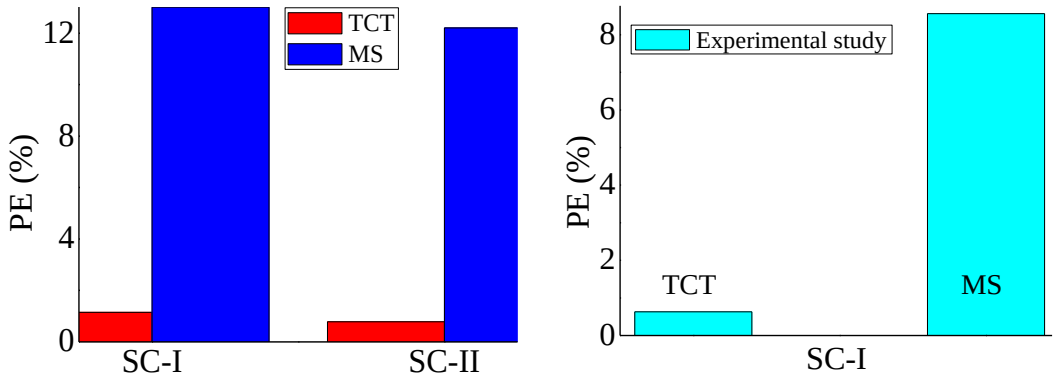

(a) (b)

Fig. 7.17 PE analysis for (a) MATLAB/Simulink study (b) Experimental study

7.5 SUMMARY

In the manuscript, traditionally generated MS configurations under PSCs are compared and analyzed with conventional SP and TCT puzzle-based configurations. Results are experimentally validated based on extensive MATLAB/Simulink based research. The performance measuring variables PL, FF, ER, and PE were also looked at. A minimum power maximum point with better values is present in the MS puzzle-based PV array architecture, per thorough research. Important elements of a thorough MATLAB/Simulink study and experiment include the following:

- The performance metrics estimated and observed in instance I of shadowing through simulation research, such as maximum power at GMPP, % PE, FF, and reduced PL (%), are recognized as significantly superior to TCT and SP

as 49.05 W, 13.01 %, 67.8 %, and 31.04 %, respectively, to MS puzzle-based PV array design. A validation experiment was also run, which examined comparable performance metrics like 46.01 W, 8.56 %, 66.4 % and 34.08 %.

- The MATLAB/Simulink results for the shading scenario II favor the MS puzzle-based PV array design with 51.35 W, 12.21 %, 63.5 %, and 28.74 % power at GMPP, % PE, FF and insignificant PL.

CHAPTER 8
CONCLUSION

In this thesis, we present and evaluate the proposed shade dispersion approach, which has been shown to be effective at lowering PS losses on PV modules. Improvements in efficiency and MPP have been demonstrated through simulations and experimental validations of this approach in a variety of PS settings. Educators and researchers need access to a cost-effective, dependable, and low-priced sensor network for PV system monitoring and data acquisition. The current generation of data collecting equipment is reliant on licensed software and wiring, which are both notoriously difficult to get and very costly. Only in close proximity to the PV arrays can you gain access to the wired data acquisition systems. They need people to be stationed close to the remote PV plant to operate the system if it is either permanently wired to power or manually controlled. Some wireless data acquisition systems are available, but they require paid software or cloud storage to function. Open-source software is used by only a small fraction of the available wireless data acquisition systems; these systems monitor and record a handful of parameters at exorbitant prices. These issues will be rendered obsolete by the planned IoT-based data collection system (DAQ). The proposed system for data acquisition uses free, online tools and a web-based storage and processing platform. This paper details the architecture of a low-priced data acquisition system for permanently accessible data collection on PV system operations, with the goal of facilitating their evaluation. From what we can tell from our tests, The suggested data collecting system is adequate, dependable, cost-effective, and appropriate for hard outdoor situations; it can be used to monitor and obtain real - time data of the PV system in order to assess its performance. These findings have been derived:

- Extensive testing of three distinct shadow scenarios (lamp post, three-cornered and single vertex shading) are extensively tested and described in Chapter 3. It

has been calculated that the SM-TCT arrangement provides a 15.81 % improvement in performance over the TCT case II scenario.

- ❖ According to Chapter 4, the most efficient LS-TCT configurations are those based on a puzzle, which leads to an 8.4 % PE, a decrease in power mismatch losses to 867 W, and an increase in FF of up to 0.037 under Shade Scenario 1. It is clear that the LS-TCT has the greatest output at GMPP and improved PL at 2368 W and 242 W respectively, in the first scenario of shading pattern 1 as compared to the SP-TCT, BL-TCT, BL-HC, TCT, HC, BL, and SP.
- ❖ Chapter 5's quantitative analysis using MATLAB/Simulink shows that case II's power at GMPP is 2349 W and PL is 311 W, while chapter 6's experimental study shows that SM-power TCT's at GMPP is 55.46 W and PL is 6.93 W, outperforming TCT, NTCT, and Shape-do-Ku in all three categories.
- ❖ SC-I for DPVM-SEC is shown to have an enhancement ratio of 66.45 % and a performance gain of 22.59 % when compared to TCT and SP in chapter 6.
- ❖ In chapter 7, it is found that the power at GMPP for shading pattern-II in MATLAB/Simulink based quantitative analysis is 49.05 W and the power at PL for shading pattern-II in Experimental study is 46.01 W and the power at PL for shading pattern-II in MS is 34.08 W, when compared to TCT and SP.

Using the proposed DAQ system to achieve the Internet of Things, detecting and monitoring PV systems in the household and commercial spheres may be done at reduced cost. In the near future, metaheuristic approaches will be able to be opted for optimal interconnections of PV modules for improvements in PV array performance when operating under PSCs.

REFERENCES

- Ahmad, R., Murtaza, A. F., Sher, H. A., Shami, U. T., & Olalekan, S. (2017). An analytical approach to study partial shading effects on PV array supported by literature. *Renewable and Sustainable Energy Reviews,* 74, 721-732.
- Ahmed, J., & Salam, Z. (2015). A critical evaluation on maximum power point tracking methods for partial shading in PV systems. *Renewable and Sustainable Energy Reviews*, 47, 933–953.
- Alahmad, M., Chaaban, M. A., Lau, S. K., Shi, J., & Neal, J. (2012). An adaptive utility interactive PV system based on a flexible switch matrix to optimize performance in real time. *Solar Energy*, 86(3), 951-963.
- Alajmi, B. N., Ahmed, K. H., Finney, S. J., & Williams, B. W. (2013). A maximum power point tracking technique for partially shaded PV systems in micro grids. *IEEE Transactions on Industrial Electronics*, 60(4), 1596-1606.
- Alonso-Garcia, C., Ruizb, J. M., & Herrmann, W. (2006). Computer simulation of shading effects in PV arrays. *Renewable Energy*, 31(12), 1986–1993.
- Anand, R., Chauhan, Y. K., Kumar, V., & Pachauri, R. (2020). Experimental system design for online characterization and performance analysis of PV module under distinguish environment. *EAI Endorsed Transactions on Energy Web*, 7(28), 1-11.
- Babu, T. S., Ram, J. P., Dragicevi, T., Miyatake, M., Blaabjerg, F., & Rajasekar, N. (2018). Particle Swarm Optimization Based Solar PV Array Reconfiguration of the Maximum Power Extraction Under Partial Shading Conditions. *IEEE Transactions on Sustainable Energy,* 9, 74-85.
- Babu, T. S., Yousri, D., & Balasubramanian, K. (2020). PV Array Reconfiguration System for Maximizing the Harvested Power using Population-based Algorithms. *IEEE Access*, 8, 109608-109624.

- Bai, J., Cao, Y., Hao, Y., Zhang, Z., Liu, S., & Cao, F. (2015). Characteristic output of PV systems under partial shading or mismatch conditions. *Solar Energy*, 112, 41–54.
- Balato, M., Costanzo, L., & Vitelli, M. (2016). Reconfiguration of PV modules: a tool to get the best compromise between maximization of the extracted power and minimization of localized heating phenomena. *Solar Energy*, 138,105–118.
- Bana, S., & Saini, R. P. (2017). Experimental investigation on power output of different PV array configurations under uniform and partial shading scenarios. *Energy*, 127, pp. 438-453.
- Bastidas, J. D., Franco, E., Petrone, G., Ramos-Paja, C. A., & Spagnuolo, G. (2013). A model of PV fields in mismatching conditions featuring an improved calculation speed. *Electric Power Systems Research*, 96, 81– 90.
- Batzelis, E. I., Georgilakis, P. S., & Papathanassiou, S. A. (2015). Energy models for PV systems under partial shading conditions: A Comprehensive Review. *IET Renewable Power Generation*, 9(4), 340–349.
- Batzelis, E. I., Routsolias, I. A., & Papathanassiou, S. A. (2014). An explicit PV string model based on the lambert W function and simplified MPP expressions for operation under partial shading. *IEEE Transactions on Sustainable Energy*, 5(1), 301-312.
- Bauwens, P., & Doutreloigne, J. (2014). Reducing partial shading PL with an integrated smart bypass. *Solar Energy*, 103, 134–142.
- Belhachat, F., & Larbes, C. (2015). Modeling, analysis and comparison of solar PV array configurations under partial shading conditions. *Solar Energy*, 120, 399–418.
- Belhaouas, N., Cheikh, M. S. A., Agathoklis, P., Oularbi, M. R., Amrouche, B., Sedraoui, K., & Djilali, N. (2017). PV array power output maximization

under partial shading using new shifted PV array arrangements. *Applied Energy*, 187, 326–337.

- Bellini, A., Bifaretti, S., & lacovone, V. (2010). MPPT algorithm for current balancing of partially shaded PV modules. *IEEE International Symposium on Industrial Electronics*, 933-938.
- Bishop, J. W. (1988). Computer simulation of the effects of electrical mismatches in PV cell interconnection circuits. *Solar Cells*, 25, 73 – 89.
- Blas, M. A. de., Torres, J. L., Prieto, E., & Garcia, A. (2002). Selecting a suitable model for characterizing a PV device. *Renewable Energy*, 25(3), 371–380.
- Bleicher, A., Pachauri, R. K., Kuchhal, P., & Bansal, K. (2020). Experimental study on electrical connections of PV system for improved performance under shadow test cases. *EAI Endorsed Transactions on Energy Web*, 7(30), 1-11.
- Bosco, M. J., & Mabel, M. C. (2017). A novel cross diagonal view configuration of a PV system under partial shading condition. *Solar Energy*, 158, 760-73.
- Boukenoui, R., Salhi, H., Bradai, R., & Mellit, A. (2016). A new intelligent MPPT method for off-grid PV systems operating under fast transient variations of shading patterns. *Solar Energy*, 124, 124–142.
- Braun, H., Buddhaa, S.T., Krishnan, V., Tepedelenlioglu, C., Spanias, A., Banavar, M., & Srinivasan, D. (2016). Topology reconfiguration for optimization of PV array output. *Sustainable Energy, Grids and Networks*, 6, 58–69.
- Buddala, S. S., Vemuru, S., & Devabhaktuni. V. (2013). Small signal modeling of diode in a parallel module subjected to partial shading. *IEEE International Conference on Electro-Information Technology*, 1-5.

- Candela, R., Dio, V. D., Sanseverino, E. R., & Romano, P. (2007). Reconfiguration techniques of partial shaded PV systems for the maximization of electrical energy production. *International Conference on Clean Electrical Power*, 716-719.
- Celik, B., Karatepe, E., Silvestre, S., Gokmen, N., & Chouder, A. (2015). Analysis of spatial fixed PV arrays configurations to maximize energy harvesting in BIPV applications. *Renewable Energy*, 75, 534-540.
- Chao, H., Lai, P. L., & Liao, B. J. (2015). The optimal configuration of PV module arrays based on adaptive switching controls. *Energy Conversion and Management*,100, 157–167.
- Cherukuri, S. K., Kumar, B. P., Kaniganti, K. R., Muthubakaji, S., Devadasu, G., Babu, T. S., & Alhelou, H. H. (2022). A Novel Array Configuration Technique for Improving the Power Output of the Partial Shaded PV System. *IEEE Access*, 10, 15056-15067.
- Chowdhury, S. R., & Saha, H. (2010). Maximum power point tracking of partially shaded solar PV arrays. *Solar Energy Materials and Solar Cells*, 94, 1441–1447.
- Daliento, S., Napoli, F. D., Guerriero, P., & Alessandro, V. D. (2016). A modified bypass circuit for improved hot spot reliability of solar panels subject to partial shading. *Solar Energy*, 134, 211–218.
- Deshkar, S. N., Dhale, S. B., Mukherjee, J. S., Babu, T. S., & Rajasekar, N. (2015). Solar PV array reconfiguration under partial shading conditions for maximum power extraction using genetic algorithm. *Renewable and Sustainable Energy Reviews*, 43(2015), 102–110.
- Ding, K., Bian, X. G., Liu, H. H., & Peng, T. (2012). A MATLAB/Simulink based PV module model and its application under conditions of non-uniform irradiance. *IEEE Transactions on Energy Conversion*, 27(4), 864-872.

- Dio, V. D., Cascia, D. L., Miceli, R., & Rando, C. (2009). A mathematical model to determine the electrical energy production in PV fields under mismatch effect. *IEEE Conference on Clean Electrical Power*, 46-51.
- Dorado, E. D., Garcia, A. S., Carrillo, C., & Cidras, J. (2010). Influence of the shadows in PV systems with different configurations of bypass diodes. *IEEE International Symposium on Power Electronics, Electrical Drives, Automation and Motion*, 134-139.
- Dorado, E.D., Cidra, J., & Carrillo, C. (2014). Discrete I–V model for partially shaded PV arrays. *Solar Energy*, 103, 96–107.
- El-Dein, M. Z. S., Kazerani, M., & Salama, M. M. A. (2011). Novel configurations for PV farms to reduce partial shading losses. *IEEE Conference on Power and Energy Society General Meeting*, 1-5.
- El-Dein, M. Z. S., Kazerani, M., & Salama, M. M. A. (2013). Optimal PV array reconfiguration to reduce partial shading losses. *IEEE Transactions on Sustainable Energy*, 4(1), 145- 153.
- Energy Information Administration, International Energy Annual, 2021 (https://www.eia.gov/outlooks/ieo/tables_side_xls.php)
- Fathy, A. (2015). Reliable and efficient approach for mitigating the shading effect on PV module based on modified artificial bee colony algorithm. *Renewable Energy*, 81, 78-88.
- Fathy, A. (2018). Recent meta-heuristic grasshopper optimization algorithm for optimal reconfiguration of partially shaded PV array. *Solar Energy*, 171, 638-651.
- Fathy, A. (2020). Butterfly optimization algorithm-based methodology for enhancing the shaded PV array extracted power via reconfiguration process. *Energy Conversion and Management*, 220, 1-21.

- Fialho, L., Melicio, R., Mendes, V.M.F., Figueiredo, J., & Pereira, M. (2014). Effect of shading on series solar modules: Simulation and Experimental Results. *Procedia Technology*, 17, 295 – 302.
- Forcan, M., Durisc, Z., & Mikulovi, J. (2016). An algorithm for elimination of partial shading effect based on a theory of reference PV string. *Solar Energy*, 132, 51–63.
- Gao, L., & Dougal, R. A. (2009). Parallel connected solar PV system to address partial and rapidly fluctuating shadow conditions. *IEEE Transactions on Industrial Electronics*, 56(5), 1548-1556.
- Gautam, N. K., & Kaushika, N. D. (2002). An efficient algorithm to simulate the electrical performance of solar PV arrays. *Energy*, 27, 347-361.
- Goss, B., Cole, I., Betts, T., & Gottschalg, R. (2014). Irradiance modelling for individual cells of shaded solar PV arrays. *Solar Energy*, 110, 410–419.
- Grisales, L. A. T., Paja, C. A. R., & Montes, A. J. S. (2015). Equivalent circuits for simulating irregular PV arrays under partial shading conditions. *Tecno Logicas*, 18(35), 57-69.
- Gul, S., Haq, A. U., Jalal, M., Anjum, A., & Khalil, I. U. (2020). A unified approach for analysis of faults in different configurations of PV arrays and its impact on power grid. *Energies*, 13, 1-23.
- Haq, A. U., Alammari, R., Iqbal, A., Jalal, M., & Gul, S. (2020). Computation of power extraction from PV arrays under various fault conditions. *IEEE Access*, 8, 47619- 47639.
- Huynh, D.C., Nguyen, T. M., Dunnigan, M. W., & Mueller, M. A. (2013). Global MPPT of solar PV modules using a dynamic PSO algorithm under partial shading conditions. *IEEE Conference on Clean Energy and Technology*, 134-139.

- Ishaque, K., Salam, Z., & Syafaruddin. (2011). A comprehensive MATLAB/Simulink PV system simulator with partial shading capability based on two diode model. *Solar Energy*, 85(9), 2217–2227.
- Jiang, L.L., Nayanasiri, D. R., Maskell, D. L., & Vilathgamuwa, D. M. (2015). A hybrid maximum power point tracking for partially shaded PV systems in the tropics. *Renewable Energy*, 76, 53-65.
- Jung, T. H., Ko, J. W., Kang, G. H., & Ahn, H. K. (2013). Output characteristics of PV module considering partially reverse biased conditions. *Solar Energy*, 92, 214–220.
- Kadri, R., Andrei, H., Gaubert, J. P., Ivanovici, T., Champenois, G., & Andrei, P. (2012). Modeling of the PV cell circuit parameters for optimum connection model and real time emulator with partial shadow conditions. *Energy*, 42(1), 57-67.
- Kansal I. & Pachauri, R. (2021). Mathematical puzzle based PV array configuration for GMP enhancement under non-uniform irradiation. EAI Endorsed Trans. *Energy Web*, 8(32), 1–10.
- Karatepe, E., Boztepe, M., & Colak, M. (2007). Development of a suitable model for characterizing PV arrays with shaded solar cells. *Solar Energy*, 81(8), 977-992.
- Kaushika, N. D., & Gautam, N. K. (2003). Energy yield simulations of interconnected solar PV arrays. *IEEE Transactions on Energy Conversion*, 18(1), 127-134.
- Kawamura, H., Naka, K., Yonekura, N., Yamanaka, S., Kawamura, H., Ohno, H., & Nait, K., 2003. Simulation of I-V characteristics of a PV module with shaded PV cells. *Solar Energy Materials & Solar Cells*, 75, 613–621.

- Kouchaki, A., Eini, H. I., & Asaei, B. (2013). A new maximum power point tracking strategy for PV arrays under uniform and non-uniform insolation conditions. *Solar Energy*, 91, 221–232.
- Krishna, G. S., & Moger, T. (2019). Improved Su-Do-Ku reconfiguration technique for TCT PV array to enhance maximum power under partial shading conditions. *Renewable and Sustainable Energy Reviews*, 109, 333–348.
- Kumar, A., Pachauri, R. K., & Chauhan, Y. K. (2016). Experimental analysis of SP/TCT PV array configurations under partial shading conditions. *IEEE International Conference on Power Electronics, Intelligent Control and Energy Systems*, 1648-1653.
- Kumar, H., Gupta, A., Pachauri, R. K., & Chauhan, Y. K. (2015). PI/FL based blade pitch angle control for wind turbine used in wind energy conversion system. *IEEE Conference on Recent Developments in Control, Automation and Power Engineering*, 1-6.
- Li, S., Haskew, T., Li, A. D., & Hu, F. (2011). Integrating PV and power converter characteristics for energy extraction study of solar PV systems. *Renewable Energy*, 36, 3238-3245.
- Lorente, D. G., Pedrazzi, S., Zini, G., Rosa, A. D., & Tartarini, P. (2014). Mismatch losses in PV power plants. *Solar Energy*, 100, 42–49.
- Lu, F., Guo, S., Walsh, T. M., & Aberle, A. G. (2013). Improved PV module performance under partial shading conditions. *Energy Procedia*, 33, 248 – 255.
- Lun, S., Wang, S., Guo, T., & Du, C. (2014). An I–V model based on time warp invariant echo state network for PV array with shaded solar cells. *Solar Energy*, 105, 529–541.
- Ma, T., Yang, H., & Lu, L. (2014). Development of a model to simulate the performance characteristics of crystalline silicon PV modules/strings/arrays. *Solar Energy*, 100, 31–41.

- Madhusudanam, G., Senthilkumar, S., Anand, I., & Sanjeevkumar, P. (2018). A shade dispersion Scheme using Latin Square Arrangement to enhance Power Production in Solar PV Array under Partial Shading Conditions. *Journal of Renewable and Sustainable Energy*, 10, 1-14.
- Maki, A., & Valkealahti, S. (2012). Power Losses in long string and parallel connected short strings of series-connected silicon-based PV modules due to partial shading conditions. *IEEE Transactions on Energy Conversion,* 27(1),173-183.
- Maki, A., & Valkealahti, S. (2014). Differentiation of multiple maximum power points of partially shaded PV power generators. *Renewable Energy*, 71, 89-99.
- Maki, A., Valkealahti, S., & Leppaaho, J. (2012). Operation of series connected silicon-based PV modules under partial shading conditions. *Progress in Photovoltaics: Research and Applications,* 20, 298–309.
- Malathy S., & Ramaprabha, R. (2015). Comprehensive analysis on the role of array size and configuration on energy yield of PV systems under shaded conditions. *Renewable and Sustainable Energy Reviews*, 49, 672–679.
- Malathy, S., & Ramaprabha, R. (2015). A static PV array architecture to enhance power generation under partial shaded conditions. *Proceedings of IEEE Conference on Power Electronics and Drives System*, 1-6.
- Malathy, S., & Ramaprabha, R. (2018). Reconfiguration strategies to extract maximum power from PV array under partially shaded conditions. *Renewable and Sustainable Energy Reviews,* 81, 2922-34.
- Manna, D. L., Vigni, V. L., Sanseverino, E. R., Dio, V. D., & Romano, P. (2014). Reconfigurable electrical interconnection strategies for PV arrays: a review. *Renewable and Sustainable Energy Reviews,* 33, 412–426.

- Mishra, N., Yadav, A. S., Pachauri, R., Chauhan, Y. K., & Yadav, V. K. (2017). Performance enhancement of PV system using proposed array topologies under various shadow patterns. *Solar Energy*, 157, 641-656.
- Mishra, V. L., Chauhan, Y. K., & Verma, K. S. (2022). A novel PV array reconfiguration approach to mitigate non-uniform irradiation effect. *Energy Conversion and Management*, 265, 1-36.
- Moballegh S., & Jiang, J. (2014). Modeling, prediction, and experimental validations of power peaks of PV arrays under partial shading conditions. *IEEE Transactions on Sustainability Energy*, 5(1), 293–300.
- Moballegh, S., & Jiang, J. (2011). Partial shading modeling of PV system with experimental validations. *Proceedings of IEEE Conference on Power and Energy Society General Meeting*, 1-9.
- Mohammadnejad, S., Khalafi, A., & Ahmadi, S. M. (2016). Mathematical analysis of TCT PV array under partial shading condition and its comparison with other configurations. *Solar Energy*, 133, 501–511.
- Moreno, F. M., Munoz, J., & Lorenzo, E. (2010). Experimental model to estimate shading losses on PV arrays. *Solar Energy Materials & Solar Cells*, 94, 2298–2303.
- Moschitta, A., Damiani, A., & Carbone, P. (2012). A simple and accurate model for predicting mismatch effects in PV arrays. *Proceedings of IEEE Conference on Energy and Exhibition*, 818-822.
- Nasiruddin, I., Khatoon, S., Jalil, M. F., & Bansal, R. C. (2019). Shade diffusion of partial shaded PV array by using odd-even structure. *Solar Energy*, 181, 519–529.
- Nezhad, M. E., Asaei, B., & Farhangi, S. (2013). Modified analytical solution for tracking PV module maximum power point under partial shading condition. *IEEE Conference on Environmental and Electrical Engineering*, 1-6.

- Nguyen, D., & Lehman, B. (2006). Modeling and simulation of solar PV arrays under changing illumination conditions. *IEEE Conference on Computers in Power Electronics*, 295-299.
- Nihanth, M. S. S., Ram, J. P., Pillai, D. S., Ghias, A. M. Y. M., Garg, A., & Rajasekar N. (2019). Enhanced power production in PV arrays using a new skyscraper puzzle based one-time reconfiguration procedure under partial shade conditions (PSCs). *Solar Energy*, 194, 209–224.
- Ola, S. R., Sarswat, A., Goyal, S. K., Jhajharia, S. K., Khan, B., Mahela, O. P., Alhelou, H. H., & Siano, P. (2020). A protection scheme for a power system with solar energy penetration. *Applied Sciences*, 10, 1-22.
- Pachauri, R. K., Bai, J., Kansal, I., Mahela, O. P., & Khan, B. (2021). Shade dispersion methodologies for performance improvement of classical total cross-tied PV array configuration under partial shading conditions. *IET Renewable Power Generation*, 15(8),1796–1811.
- Pachauri, R. K., Kansal, I., Babu, T. S., & Alhelou, H. H. (2021). Power Losses Reduction of Solar PV Systems under Partial Shading Conditions Using Re-Allocation of PV Module-Fixed Electrical Connections. *IEEE Access*, 9, 94789–94812.
- Pachauri, R. K., Thanikanti, S. B., Bai, J., Yadav, V. K., Aljafari, B., Ghosh, S., & Alhelou, H. H. (2022). Ancient Chinese magic square-based PV array reconfiguration methodology to reduce Power Loss under Partial shading conditions. *Energy Conversion and Management*, 253(3), 115-148.
- Pachauri, R. K., Yadav, A. S., Chauhan, Y. K., Sharma, A., & Kumar, V. (2018). Shade dispersion-based PV array configurations for performance enhancement under partial shading conditions. *International Transaction on Electrical Energy System*, 28(7), 1-32.

- Pachauri, R., Singh, R., Gehlot, A., Samakaria, R., & Choudhury, S. (2019). Experimental analysis to extract maximum power from PV array reconfiguration under partial shading conditions. *Engineering Science and Technology, an International Journal*, 22, 109–130.
- Pareek, C., Chaturvedi, N., & Dahiya, R. (2017). Optimal interconnections to address partial shading losses in solar PV arrays. *Solar Energy*, 155, 537-551.
- Pareek, S., & Dahiya, R. (2014). Output power maximization of partially shaded 4×4 PV field by altering its topology. *Energy Procedia*, 54, 116 – 126.
- Pareek, S., & Dahiya, R. (2016). Enhanced power generation of partial shaded PV fields by forecasting the interconnection of modules. *Energy*, 95, 561–572.
- Pareek, S., Runthala, R., & Dahiya, R. (2013). Mismatch losses in SPV systems subjected to partial shading conditions. *Proceedings of IEEE Conference on Advanced Electronics Systems*, 343-345.
- Parlak, K. S. (2014). FPGA based new MPPT method for Photovoltaic array system operating partially shaded conditions. *Energy*, 68, 1-12.
- Parlak, K. S. (2014). PV array reconfiguration method under partial shading conditions. *Electrical Power and Energy Systems*, 63, 713–721.
- Patel, H., & Agarwal, V. (2008). MATLAB-based modeling to study the effects of partial shading on PV array characteristics. *IEEE Transactions on Energy Conversion*, 23(1), 302-310.
- Patel, H., & Agarwal, V. (2008). Maximum power point tracking scheme for PV systems operating under partially shaded conditions. *IEEE Transactions on Industrial Electronics*, 55(4), 1689-1698.
- Patnaik, B., Sharma, P., Trimurthulu, E., Duttagupta, S. P., & Agarwal, V. (2011). Reconfiguration strategy for optimization of solar PV array under non-uniform illumination conditions. *Proceedings of IEEE Conference on PV Specialists*, 1859-1864.

- Penaranda, R. C., Quiroz, F. A. R., Montoya, D. G., Martinez, F., & Ramos-Paja, C. A. (2015). Reconfiguration of PV arrays based on genetic algorithm. *Revista Facultad de Ingeniería Universidad de Antioquia*, 75, 95-107.
- Petronea G., & Ramos-Paja, C. A. (2011). Modeling of PV fields in mismatched conditions for energy yield evaluations. *Electric Power Systems Research*, 81(4), 1003–1013.
- Piazza, C. D., & Vitale, G. (2010). PV field emulation including dynamic and partial shadow conditions. *Applied Energy*, 87, 814–823.
- Picault, D., Raison, B., Bacha, S., De la Casa, J., & Aguilera, J. (2010). Forecasting PV array power production subject to mismatch losses. *Solar Energy*, 84, 1301-1309.
- Pillai, D. S., Ram, J. P., Nihanth, M. S. S., & Rajasekar, N. (2018). A Simple, sensor less and fixed reconfiguration scheme for maximum Performance Enhancement in PV systems. *Energy Conversion and Management*, 172, 402-417.
- Potnuru, S. R., Pattabiraman, D., Ganesan, S. I., & Chilakapati, N. (2015). Positioning of PV panels for reduction in line losses and mismatch losses in PV array. *Renewable Energy*, 78, 264-275.
- Premkumar, M., Subramaniam, U., Babu, T. S., Elavarasan, R. M., & Popa, L. M. (2020). Evaluation of Mathematical Model to Characterize the Performance of Conventional and Hybrid PV Array Topologies under Static and Dynamic Shading Patterns. *Energies*, 13, 1-37.
- Qi, J., Zhang, Y., & Chen, Y. (2014). Modeling and maximum power point tracking (MPPT) method for PV array under partial shade conditions. *Renewable Energy*, 66, 337–345.
- Quesada, G. V., Gispert, F. G., Lopez, R. P., Lumbreras, M. R., & Roca, A. C. (2009). Electrical PV array reconfiguration strategy for energy extraction

improvement in grid connected PV systems. *IEEE Transactions on Industrial Electronics*, 56, 4319- 4331.

- Rakesh, N., & Madhavaram, T. V. (2016). Performance enhancement of partially shaded solar PV array using novel shade dispersion technique. *Frontiers in Energy*, 10(2), 227-239.
- Ram, P., & Rajasekar, N. (2016). A new global maximum power point tracking technique for solar PV (PV) system under partial shading conditions (PSC). *Energy*, 118, 1-14.
- Ramaprabha, R. (2014). Selection of an optimum configuration of solar PV array under partial shaded condition using particle swarm optimization. *International Journal of Electrical, Computer, Energetic, Electronic and Communication Engineering*, 8(1), 89-96.
- Ramaprabha, R., & Mathur, B.L. (2012). A comprehensive review and analysis of solar PV array configurations under partial shaded conditions. *International Journal of Photoenergy*, 2012, 1-16.
- Ramos-Paja, C. A., Bastidas, J. D., & Saavedra-Montes, A. J. (2013). Experimental validation of a model for PV arrays in TCT configuration. *Dyna*, 80, 191-199.
- Rani, B. I., Ilango, G. S., & Nagamani, C. (2013). Enhanced power generation from PV array under partial shading conditions by shade dispersion using Su-Do-Ku configuration. *IEEE Transaction Sustainable Energy*, 4(3), 594–601.
- Rao, P. S., Dinesh, P., Ilango, G. S., & Nagamani, C. (2015). Optimal Su-Do-Ku based interconnection scheme for increased power output from PV array under partial shading conditions. *Frontier Energy*, 9(2), 199–210.
- Reinoso, R. S., Milone, D. H., & Buitrago, R. H. (2013). Simulation of PV centrals with dynamic shading. *Applied Energy*, 103, 278–289.

- Renaudineau, H., Houari, A., Martin, J. P., Pierfederici, S., Tabar, F. M., & Gerardin, B. (2011). A new approach in tracking maximum power under partially shaded conditions with consideration of converter losses. *Solar Energy*, 85, 2580–2588.
- Report on World Energy Outlook, 2021 (https://www.iea.org/fuels-and-technologies/renewables)
- Rezk, H., Fathy, A., & Aly, M., (2021). A robust PV array reconfiguration strategy based on coyote optimization algorithm for enhancing the extracted power under partial shadow condition. *Energy Reports*, 7, 109-124.
- Rodrigo, P. M., Fernandez, E. F., Almonacid, F., & Higueras, P. J. P. (2013). A simple accurate model for the calculation of shading Power Losses in PV generators. *Solar Energy*, 93, 322–333.
- Rodriguez, D. B., Grisales, L. A. T., Montoya, D. G., Paja, A. R., & Spagnuolo, G. G. (2018). General modeling procedure for PV arrays. *Electric Power Systems Research*, 155, 67-79.
- Sagar, G., Pathak, D., Gaur, P., & Jain, V. (2020). A Su-Do-Ku puzzle-based shade dispersion for maximum Performance Enhancement of partially shade hybrid bridge-link-TCT PV array. *Solar Energy*, 204, 161-180.
- Sahu, H. S., & Nayak, S. K. (2016). Extraction of Maximum Power from a PV Array under Non-uniform Irradiation Conditions. *IEEE Transactions on Electron Devices*, 63(12), 4825–4831.
- Sahu, H. S., Nayak, S. K., & Mishra, S. (2016). Maximizing the power generation of a partially shaded PV array. *IEEE Journal of Emerging and Selected Topics in Power Electronics*, 4(2), 626–637.
- Salam, Z., & Ramli, M. Z. (2012). A simple circuit to improve the power yield of PV array during partial shading. *Proceedings of IEEE Conference Energy Conversion Congress and Exposition*, 1622- 1626.

- Samikannu, S. M., Namani, R., & Subramaniam, S. K. (2016). Performance Enhancement of partially shaded PV arrays through shade dispersion using magic square configuration. *Journal of renewable and sustainable energy and reviews*, 8, 1-20.
- Santos, D., Vicente, E. M., & Ribeiro, E. R. (2011). Relationship between the shading position and the output power of a PV panel. *IEEE Conference on Power Electronics*, 676-681.
- Satpathy, R., Sharma, R., & Jena, S. (2017). A shade dispersion interconnection scheme for partially shaded modules in a solar PV array network. *Energy*, 139, 350-365.
- Seyedmahmoudian, M., Mekhilef, S., Rahmani, R., Yusof, R., & Renani, E. T. (2013). Analytical modeling of partially shaded PV systems. *Energies*, 6, 128-144.
- Shankar, G., & Mukherjee, V. (2015). MPP detection of a partially shaded PV array by continuous GA and hybrid PSO. *Ain Shams Engineering Journal*, 6(2), 471–479.
- Shirzadi, S., Hizam, H., & Wahab, N. I. A. (2014). Mismatch losses minimization in PV arrays by arranging modules applying a genetic algorithm. *Solar Energy*, 108, 467–478.
- Silvestre, S., Boronat, A., & Chouder, A. (2009). Study of bypass diodes configuration on PV modules. *Applied Energy*, 86, 1632–1640.
- Silvestre, S., & Chouder, A. (2008). Effects of shadowing on PV module performance. *Progress in PVs: Research and Applications*, 16, 141–149.
- Singh, A. K., Pandey, V., & Pachauri, R. K. (2021). Estimation of solar radiation at FARASAN Island with two-step ANN concepts. *Proceedings of International Conference on Intelligent Communication, Control and Devices*, 1-10.

- Srinivasan, A., Devakirubakaran, S., & Sundaram, B. M. (2020). Mitigation of mismatch losses in solar PV system- two step reconfiguration approach. *Solar Energy*, 206, 640-654.
- Storey, J., Wilson, P. R., & Bagnall, D. (2014). The optimized string dynamic PV array. *IEEE Transactions on Power Electronics*, 29(4), 1768-1776.
- Sundareswaran, K., Kumar, V.V., & Palani, S. (2015). Application of a combined particle swarm optimization and perturb and observe method for MPPT in PV systems under partial shading condition. *Renewable Energy*, 75, 308-317.
- Tabish, S., & Ashraf, I. (2017). Simulation of partial shading on solar PV modules with experimental verification. *International Journal of Ambient Energy*, 38(2), 161-170.
- Tian, H., David, F. M., Ellis, K., Muljadi, E., & Jenkins, P. (2013). Determination of the optimal configuration for a PV array depending on the shading condition. *Solar Energy*, 95, 1–12.
- Tossa, A. K., Soro, Y. M., Azoumah, Y., & Yamegueu, D. (2014). A new approach to estimate the performance and energy productivity of PV modules in real operating conditions. *Solar Energy*, 110, 543–560.
- Tsai, H. L. (2010). Insolation oriented model of PV module using MATLAB/Simulink. *Solar Energy*, 84, 1318–1326.
- Vengatesh, P., & Rajan, S. E. (2017). Analysis of PV module connected in different configurations under uniform and non-uniform solar radiations. *International Journal of Green Energy*, 14(13), 1507-1516.
- Venkateswari, R., & Rajasekar, N. (2020). Performance Enhancement of PV system via physical array configuration-based Lo-Shu technique. *Energy Conversion and Management*, 215, 1-22.

- Vicente, D. S., Pimenta, T. C., & Ribeiro, E. R. (2015). Photovoltaic array reconfiguration strategy for maximization of energy production. *International Journal of Photo Energy*, 2-11.
- Vijayalekshmy, S., Bindu, G. R., & Iyer, S. R. (2015). Analysis of various PV array configurations under dispersion by Su-Do-Ku arrangement during passing cloud conditions. *Indian Journal of Science and Technology*, 8(35), 1-7.
- Vijayalekshmy, S., Bindu, G. R., & Iyer, S. R. (2016). A novel Zig-Zag scheme for Performance Enhancement of partially shaded solar arrays. *Solar Energy*, 135, 92–102.
- Vijayalekshmy, S., Bindu, G. R., & Iyer, S. R. (2016). Performance improvement of partially shaded PV arrays under moving shadow conditions through shade dispersion. *Journal of the Institution of Engineers (India): Series-B*, 97(4), 569-575.
- Vijayalekshmy, S., Iyer, S. R., & Beevi, B. (2014). Comparative analysis on the performance of a short string of series connected and parallel connected PV array under partial shading. *Journal of the Institution of Engineers (India) Series B*, 96(3), 217-226.
- Villa, F. L., Picault, D., Raison, B., Bacha, S., & Labonne, A. (2012). Maximizing the power output of partially shaded PV plants through optimization of the interconnections among its modules. *IEEE Journal of Photovoltaics*, 2(2), 154-163.
- Wang, Y. J., & Hsu, P. C. (2010). Analytical modelling of partial shading and different orientation of PV modules. *IET Renewable Power Generation*, 4(3), 272–282.
- Wang, Y. J., & Lin, S. S. (2012). Analysis of a partially shaded PV array considering different module connection schemes and effects of bypass diodes.

IEEE Conference on Utility Exhibition on Power and Energy Systems: Issues and Prospects for Asia. 1-7.

- Wang, Y., Lin, X., Kim, Y., Chang, N., & Pedram, M. (2014). Architecture and control algorithms for combating partial shading in PV systems. *IEEE Transactions on Computer Aided Design of Integrated Circuits and Systems,* 33(6), 917- 929.
- Wanko, J. J., & Nickell, J. V. (2013). Shape-do-Ku puzzles combine logic and spatial reasoning with an understanding of basic geometric concepts. *The Mathematics Teacher,* 107(3), 188-194.
- Woytea, A., Nijsa, J., & Belmansa, R. (2003). Partial shadowing of PV arrays with different system configurations: literature review and field test results. *Solar Energy*, 74, 217–233.
- Xiao, W., Ozog, N., & Dunford, W. G. (2007). Topology study of PV interface for maximum power point tracking. *IEEE Transactions on Industrial Electronics*, 54(3), 1696-1704.
- Xueye, J. W., & Tianlong, Z. (2015). Research on the output characteristics of PV array under the non-uniform light. *International Journal of control and automation*, 8(10), 431-444.
- Yadav, A. S., Pachauri, R. K., Chauhan, Y. K., Choudhury, S., & Singh, R. (2017). Performance enhancement of partially shaded PV array using novel shade dispersion effect on magic-square puzzle configuration. *Solar Energy*, 144, 780–797.
- Yadav, A. S., Pachauri, R. K., & Chauhan, Y. K. (2016). Comprehensive investigation of PV arrays with puzzle shade dispersion for improved performance. *Solar Energy*, 129, 256–285.
- Yadav, P., Kumar, A., Gupta, A., Pachauri, R. K., Chauhan, Y. K., & Yadav, V. K. (2016). Investigations on the effects of partial shading and dust

accumulation on PV module performance. *Advances in Intelligent Systems and Computing*, 479, 1005-12.

- Yadav, S., Pachauri, R. K., & Chauhan, Y. K. (2015). Comprehensive investigation of PV arrays under different shading patterns by shade dispersion using puzzled pattern-based Su-do-Ku puzzle configuration. *Proceedings of IEEE Conference on Next Generation Computing Technologies*, 824-830.
- Yousri, D., Allam, D., & Eteiba, M. B. (2020). Optimal PV array reconfiguration for alleviating the partial shading influence based on a modified harris hawks optimizer. *Energy Conversion and Management*, 206, 1-25.
- Zhang, F., Ali, J., Feng, C., & Wu, Y. (2012). In-depth investigation of effects of partial shading on PV array characteristics. *Proceedings of International Conference on Power Engineering and Automation*, 1-4.
- Zheng, H., Li, S., Challoo, R., & Proano, J. (2014). Shading and bypass diode impacts to energy extraction of PV arrays under different converter configurations. *Renewable Energy*, 68, 58-66.
- Ziar, H., Mansourpour, S., Afjei, E., & Kazemi, M. (2012). Bypass diode characteristic effect on the behavior of solar PV array at shadow condition. *IEEE Conference on Power Electronics and Drive Systems Technology*, 229-233.

PUBLICATIONS

- **I. Kansal**, R. K. Pachauri, "**Mathematical Puzzle-Based PV Array Configuration for GMP Enhancement under Non-Uniform Irradiation**", EAI Endorsed Transactions on Energy Web, vol. 8(32), pp. 1-10, 2020. 165915. **(Scopus Indexed)**
- **I. Kansal**, R. K. Pachauri, "**Game Theory-Based Photovoltaic Array System Reconfigure Method: Experimentation Validation**", International Journal of Advanced Technology and Engineering Exploration, vol. 10 (99), pp. 202-217, 2023. **(Scopus Indexed)**
- **I. Kansal**, R. K. Pachauri, "**DPVM-SEC based Methodology to Reconfigure PV System and Characterization during PSCs: Experimental Study using Data Acquisition System**" in Materials Today Proceedings, vol. 80(2), pp. 731-739, 2023. **(Scopus Indexed)**
- R. K. Pachauri, **I. Kansal**, et. al., "**Power Losses Reduction of Solar PV Systems under Partial Shading Conditions using Re-allocation of PV Module-Fixed Electrical Connections**", IEEE Access, vol. 9, pp. 94789-94812, July 2021. **SCI (IF- 3.745)**

PUBLICATIONS

- **I. Kansal**, R. K. Pachauri, "**Mathematical Puzzle-Based PV Array Configuration for GMP Enhancement under Non-Uniform Irradiation**", EAI Endorsed Transactions on Energy Web, vol. 8(32), pp. 1-10, 2020. 165915. **(Scopus Indexed)**
- **I. Kansal**, R. K. Pachauri, "**Game Theory-Based Photovoltaic Array System Reconfigure Method: Experimentation Validation**", International Journal of Advanced Technology and Engineering Exploration, vol. 10 (99), pp. 202-217, 2023. **(Scopus Indexed)**
- **I. Kansal**, R. K. Pachauri, "**DPVM-SEC based Methodology to Reconfigure PV System and Characterization during PSCs: Experimental Study using Data Acquisition System**" in Materials Today Proceedings, vol. 80(2), pp. 731-739, 2023. **(Scopus Indexed)**
- R. K. Pachauri, **I. Kansal**, et. al., "**Power Losses Reduction of Solar PV Systems under Partial Shading Conditions using Re-allocation of PV Module-Fixed Electrical Connections**", IEEE Access, vol. 9, pp. 94789-94812, July 2021. **SCI (IF- 3.745)**

UPES
UNIVERSITY OF TOMORROW

PLAGIARISM CERTIFICATE

1. I **Dr. Rupendra Kumar Pachauri** (Supervisor) certify that the Thesis titled "**Optimal interconnections of PV Modules for Performance Enhancement of PV Array under Partial Shading Conditions**" submitted by Scholar **Ms. Isha Kansal** having SAP ID 500057724 has been run through a Plagiarism Check Software and the Plagiarism Percentage is reported to be 10%.

2. Plagiarism Report generated by the Plagiarism Software is attached.

11.8.23

Signature of the Internal Guide

Signature of the Scholar

ik1 Isha Kansal (SAP ID: 500057724)

ORIGINALITY REPORT

10%	7%	9%	1%
SIMILARITY INDEX	INTERNET SOURCES	PUBLICATIONS	STUDENT PAPERS

RIMARY SOURCES

1	www.researchgate.net Internet Source	2%
2	eprints.eudl.eu Internet Source	1%
3	www.sciopen.com Internet Source	<1%
4	Shahroz Anjum, Vivekananda Mukherjee. "Static and Dynamic Reconfiguration Strategies for Reducing Partial Shading Effects in Photovoltaic Array: A Comprehensive Review", Energy Technology, 2022 Publication	<1%
5	Rupendra Kumar Pachauri, Ankur Kumar Gupta, Ahmad Faiz Minai, Mohit Kumar, Shashikant. "Su-Do-Ku Game Puzzle for Improving Shade dispersion factor on PV Array Systems under PSCs: Experimental Validation", 2022 International Conference on Emerging Smart Computing and Informatics (ESCI), 2022 Publication	<1%